Pseudo Potential Fields on Surface-Haptic Touchscreens using Friction Modulation

T.J. Brans

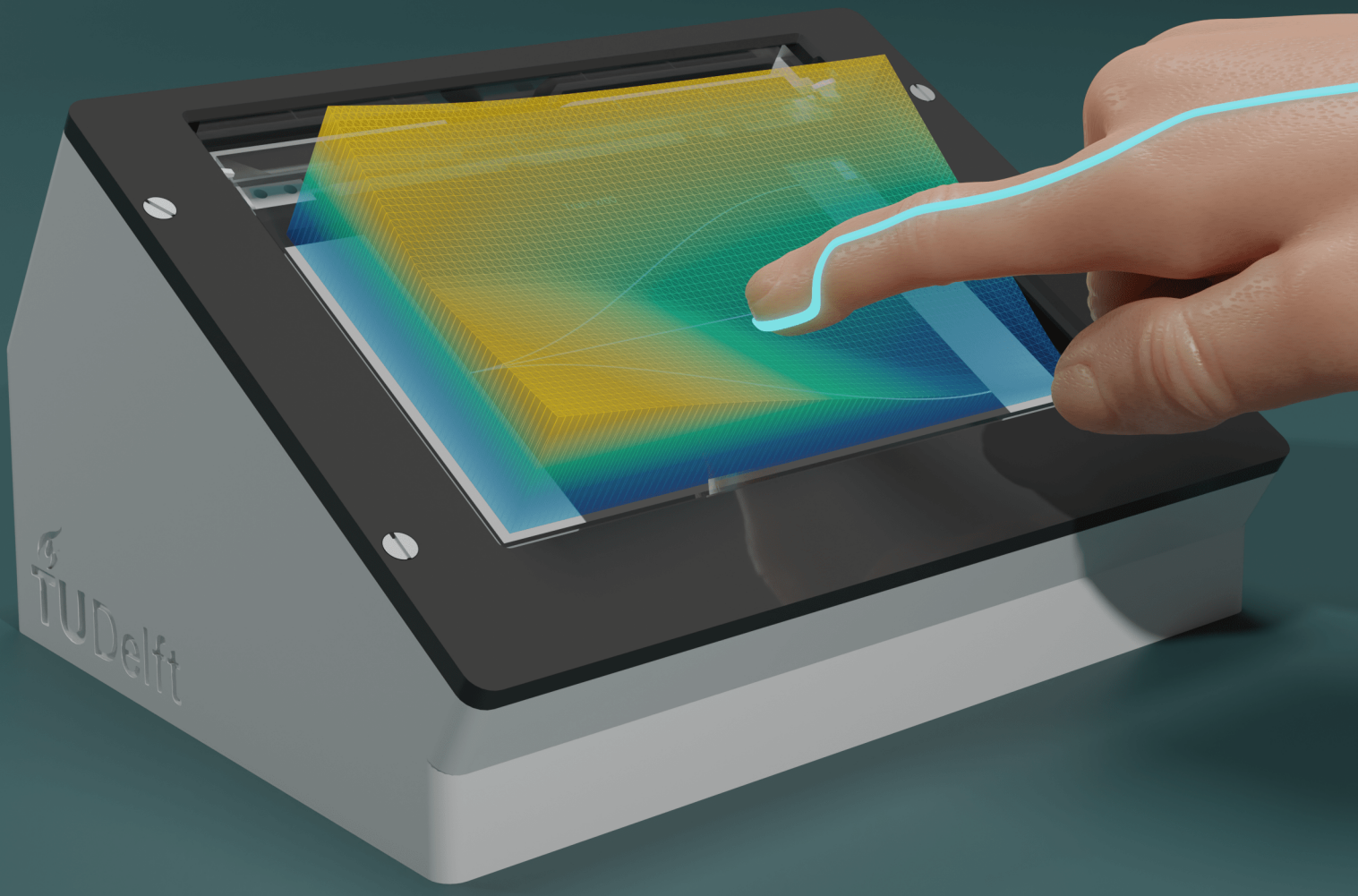

TU Delft

video abstract

Pseudo Potential Fields on Surface-Haptic Touchscreens using Friction Modulation

by

T.J. Brans

to obtain the degree of Master of Science
at the Delft University of Technology,
to be defended on July 4th 2022.

Student number:	4367553	
Project duration:	April 2021 - July 2022	
Thesis committee:	Prof. Dr. ir. D.A. Abbink	TU Delft, supervisor, chair
	Dr. M. Wiertlewski	TU Delft, daily supervisor
	Dr. B. Shyrokau	TU Delft, supervisor
	Dr. ir. D.M. Pool	TU Delft, external committee member

Acknowledgements

I experienced a great amount of help of many people around me. Discussing problems with others and having relaxing talks about everyday life helped me to stay motivated and achieve this result. For this I would like to express my gratitude.

First of all, I want to thank Michaël Wiertlewski, my daily supervisor during the entire project. I always felt welcome to walk by your office and discuss anything with you. Although the meetings sometimes got a little bit off track, I always left with new and interesting thoughts. The insights and feedback played an essential role in the progress of the thesis, for which I am thankful. Additionally, I would like to thank David Abbink and Barys Shyrokau for the feedback and suggestions made during the update meetings throughout the whole process. Furthermore, the time and expertise of Ehsan Hoseini for the design and manufacturing of the printed circuit board was invaluable.

Of course, this research would not have been possible without the many people who freed up their schedule to participate in the study. Together, you provided me with a staggering 2.2 kilometer of finger movements on the touchscreen. From this data I could extract my results and draw the conclusions.

The help of my fellow students and friends of the Cognitive Robotics department was amazing. During the joint meetings, in the lab and of course during the many coffee breaks. Not only could we discuss our projects with each other, but also comfortably talk about the struggles that are part of the master thesis.

The one I could always fall back to was Liselotte. Although, you were away for a long time chasing your own dreams I could share my experiences with you. Something I would not have wanted to miss.

Having great friends as roommates helped tremendously to relax after a day of studying. Especially during the pandemic, the extensive cooking sessions and many movie nights were very welcome. Also, the time spend with my close friends, making music as an excuse to have a nice time together makes everything more enjoyable. I cannot name all of you here, but know that I am thankful.

Finally, I would like to express my appreciation to my parents, brother and sister, who always provided me with an unlimited amount of support.

Contents

1

Introduction

The body of this thesis is built around the paper "Pseudo potential fields on surface-haptic touchscreens using friction modulation" in Chapter 2. This includes the majority of the research and its main takeaways. For further elaboration on the subject, the author would like to refer to the included appendices.

The detailed design of the haptic touchscreen is explained in Appendix A, together with the schematics of the electronics in Appendix B. Notes on the manufacturing and assembly are found in Appendix C. The characterisation of the most important part of the system, the glass plate, is presented in Appendix D. This includes the validation of the design as well. The code that is used to render the effects and run the experiments is given in Appendix F and Appendix G. The safety inspection report and ethics checklist are included in the appendix as well for completeness sake (Appendix H).

As part of the master thesis, multiple pilot experiments are conducted before settling for the design of the main experiment. At the start of the research the focus was on relating the results to the steering law [1]. During the design process and due to the findings of the pilot experiments, the focus shifted to the perception of the pseudo-potential field rendering method. The results are included in Appendix I, to share the findings of these pilot studies as well.

The experimental procedure (Appendix J) and notes made during the experiment (Appendix K) are shared as well. The datasets per participant are included in Appendix L to provide insight in the inter- and intra- subject variability.

2

Paper: Pseudo potential fields on surface-haptic touchscreens using friction modulation

Pseudo Potential Fields on Surface-Haptic Touchscreens using Friction Modulation

T.J. Brans

Abstract—It is impossible to imagine modern day interaction with technology without the use of touchscreens. It is a go-to interface to use for many applications, because of the high stimuli-response compatibility and adaptability of the graphical user interface. But the haptic feedback one would have with physical buttons and dials, is lost with the use of touchscreens. High potential to improve the interaction with high resolution haptic feedback is often ignored. In this paper, the use of a haptic pseudo-potential field rendering method on a friction modulated touchscreen is proposed. With this method, the user is assisted in moving towards a target by lowering the friction and impeded in moving away by increasing the friction coefficient. In a human factors experiment, this rendering method is compared to a position-based friction modulation method. Subjects are instructed to find a target path, based on the haptic feedback. The results show that the position-based rendering method has a higher hit-rate and lower movement times. This demonstrates that the pseudo-potential field method is difficult to perceive, however it is expected that advancements in rendering larger friction coefficient ranges or even active lateral force feedback will improve this rendering method.

Index Terms—surface haptics, ultrasonic friction modulation, pseudo-potential fields

1 Introduction

Touchscreens are used in everyday life increasingly more. Not only with mobile phones and tablets but also replacing buttons, dials and sliders used in everyday interaction. They have great stimuli-response compatibility due to the colocation of the touch input and visual feedback [1]. Together with the high resolution input and output and the highly adaptable user interface, this results in intuitive and efficient interaction. In spite of these advantages, touchscreens lack in providing rich haptic feedback. With touchscreens the user always feels the same piece of glass, instead of the tactile cues a user receives when interacting with physical buttons and dials. The addition of vibrotactile feedback (using eccentric rotating mass motors, voice coils or solenoids) can provide extra information, improving the interaction. But this feedback is coarse and limited to confirmatory cues [2],[3]. This low resolution haptic feedback does not align with the high resolution input method and visual feedback of touchscreens.

The interaction with touchscreens relies heavily on the visual feedback modality, which can deteriorate in real life scenarios. For example, when visual attention has to be shared during multitasking or when the visuals are masked due to external factors. In general, multi-modal feedback is superior because additional, redundant information is provided [4]. But in touchscreen interaction, no advantage is taken of the many mechanoreceptors the human has in each fingertip. This leaves high potential to improve the interaction. The tactile information encoded by these mechanoreceptors provides feedback to the motor system and, at the same time, conveys perceptual information about the object, such as weight, softness and texture [5],[6]. Information far beyond simple vibrations and clicks.

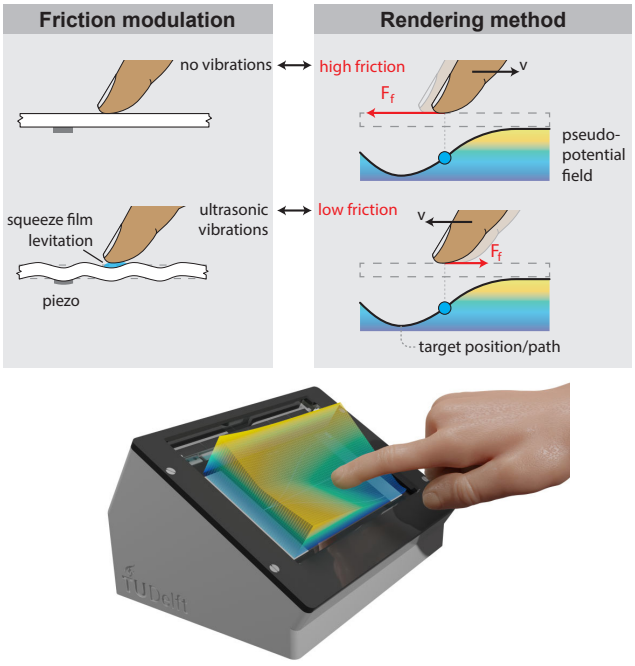

Fig. (1) Visual representation of the proposed haptic rendering method used for guidance to a target.

For efficient and intuitive haptic feedback, continuous evolving haptics is preferred. Such that the high resolution visual feedback can be supplemented (or sometimes replaced) by high resolution haptic feedback. With surface haptics, it is possible to continuously adapt the apparent friction coefficient between the touch surface and fingertip, by using ultrasonic vibrations [7],[8]. By inducing vibrations in a glass plate using piezoelectric elements, the plate vibrates at its ultrasonic eigenfrequency. These displacement amplitudes, in the order of microns, create a squeeze

film between the plate and fingertip. The vibrations of the plate itself are not felt by the user, but the friction reduces as the vibration amplitude increases [9],[10]. Placing an LCD screen below this surface makes the haptic effects coincide with the visual feedback. Different haptic effects can be generated by modulation of this vibration amplitude (and thus friction coefficient) based on finger position. This results in continuous haptic feedback that increases the perceived realism during interaction, by rendering textures [11],[12],[13]. Also, eyes-free interaction in slider tasks is possible by presenting a continuously changing texture, which spatial frequency correlates to the value of the setting [14]. Additionally, improved task performance for pointing and dragging tasks is found. Friction modulation can aid the user in target acquisition by creating zones of low or high friction. This haptic feedback decreases the movement time, while maintaining similar accuracy [15],[16].

However, these position-based rendering methods will only provide the user with confirmatory feedback when they hit the target. For more complex tasks or when the target is unknown to the user, continuous directional cues towards the target would be more useful. Providing active forces on the fingertip towards a target is not possible with friction modulation, but a pseudo effect is possible by continuously modulating the friction coefficient. We propose the use of a pseudo-potential field as a haptic feedback rendering principle (figure 1). Rather than modulating the friction purely based on the position of the finger, also the direction of movement is taken into account. Movement against a virtual force field will be impeded by generating high friction, while movement in the same direction as the force field will be aided by generating low friction. Hereby, this rendering principle continuously provides directional cues towards the target, as opposed to confirmatory haptic feedback.

The proposed haptic rendering principle is evaluated by conducting a human factors experiment. It is researched whether subjects are able to properly perceive the haptic guidance to a certain predefined target path. The pseudo-potential field method is compared to position dependent friction modulation. The results of this experiment are used to answer the question, which rendering method is best suited to guide users to a specific target on a friction modulated touchscreen interface, using ultrasonic vibrations. It is tested which feedback principle provides the highest hit-rate and the lowest movement times.

Improved haptic rendering methods will bring the valuable haptic feedback, that physical buttons and dials have, to touchscreens. While touchscreens also take advantage of the high stimuli-response compatibility and graphical adaptability of touchscreens. Thus, it combines the best of both worlds.

2 Related work

Research into both surface haptics and the addition of haptic feedback in touchscreens have gathered a lot of momentum in the last decades.

2.1 Surface haptic technologies

Nowadays, the implementation of embedded vibrators is found in many consumer touchscreen devices. The simplistic feedback increases the performance during interaction [2]. For example a confirmation vibration while touching a user interface element can replicate the feeling of a mechanical button being pressed [3]. However, this feedback principle is limited to providing discontinuous or binary feedback.

A method to incorporate continuous force feedback in touchscreens is to use ultrasonic vibrations on the touch surface. As explained before, a transparent plate located just above the screen is actuated at its eigenfrequency, causing vertical displacements in the order of microns. These low amplitude, high frequency vibrations are not perceived by the user directly, but a squeeze film effect is generated between the finger and the touch surface. This mechanism reduces the effective friction coefficient between finger and touch surface [17],[18]. A wide range of friction forces can be generated by modulating the amplitude of the vibrations. Multiple touchscreen devices are presented in literature that utilize this feedback principle [19], also for improving task performance [15],[16].

An alternative to actively modulate the friction force is the use of electroadhesion, or sometimes referred to as electrovibration. By supplying an alternating voltage to an electrode just below an insulating touch surface, the resulting electrostatic forces periodically attract the finger. The increase in normal force in turn results in a higher friction force [20],[21]. Note that the normal force is changed rather than the apparent friction, as is the case with ultrasonic vibrations. Several touchscreen interfaces implementing this effect are presented as well [22],[23]. The proposed rendering method in this paper could work similarly for electroadhesion touchscreens, but this is not evaluated. For an in depth review of different surface haptic technologies, the author would like to refer the reader to a literature review of Basdogan et al. [24] or Costes et al. [25].

2.2 Touchscreen task performance

Haptic feedback on touchscreens is often researched in situations where multiple tasks have to be executed. An example is the execution of secondary tasks on a touchscreen in automotive situations. This includes setting a slider or pressing a button on a touchscreen while driving. Research has shown that (simplistic) haptic feedback can reduce eyes-off-road time [26],[27] and result in lower error rates [3].

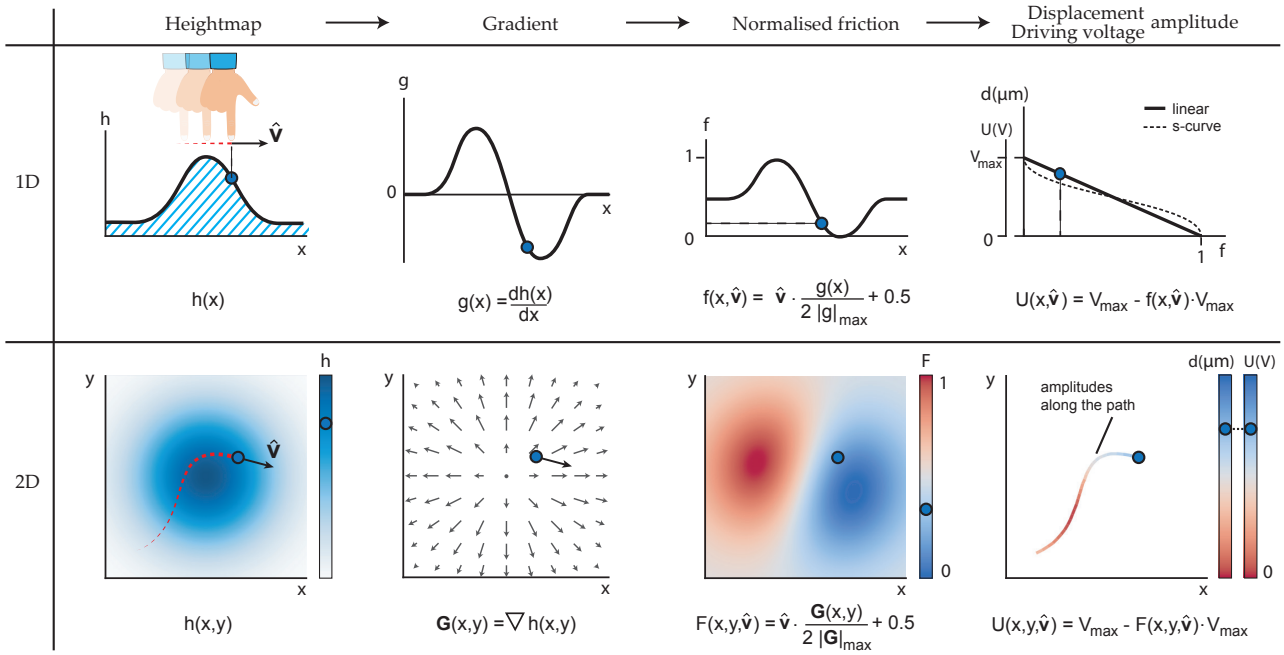

Fig. (2) Visualisation of the pseudo-potential haptic rendering method, for an one- and two-dimensional case. The unit velocity vector is multiplied by the gradient at the finger position. Normalising this to the driving signal range results in the rendering of a pseudo-potential field.

The advantages of haptic feedback are not limited to scenarios including multitasking. Surface haptic technologies are also implemented in target acquisition tasks. The performance during these tasks can be well related to Fitts' law, where the movement time to select a target is formulated as a function of the distance to, and size of the target [28]. By creating zones of high friction on a target and low friction elsewhere, it is shown that the feedback assists the user, essentially reducing the difficulty of the task [15]. The movement time was reduced with the addition of the friction modulation feedback, while maintaining similar accuracy. Also, the addition of haptic distractor targets did not adversely affect the targeting performance [15],[16]. Similar results are found using an electroadhesive technology [29].

All of the before mentioned research have in common that the friction modulation is only dependent on finger position and only provides binary feedback for when the user is on the target or not. However, a continuously evolving feedback principle is preferred for effective haptic feedback. To the best of the authors knowledge, no research is done towards improving tasks performance with a haptic rendering method, where the direction of movement is taken into account. This extra information layer can be of benefit to provide rich and continuous feedback. We propose to use a similar rendering principle as employed for rendering textures on touchscreens. As described by Kim et al., the position and direction of movement can be taken into account when rendering heightmaps of a texture [30].

3 Haptic Rendering Method

The haptic rendering of a pseudo-potential field is fundamentally different, by taking the direction of movement into account as well as the finger position, rather than just the finger position. With this extra information, the feeling of a force field can be generated, instead of just sections of high or low friction. Because on a friction modulated touchscreen no active lateral forces can be generated, the term 'psuedo' is included. Only friction forces opposite to the direction of movement are modulated.

3.1 Pseudo-potential field

The pseudo-potential field essentially acts as a force field on the finger. Moving with the direction of the force field is assisted by lowering the friction, while moving against the force field is impeded by generating a high friction. This way, a different friction coefficient is rendered at the same position, depending on the direction of movement. The method is best explained by the use of heightmaps, which are a type of potential field.

Starting with an one-dimensional case, as in figure 2. A potential function $h(x)$ is proposed across the screen size domain. The derivative, or gradient, $g(x)$ is calculated and normalised. The reason for the normalisation is to map the full range of gradient to the whole range of vibration amplitudes. The unit velocity vector of a user's finger sliding across the screen is measured (in the one dimensional example moving to the right ($\hat{v} = 1$) or moving to the left ($\hat{v} = -1$)). The unit velocity is multiplied by the gradient $g(x)$ at the position of the finger. This product provides

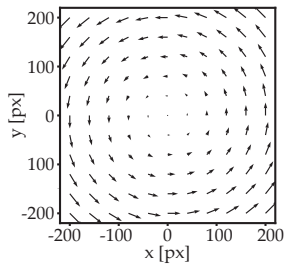

Fig. (3) Example of a non-conservative force field: $\boldsymbol{G}(x, y) = \langle -y, x \rangle$

the required friction, that needs to be rendered. The friction is inversely related to the displacement amplitude of the glass plate, thus the required friction needs to be converted to a displacement amplitude. For the sake of simplicity this is assumed to be linear, but the system can be easily adapted to other curves that are described in literature (such as s-shaped curves [9],[19]). The displacement amplitude is directly proportional to the driving voltage amplitude of the piezo electric actuators.

This rendering method is then converted into the two-dimensional case, where the heightmap function $h(x, y)$ is dependent on both x and y. The partial derivatives of this function, give the gradient function $\boldsymbol{G}(x, y)$. The dot product between the unit velocity vector and the gradient vector gives the scalar value of the rendered friction.

This analogy to a heightmap gives an easily understandable physical representation to the user, but this method is not limited to the construction of heightmaps. The gradient of a heightmap (scalar potential function) is an example of a conservative field. A simple example of a non-conservative field is $\boldsymbol{G}(x, y) = \langle -y, x \rangle$ resulting in an anti-clockwise vector field (see figure 3) which cannot be represented by a potential function [31]. Other vector fields can provide a wide range of interaction modes. Similar terms as in phase plane figures can be used to describe the vector (or gradient) fields, consisting of sinks, sources, spirals and saddlepoints.

By modelling several potential fields as simple sink points and paths, these individual elements can easily be added to provide complex combined vector fields. The individual elements can be assigned with specific weights according to their importance in the final interaction. The pseudo-potential field in the experiment consists of a combined point sink (equation 1) and path sink (equation 2). Adding both potential fields with equal weights results in a valley with a slope towards the target point, as depicted in figure 4. This rendering method is referred to as the heightmap condition.

$$H_{\text{Point}}(x, y) = \sqrt{\left(x - x_{\text{target}}\right)^2 + \left(y - y_{\text{target}}\right)^2} \tag{1}$$

$$H_{\text{Path}}(x, y) = \left| \frac{1}{a} \cdot tan^{-1}(a \cdot (y - y_{\text{path}}(x))) - (y - y_{\text{path}}(x)) \right| \tag{2}$$

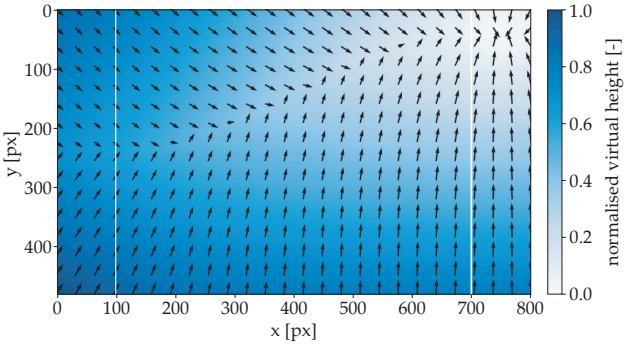

Fig. (4) Example of pseudo-potential field rendering with a combined point sink and path sink to the top right corner. Resulting in a valley with a slope towards the target point.

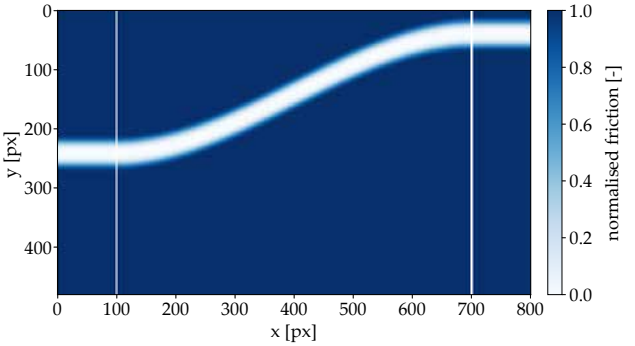

Fig. (5) Example of position based rendering where the white represents the low friction path to the top right.

3.2 Position based rendering

The position based rendering principle describes the rendered friction across the touchscreen with a scalar function $F(x, y)$, directly defining the required vibration amplitude for each finger position. This feedback principle is explored in earlier works for target acquisition [15],[16]. A target point is rendered to have high friction, while the surrounding area is rendered with low friction. The inverse of this rendering (low friction target, high friction elsewhere), has shown similar improvements in the interaction [15].

This principle is implemented in the position based condition, where the target path is rendered to have low friction and the surrounding area high friction. With this rendering method the user would explore the active area to find the low friction path, after which the low friction path would assist the user in moving towards the target. A resulting depiction of this principle is seen in figure 5. A smoothstep (sigmoid) function [32] is used to smooth the transition between the target path and the surrounding area. This method is referred to as the frictionmap condition in the rest of this paper.

4 MATERIALS

A haptic touchscreen test setup is developed for this experimental study. It utilizes the squeeze film principle generated by ultrasonic vibrations to modulate the friction on a glass plate. This plate is located above a 7 inch LCD screen. In this way, the visual feedback and haptic feedback coincides.

4.1 Hardware

The visual feedback is provided by the LCD screen, which is connected to a single-board computer (Raspberry Pi 4, Model B), which runs a Python program to provide the required visuals. The haptic feedback loop is controlled by a microcontroller (Teensy 3.6 Development Board), which is programmed using the Arduino IDE. The microcontroller is connected to a custom made PCB, which uses an AD9834 chip to generate the ultrasonic waveform. The frequency of this waveform is tuned once and the amplitude is actively modulated by the microcontroller during interaction. The output signal is pre-amplified using op-amps to a maximum of 10Vpp. This signal is sent to two external amplifiers (PiezoDrive PD200) with an amplification factor of 20. The signal is fed back into the housing, actuating the piezo electric actuators, which are glued to the glass plate.

Also connected to this PCB, via I^2C, is an optical position sensor (Neonode touch sensor module, NNAMC1581PCEV), which uses an array of infrared light to sense the position of objects, in this case a finger, in two dimensions. This device is located at the top of the glass plate and is positioned such that the active sensing plane is just above the glass surface. Lastly, four loadcells (CZL611CD) are mounted in the enclosure to which the glass plate is connected. In this way, the normal force on the glass plate can be measured. The loadcells are connected to four individual instrumental amplifiers on the PCB, which in turn send an analog signal to the microcontroller. The schematic of this device is seen in figure 6.

The main component of this system is the glass plate which is vibrating at its resonance frequency, resulting in a specifically designed banded (0;14) mode shape. The mode shape is chosen to have only horizontal nodal lines, which makes the amplitude in one dimension constant. It is recognised that the amplitude of the glass plate is not constant across the vertical dimension. However, due to the high resonance frequency the nodal lines are close together and because the contact area of the finger is relatively large this averages out the haptic effect.

With an analytical analysis, using Bernoulli beam theory [33], the length and width of the glass plate are chosen such that vertical dimension is at a resonance length, while the horizontal dimension is in between two resonance lengths. The mode shape across the resonance length is calculated using the formula for

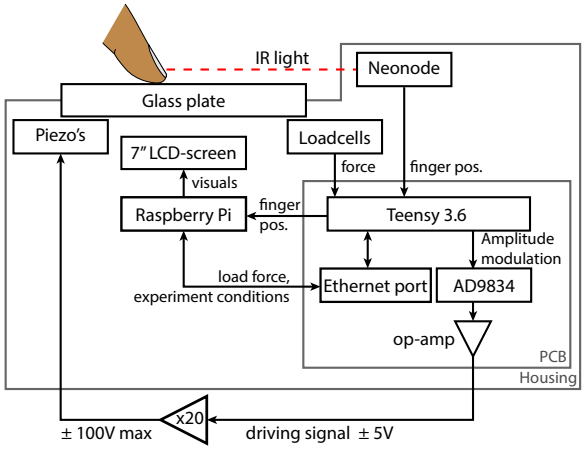

Fig. (6) Schematic overview of the haptic touchscreen. Haptic feedback is provided by actuation of the piezos. Finger position is sensed by an optical position sensor and the visual feedback is provided by a LCD screen connected to a Raspberry Pi.

a free-free beam [34]. From this formula the first and last anti-node is extracted providing the location of the piezos.

The piezo ceramic plates (SMPL26W8T07111) are selected such that the width of the elements is just below half the wavelength of the mode shape of the glass plate. The piezos are glued (using 3M Skotch-Weld DP490) on the bottom of the glass plate in two rows of six at the first and last anti-node. Each row of actuators is connected in parallel to one of the two external amplifiers. The polarities of the two circuits are opposite such that, with the same output signal of the PCB, the correct curvature of the mode shape is achieved.

The analytical calculations are confirmed using a finite element model in COMSOL. The glass plate and the piezo electric elements are modelled. A preliminary eigenfrequency search confirmed the expected mode shape. A second study, using a piezoelectric frequency sweep around the eigenfrequency, showed a spike in the total displacement of the top surface at a frequency of 42.5 kHz.

To aid the user in the interaction with the touchscreen, the LCD and glass plate are angled at 30 degrees with respect to the horizontal. As a result, the users do not have to lean forward or strain their neck in order to properly see the screen. Any offset in finger position and visual rendering due to the vertical distance between the surface of the glass plate and LCD is also minimised. Additionally the finger can be kept horizontally as well, while ensuring that the finger pad is in contact with the glass plate, instead of the more stiff tip of the finger.

4.2 Software

The system consists of two main building blocks, this being the visual feedback and the haptic feedback system. The haptic feedback loop is separated, because of the need of a high refresh rate. Rendering the visuals at this refresh rate was not possible with the hardware used.

4.2.1 Haptic feedback loop

The Arduino program on the microcontroller consists of three main functions (apart from initialisation). In the main loop, the communication with the Raspberry Pi (visual loop) is handled. It sends the finger position coordinates as cursor positions over the USB HID (Human Interface Devices) protocol, sends the normal force data over ethernet (UDP) and reads any incoming messages on the Ethernet port (WIZ820io). The UDP messages from the Raspberry Pi include the specific conditions that need to be rendered haptically. An interrupt function is executed when the Neonode position sensor indicates data is ready to be read out (at approx. 200 Hz). The finger position in x and y is communicated via I^2C to the microcontroller and stored. The last function is an internal interrupt function running at 2000Hz, which takes the most recent and previous position data to linearly extrapolate the finger position. This is followed by a 1 euro filter [35], which is a first order low-pass filter with an adaptive cutoff frequency, based on velocity. The output signal for the piezo elements is also calculated in this loop, based on the finger position and velocity, as well as the requested feedback condition, according to the haptic rendering method described in section 3.

4.2.2 Visual feedback loop

The visual feedback loop is programmed in Python and executed on a Raspberry Pi single-board computer. The loop is refreshed at 80 Hertz and includes the rendering of visual elements. This is done by taking advantage of the pygame library. The specific conditions needed for the experiment are communicated with UDP messages to the microcontroller. The data acquisition is handled by the python program as well. For the duration of each trial the timestamp, finger position and normal force are stored, as well as summary metrics for each trial.

4.3 Validation/characterisation

The working principles of the haptic touchscreen are validated and the response of the glass plate is measured. The displacement amplitude of the glass plate surface is measured with the use of a laser interferometer (Polytec OFV505), controlled with a vibrometer controller (Polytec OFV5000).

First of all, the eigenfrequency is checked by sending a frequency sweep signal (25kHz to 70kHz in 30 seconds at an amplitude of 20V) to the actuators using a function generator (Tektronix AFG 1062). The resulting frequency response results in several local maxima corresponding to different eigenmodes. These eigenmodes are confirmed by actuation of the system at the found frequencies and placing fine grained salt on the glass plate. The nodal lines, that become visible due to the accumulation of the salt, are counted to find the mode number. The designed (0;14) mode is found at 46.4 kHz, but the actuation of the plate at the (0;12) mode with a frequency of 34.9 kHz resulted in higher displacement amplitudes. Consequently the test setup is used with at the latter frequency.

This experiment is followed by the actuation of the system using a modulating ramp -up and -down (from 0V to 100V and back in 5 seconds) signal. This is used to confirm the linearity of the system and to find the peak vibration amplitude. A maximum displacement amplitude of 5 micrometer is measured at the maximum actuation amplitude of 100V. The experiment showed that this actuation voltage is within the linear regime of the piezos.

Lastly, the glass plate and its components are connected in the final setup. A step-up and -down signal is initiated by the microcontroller and the amplitude response is measured. The results show a 5%-rise time of 6.3 ms and a 5%-fall time of 7.6 ms.

5 Experiment

In the human factors experiment, the two conditions (heightmap and frictionmap) are presented to the participants and resulting metrics are analysed to find which haptic rendering method is best suited for guiding users to a specific target. The system provides the feedback, such that the subjects are guided to one of three possible targets, as well as the paths leading to these targets. The visuals are as presented in figure 7. This design is used to test the perception and thus effectiveness of the different haptic feedback conditions in a task where two dimensional movement is needed.

Twenty-two Participants were recruited to participate in the experiment: aged 22-65 (mean: 29, SD: 11), 20 right handed, 16 male/ 6 female. Before the start of the experiment, the participant information letter is read by, or to, the participant, briefly explaining the technology and the procedure of the experiment. Written informed consent is obtained from each participant hereafter. Before starting the experiment, the participant is asked to thoroughly clean their hands with water and soap and dry their hands. The glass plate is cleaned with isopropyl alcohol before each experiment.

The experiment took place in a closed room in which participants were seated in front of the touchscreen. They were able to adjust the height of the office chair and reposition the touchscreen to a comfortable position. The two amplifiers were on the far edge of

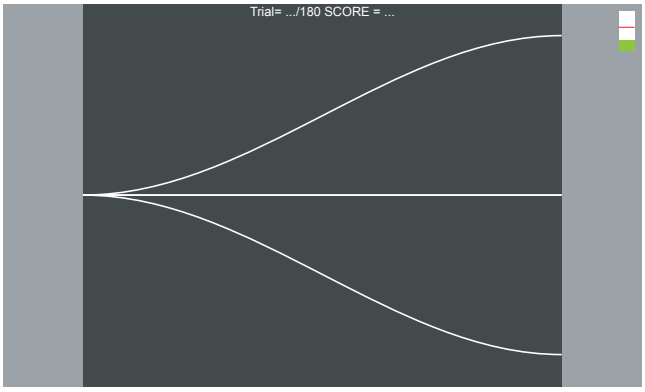

Fig. (7) Visual feedback as presented to the participant at the start of each trial.

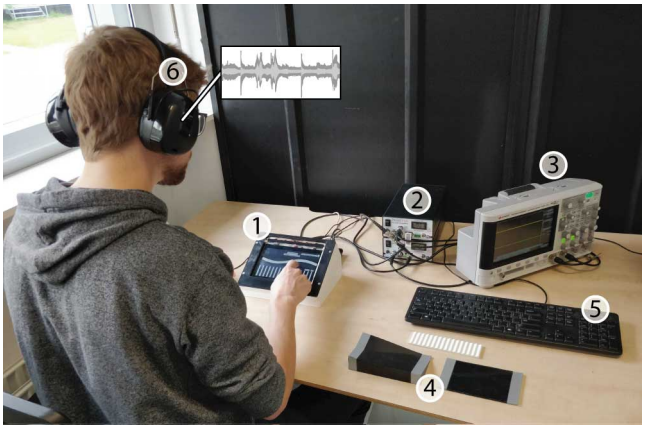

Fig. (8) Experimental setup in a closed room, with: (1) haptic touchscreen, (2) amplifiers, (3) oscilloscope, (4) 3D printed models, (5) keyboard and (6) headphones playing a combination of white noise and music.

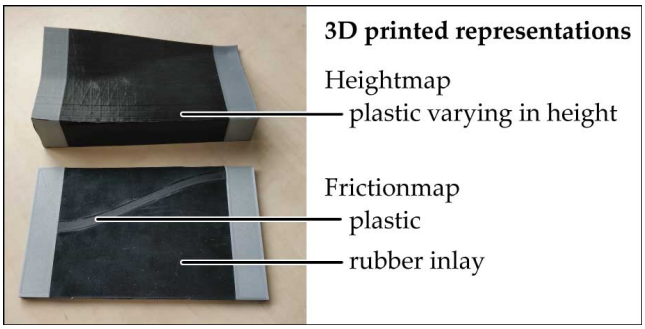

Fig. (9) Physical representation of the heightmap and frictionmap, presented to the participants to get familiar with the working principles.

the table and an oscilloscope was used to confirm that the system was working as intended. The screen of the oscilloscope was only visible to the experimenter. The general setup is depicted in figure 8. The haptic touchscreen is inspected by the safety manager of the faculty of Mechanical Engineering at the TU Delft and the experimental procedure is approved by the ethics committee of the TU Delft.

Before the main trials, the participant is presented with a familiarisation phase to experience the working principle of the touchscreen, because this is something the participants are not used to. During this phase, a representation of a winding path with low friction surrounded by high friction, as well as a sinusoidal heightmap is rendered. This exemplified the working principle of the two conditions tested later during the experiment. Besides the touchscreen, several physical 3D-printed models where available to explore (figure 9). These models represented the physical principles of the rendering methods and made it easier for the participant to grasp the different rendering techniques. The familiarisation screen also included a normal force indicator, which turned red at a normal force above 0.5 N, to let participants know that only a small normal force is required. This force indicator was visible throughout the experiment but did not enforce any re-trials if the force was exceeded. The experimenter paid close attention to the exerted force, and provided feedback if needed.

During the whole procedure, the participant is wearing passive noise canceling headphones (3M Peltor Wortunes Pro, SNR=32 dB). Additionally, a mix of white noise and music is playing on these headphones (at an average sound level of 60 dBA, measured by Sauter SU130 sound level meter). This is required to limit any auditory feedback emitted by the actuation of the haptic system. Although special care is taken to limit the emission of the auditory frequencies, the headphones provide that the haptic feedback is the only feedback modality. During pilot experiments it was evident that white noise only could not mask the transient noises from the touchscreen, hence the addition of music.

The main experiment is presented to the participants in two parts, with a forced break in between, as well as halfway the two conditions. The two feedback conditions are presented in two separate blocks. The order in which they are presented is counterbalanced. The full experiment consists of 2x3x3x10 = 180 trials. This being; 2 feedback conditions ($heightmap, frictionmap$), 3 vibration amplitudes ($1.65, 3.3, 5 \mu m$), 3 target positions ($top, middle, bottom$) and 10 repetitions for each condition. The trials are presented in randomised order within the 2 sets of haptic feedback conditions.

The amplitudes of the ultrasonic vibrations are varied in order to relate the resulting hit rates to psychological curves. The haptic strength is varied by changing the range of the possible vibration amplitudes. Instead of just lowering the maximum amplitude, the range is scaled around its center point. The three scales are chosen to be 1, 0.66 and 0.33 of the maximum achievable driving voltage of the system. These haptic percentages correspond to the following driving voltage amplitude ranges: $[0, 100]$,

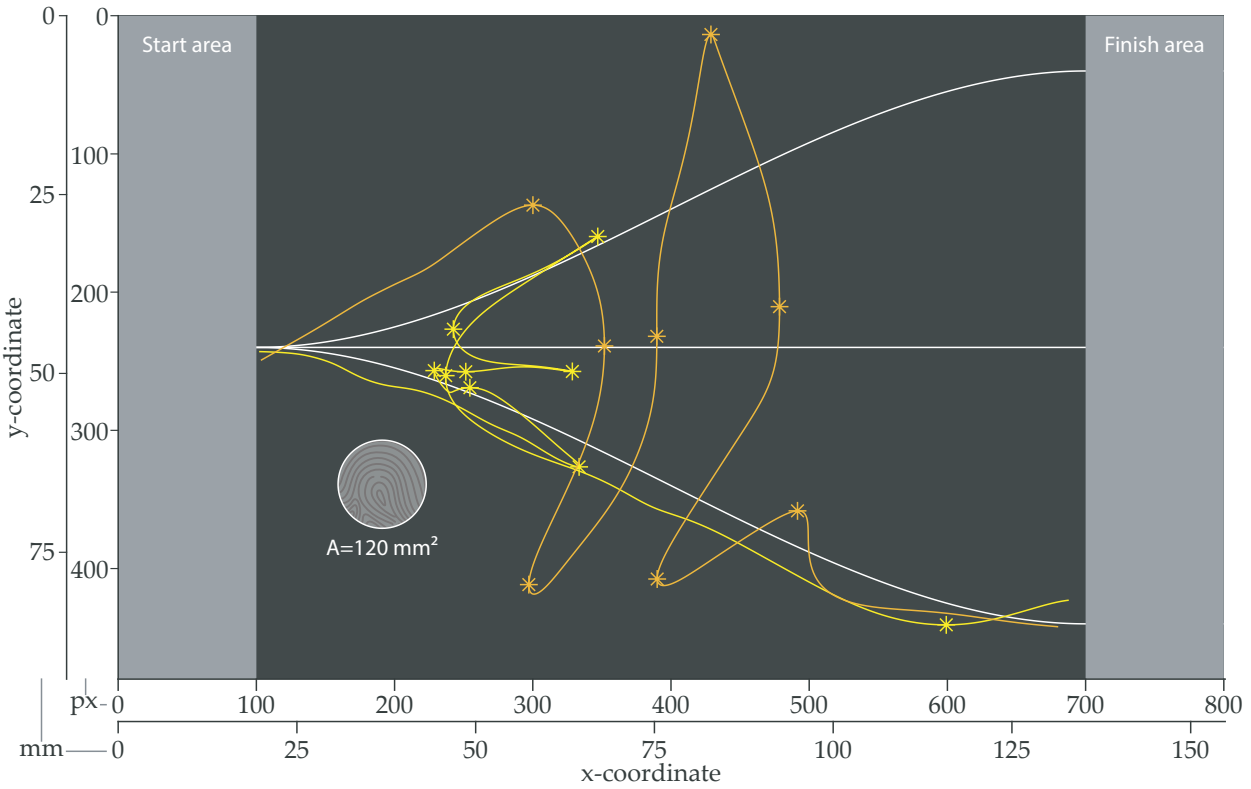

Fig. (10) Typical position data visualise the two main strategies: movement back and forth along the three different paths (yellow) and trajectories perpendicular to the paths (orange). On the trajectories, the direction changes are indicated with a star. The white circle represents the approximate index finger size. When printed on A4, the image is true to size.

$[17, 83]$ and $[33.5, 66.5]$ V respectively. The steady-state, free-air vibration amplitudes at the central anti-node are measured with the laser interferometer and have corresponding displacement amplitude ranges (ΔA) of $5\mu m$, $3.3\mu m$ and $1.65\mu m$.

The participants are instructed to explore the touch-screen with their index finger, in any way they felt fit. When they were convinced in knowing where the haptic feedback was trying to guide them, the participant could lock in the decision by moving to a target position on the right side of the screen. Hereafter, the correctness of their choice was visually represented by a red or green bar. On top of that, the correct target is visualised by an image of a cookie. Throughout the experiment the score (amount of correct answers) is visualised at the top of the screen. The participants were encouraged to find as many targets (cookies) as possible. The self-paced trails are started by moving the finger to a circle on the left side of the screen. The time needed to complete all trails was between 13 and 49 minutes (mean: 26, SD: 10), excluding pre-planned and participant induced breaks.

The results of this experiment are used to test the null-hypothesis that the hit-rate is equal for both haptic feedback conditions, with the alternative hypothesis that one condition results in a higher hit-rate than the other. Additionally, it is tested whether the completion time of acquiring the target is equal for both haptic feedback conditions.

6 Results

The raw data of each trial is analysed and any large jumps in the finger position data are flagged. These trials are manually reviewed and removed from the further analysis when data errors were present. From the 3960 trials, 51 trials are removed due to data errors or the presence of another finger in the sensing plane.

In figure 10, typical trial data is visualised. The visuals are the same as presented to the participant; a solid black background with light grey start and end zones, together with the three possible paths visualised by white lines. Included in the figure but not visible to the user are the typical finger trajectories and the indication of index fingertip size (apparent contact area of $120mm^2$ [36]).

6.1 Hit rates

For each participant the hit rate for the different conditions is visualised in figure 11. A two-way repeated-measures ANOVA revealed that there is a significant main effect of vibration amplitude ($F_{2,40} = 37.0, p < 0.001$) with increasing hit rate for the three vibration amplitudes: $1.65\mu m$ (Mean=0.53, SD=0.02), $3.3\mu m$ (Mean=0.67, SD=0.03) and $5\mu m$ (Mean=0.73, SD=0.03). Post hoc Bonferroni adjusted pairwise comparisons show significant differences between any combination of the three vibration amplitudes ($p < 0.02$).

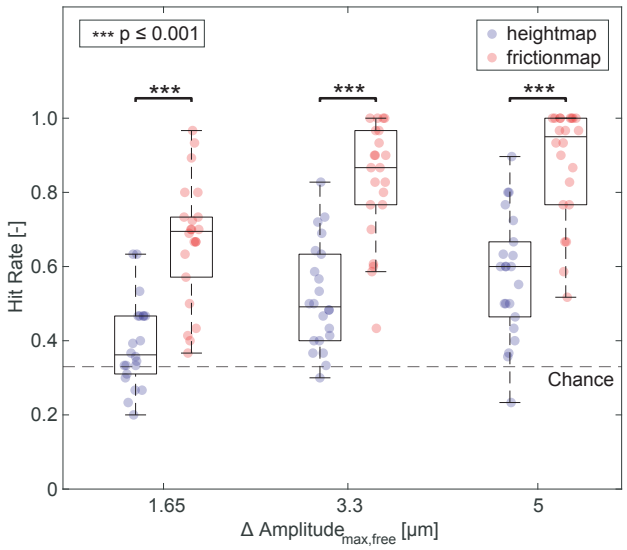

Fig. (11) Hit rates for the heightmap (blue) and frictionmap (red) at the three free-air vibration amplitudes.

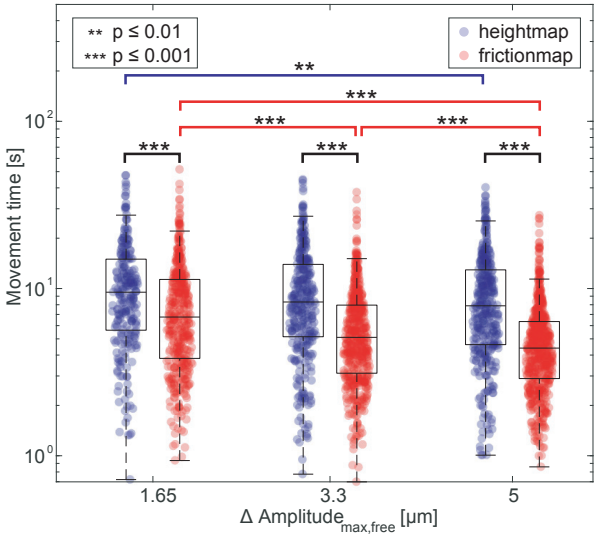

Fig. (12) Movement times for each correctly answered trial, for both the heightmap (blue) and frictionmap (red) conditions at the three free-air vibration amplitudes.

Additionally, a significant main effect of haptic condition is found ($F_{1,20} = 87.1, p < 0.001$), with higher hit rates for the frictionmap condition (Mean=0.79, SD=0.03) than the heightmap condition (Mean=0.49, SD=0.02). This effect is also found when comparing the two conditions for each vibration amplitude using the Wilcoxon signed rank test, as indicated in figure 11.

In contrast, no significant interaction was found between the independent variables ($F_{2,40} = 0.4, p > 0.05$).

6.2 Movement time

Besides the hit rates, also the movement times are analysed. As the participants were instructed to take as much time as needed to make a confident decision, the movement time reflects how difficult it is to grasp the different haptic feedback conditions. The movement time is defined by the time difference between leaving the left start area and the moment a target is selected by moving into the right end-area. In figure 12 the movement times for each correctly answered trial are visualised. The distributions of the movement times are not normally distributed and exhibit positive skewness, as can be expected with the metric of completion time. Statistical analysis using the Wilcoxon signed rank test indicates significant differences between the two feedback conditions at each vibration amplitude. A two-way repeated measures ANOVA with Greenhouse-Geisser correction on the average movement times revealed a significant main effect on both the vibration amplitude ($F_{1.4,27.2} = 10.9, p = 0.001$) and the haptic condition ($F_{1,20} = 19.5, p < 0.001$). However, only for the frictionmap condition the medians are significantly different across all vibration amplitudes, whereas movement times for the heightmap condition are only significantly different between the lowest and highest haptic strength level (1.65 and $5\mu m$ vibration amplitude) as indicated in figure 12.

6.3 Direction Changes

The required amount of searching to make a decision is captured in the metric of amount of direction changes. This value is calculated in a similar fashion to the steering reversal method [37], but extended to include two dimensions. Both the x and y positions are filtered using a low-pass, second-order Butterworth filter with a cut-off frequency of 2Hz. The stationary points (local minima and maxima) are classified where the first order derivative of the position data (velocity) is either zero, or about to cross zero. A threshold of minimum 10 pixels ($\approx 2mm$) is used for a stationary point to be classified as an unique reversal. The reversals in x and y are added to find the total number of direction changes. However, a simultaneous reversal in x and y is considered as a single direction change, with an absolute distance threshold of 15 pixels ($\approx 3mm$). The values for the filter and thresholds are tuned manually by analysing the raw data. The points of direction changes are also indicated in figure 10.

Analysis on the average direction changes per participant, using two-way repeated measures ANOVA shows a significant effect of vibration amplitude ($F_{2,40} = 10.9, p < 0.001$) and the haptic condition ($F_{1,20} = 12.6, p = 0.002$). Significant differences on all combined datapoints, using the Wilcoxon signed

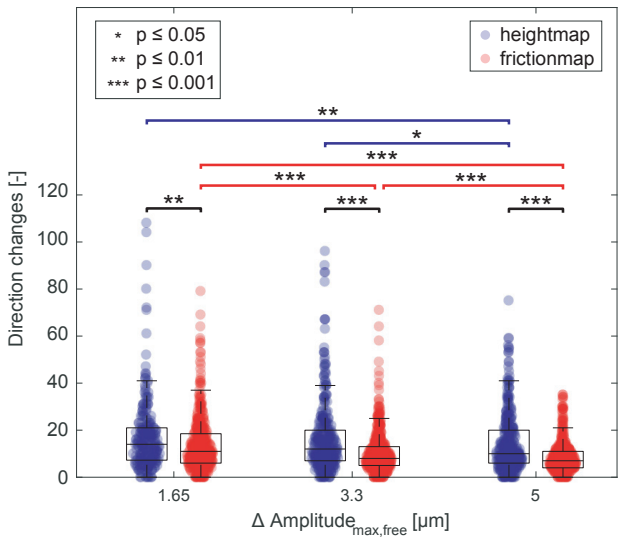

Fig. (13) Amount of direction changes for each correctly answered trial, for both the heightmap (blue) and frictionmap (red) conditions at the three free-air vibration amplitudes.

rank test are indicated in figure 13. It is observed that the amount of searching needed, reduces with the increasing vibration amplitudes.

6.4 Movement strategies

As observed during the experiment and as seen in the typical trial data (figure 10), two main strategies are present. To classify these strategies the movement direction angle for both conditions is analysed. The total number of observations of the movement directions for all participants are plotted in a histogram seen in figure 14. The main movement direction for both the conditions is to the right, which is expected due to the start position being on the left and the targets on the right. However, the vertical movement direction for the heightmap condition is more prominent than for the frictionmap condition. In contrast, the movement direction in the frictionmap condition has more occurrences along the paths.

6.5 Learning effect

No significant effect is reported on the hit rate with respect to the order in which the conditions are presented to the participant ($F_{1,20} = 2.07, p > 0.05$). This also holds true for the effect of condition order on the average movement times ($F_{1,20} = 0.015, p > 0.05$) and on the number of direction changes ($F_{1,20} = 0.014, p > 0.05$). These tests indicate that the condition order does not influence the metrics by transfer of any learning effects that may be present.

Any learning within the conditions is analysed as well. Figure 15 shows the learning in terms of hit rate as well as movement time. Each of the two haptic

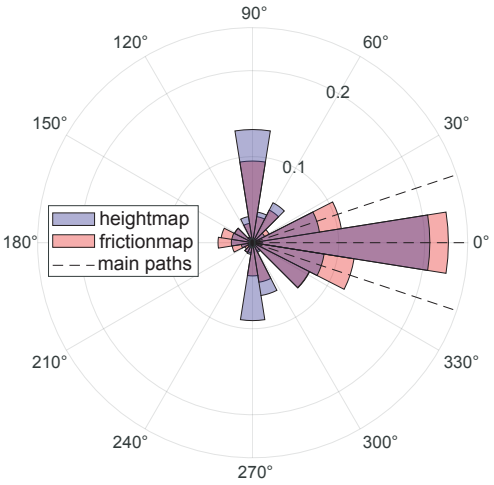

Fig. (14) Normalised histogram of the movement angle of all participants for the two feedback conditions. The dashed lines indicate the main angles of the three possible paths.

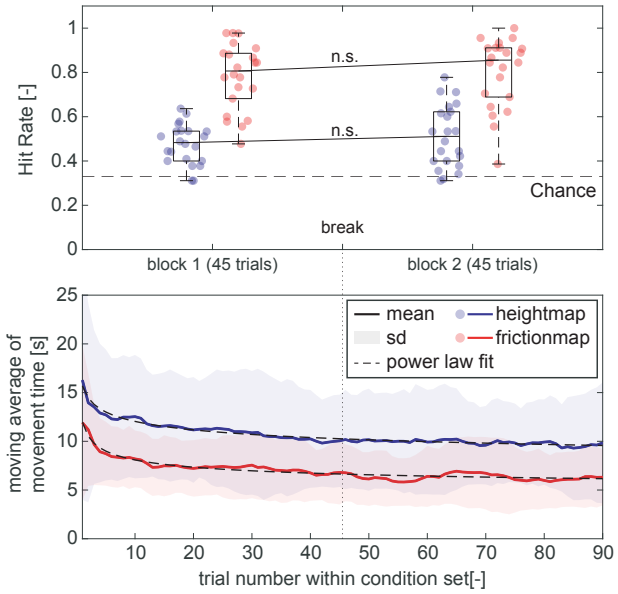

Fig. (15) Visualisation of learning effects within the two feedback conditions: Heightmap (blue) and Frictionmap (red). Top graph shows the proportion of correct responses for each block of 45 trials. Bottom graph shows the moving average of the movement times (with a window of 10 trials). Solid line represents the mean of all participants and the shaded area represents the standard deviation.

conditions is presented to the participant in 2 blocks. The hit rates for each of the two blocks are visualised. Testing the difference between the two blocks for each condition, using the Wilcoxon signed rank test, shows no significant effect for both the heightmap ($p = 0.18$) and the frictionmap ($p = 0.24$).

A moving average of the movement times is calculated for each participant using a window of 10

trials. The resulting mean and standard deviation is presented in the figure. The learning curves of the movement time can be characterized with a power law function ($y(x) = a \cdot x^{-b} + c$). This curve fitting is typical for tasks where learning is present [38]. By analysing the coefficients of the power law function the learning is characterised. The movement time at the beginning is given by $a + c$. How quickly the performance is improved is reflected by b. Finally the plateau is given by the coefficient c. The participants show longer movement times at the beginning for the heightmap condition with respect to the frictionmap condition ($a+c = 15.7$ and 12.0 respectively), but with a similar plateau value ($c = 3.3$ and 4.0 respectively). The decrease in movement, however, is faster for the frictionmap condition ($b = 0.29$) than for the heightmap condition ($b = 0.15$).

7 Discussion

Participants are able to perceive the haptic guidance on a friction modulated touchscreen and find the correct target with an average hit-rate of 0.57 for the pseudo-potential field feedback and 0.88 for the position based feedback. These hit-rates are achieved at the maximum free-air vibration amplitude of $5\mu m$. With lower vibration amplitudes (and thus lower haptic strength), the performance decreases for both conditions similar to what would be expected according to psychometric curves [39].

Moreover, the position-based feedback secures not only a higher hit-rate, but also achieves this with lower movement times. Some learning is present in this metric, but the shape of these learning curves for the two conditions is similar, albeit with an offset.

Both hypothesis regarding the equality of the proportion of correct responses and the movement time for the two haptic rendering methods are rejected. The alternative hypothesis is accepted that the position based rendering method is better suited than the pseudo-potential field method in guiding users to a specific target with higher hit rates and lower movement times.

Interestingly, the exploration tactics employed by the participants during the experiment are different for the two haptic rendering methods. More movement is observed along the possible target paths for the position-based method, while the movement perpendicular to these paths is more prominent in the pseudo-potential field rendering method. This entails that the direction in which the haptic information is most easily gathered is different. This additional result has to be taken into account when designing for control principles on touchscreens.

It has to be stated that the experiment tests the perception of the two haptic rendering methods. This is different than a target acquisition task in the fact that the user and automation would share a common goal. The subjects did not have an a priori target, but were asked to find the target initiated by the touchscreen. This perception of the intentions of the automation is only a part of the control loop. Transfer of the rendering principles to some sort of shared control task might result in different findings.

Additionally, a strong haptic interface is preferred in haptic assistance, but the mechanical aspect of this interaction principle might have a limited influence on the trajectory of the human finger. It is believed by Casiez et al. that, for a target acquisition task and position based rendering, the "system mainly provides information feedback and little or no mechanical effect"[15]. While in fact, the reduction in friction is shown by others [9]. A stronger haptic interaction principle is preferred but any device that modulates friction is limited by the fact that the feedback is only perceived on a moving finger. Meaning only the force opposite of the movement direction can be manipulated. Additionally, the friction force depends on the normal force, which is difficult to regulate and assumed to be constant to render the effects. Other tribological factors (such as sweat or humidity) add further noise to any rendered patterns. It is also found that subjects' perception of change in friction is reduced with lower spatial friction slopes (rate of change in tangential force) [12]. For both of the rendering principles, only a localised high spatial friction slope is present with slow (or no) changes elsewhere on the screen.

Research being done in active force feedback using travelling waves or combinations of standing and lateral vibrations shows that it is possible to provide forces lateral to the movement direction, as well as providing forces when the finger is static [26],[40],[41],[42]. It is hypothesised that, in this field of active haptic surfaces, the principles of the pseudo-potential field rendering method do provide to be useful. Especially in utilising haptic shared control principles to assist the user in interacting on touchscreen interfaces, because active forces can be applied to the user by the automation system. Further research in using the potential field rendering method on surface haptic devices, capable of providing active forces is recommended.

In the experiment, only a single design of each haptic rendering principle is explored, albeit at different vibration amplitude ranges. Many other parameters can be changed to conform to different kinds of interaction and haptic stimuli. As illustrated in figure 16, the haptic feedback can be implemented in many different human-machine interactions. This includes, but is not limited to, the tactical level shared control of a highly automated vehicle, typing assistance on touchscreens using swipe gestures and immersive gaming experiences on touchscreen devices.

To test the full potential of the haptic feedback on surface haptic touchscreens, it is recommended

Fig. (16) Concept applications for shared control in touchscreens for assistance in typing or haptic shared control in highly automated vehicles.

to research the added benefit of the haptic cues in multi-tasking. Testing different feedback modalities and combinations of feedback modalities, while attention is shared could yield interesting insights. As mentioned before, the implementation of potential fields on surface haptic devices with directional force feedback can prove to be even more beneficial and intuitive. Further research in this field is highly recommended.

8 Conclusion

The use of a pseudo-potential field rendering method on surface-haptic touchscreens is proposed. By taking the direction of finger movement into account, haptic feedback with directional cues can be provided. This method is compared to a position-based method in a study in which subjects had to find a specific target path. Both the position based and the pseudo-potential field rendering method can lead users to a specific target with haptic information. However, it is found that, with the current setup, the pseudo-potential field rendering method is less suited for finding target paths than a position based rendering method. The proportion of correct responses is higher for the position-based method, and movement times lower. Additionally, this higher performance required lower vibration amplitudes.

It is observed that the two rendering methods also result in a different searching strategy. More movement along the possible paths is seen in the position based rendering method, while more movement perpendicular to the paths is seen in the pseudo-potential field method. These strategies have to be taken into account when implementing such system in a haptic shared control task.

Using friction modulation for rendering a pseudo-potential field limits the richness of the feedback. Only friction forces opposite to the finger movement can be modulated. For a true potential field rendering method, there is a need of active lateral forces on the finger, even when it is static. It is hypothesised that technologies in active haptic feedback are able to take this rendering method, and its applications in haptic shared control on touchscreens, to a higher level.

Acknowledgments

This project has benefited from contributions of many individuals. I'm extremely grateful for the help of Dr. Michaël Wiertlewski, Prof. Dr. David Abbink and Dr. Barys Shyrokau and their insights during meetings. Thanks should also go to the many participants that took their time to provide valuable results, used in this study. Special thanks to ir. Ehsan Hoseini, for his work on the pcb design.

References

[1] A. Rydström, P. Bengtsson, C. Grane, R. Broström, J. Agardh, and J. Nilsson, "Multifunctional systems in vehicles: a usability evaluation," in Proceedings of CybErg 2005. The Fourth International Cyberspace Conference on Ergonomics. International Ergonomics Association Press, 2005, pp. 768–775. [Online]. Available: https://www.diva-portal.org/smash/record.jsf?pid=diva2%3A1010799&dswid=-7631

[2] M. Fukumoto and T. Sugimura, "Active click: Tactile feedback for touch panels," Conference on Human Factors in Computing Systems - Proceedings, pp. 121–122, 2001.

[3] E. Tunca, I. Zoller, and P. Lotz, "An investigation into glace-free operation of a touchscreen with and without haptic support in the driving simulator," in Proceedings - 10th International ACM Conference on Automotive User Interfaces and Interactive Vehicular Applications, AutomotiveUI 2018. Association for Computing Machinery, Inc, 9 2018, pp. 332–340. [Online]. Available: https://dl.acm.org/doi/abs/10.1145/3239060.3239077

[4] J.-H. Lee and C. Spence, "Assessing the Benefits of Multimodal Feedback on Dual-Task Performance under Demanding Conditions," in BCS-HCI '08: Proceedings of the 22nd British HCI Group Annual Conference on People and Computers: Culture, Creativity, Interaction, 9 2008, pp. 185–192. [Online]. Available: https://dl.acm.org/doi/10.5555/1531514.1531540

[5] S. J. Lederman and R. L. Klatzky, "Extracting object properties through haptic exploration," Acta Psychologica, vol. 84, no. 1, pp. 29–40, 10 1993.

[6] J. A. Pruszynski, R. S. Johansson, and J. R. Flanagan, "A Rapid Tactile-Motor Reflex Automatically Guides Reaching toward Handheld Objects," Current Biology, vol. 26, no. 6, pp. 788–792, 3 2016.

[7] M. Wiertlewski, D. Leonardis, D. J. Meyer, M. A. Peshkin, and J. E. Colgate, "A High-Fidelity Surface-Haptic Device for Texture Rendering on Bare Fingers," International Conference on Human Haptic Sensing and Touch Enabled Computer Applications, pp. 241–248, 2014.

[8] M. Biet, F. Giraud, and B. Lemaire-Semail, "Squeeze film effect for the design of an ultrasonic tactile plate," in IEEE Transactions on Ultrasonics, Ferroelectrics, and Frequency Control, vol. 54, no. 12, 12 2007, pp. 2678–2688.

[9] M. Wiertlewski, R. F. Friesen, and J. E. Colgate, "Partial squeeze film levitation modulates fingertip friction," Proceedings of the National Academy of Sciences of the United States of America, vol. 113, no. 33, pp. 9210–9215, 8 2016. [Online]. Available: www.pnas.org/cgi/doi/10.1073/pnas.1603908113

[10] T. Sednaoui, E. Vezzoli, B. Dzidek, B. Lemaire-Semail, C. Chappaz, and M. Adams, "Friction Reduction through Ultrasonic Vibration Part 2: Experimental Evaluation of Intermittent Contact and Squeeze Film Levitation," IEEE Transactions on Haptics, vol. 10, no. 2, pp. 208–216, 4 2017.

[11] C. Bernard, J. Monnoyer, and M. Wiertlewski, "Harmonious textures: The perceptual dimensions of synthetic sinusoidal gratings," Haptics: Science, Technology, and Applications 11th International Conference, EuroHaptics, pp. 685–695, 2018.

[12] M. K. Saleem, C. Yilmaz, and C. Basdogan, "Tactile Perception of Virtual Edges and Gratings Displayed by Friction Modulation via Ultrasonic Actuation," IEEE Transactions on Haptics, vol. 13, no. 2, pp. 368–379, 4 2020.

[13] M. Biet, G. Casiez, F. Giraud, and B. Lemaire-Semail, "Discrimination of virtual square gratings by dynamic touch on friction based tactile displays," Symposium on Haptics Interfaces for Virtual Environment and Teleoperator Systems 2008 - Proceedings, Haptics, pp. 41–48, 2008.

[14] C. Bernard, J. Monnoyer, S. Ystad, and M. Wiertlewski, "Eyes-Off Your Fingers: Gradual Surface Haptic Feedback Improves Eyes-Free Touchscreen Interaction," CHI Conference on Human Factors in Computing Systems, pp. 1–10, 4 2022. [Online]. Available: https://dl.acm.org/doi/10.1145/3491102.3501872

[15] G. Casiez, N. Roussel, R. Vanbelleghem, and F. Giraud, "Surfpad: Riding Towards Targets on a Squeeze Film Effect," in CHI '11: Proceedings of the SIGCHI Conference on Human Factors in Computing Systems, 2011, pp. 2491–2500. [Online]. Available: https://doi.org/10.1145/1978942.1979307

[16] V. Levesque, L. Oram, K. MacLean, A. Cockburn, N. D. Marchuk, D. Johnson, J. E. Colgate, and M. A. Peshkin, "Enhancing physicality in touch interaction with programmable friction," in Proceedings of the SIGCHI conference on human factors in computing systems, 2011, pp. 2481–2490. [Online]. Available: https://doi.org/10.1145/1978942.1979306

[17] T. Watanabe and S. Fukui, "Method for controlling tactile sensation of surface roughness using ultrasonic vibration," Proceedings - IEEE International Conference on Robotics and Automation, vol. 1, pp. 1134–1139, 1995.

[18] D. J. Meyer, M. Wiertlewski, M. A. Peshkin, and J. E. Colgate, "Dynamics of ultrasonic and electrostatic friction modulation for rendering texture on haptic surfaces," IEEE Haptics Symposium, HAPTICS, pp. 63–67, 2014.

[19] L. Winfield, J. Glassmire, J. E. Colgate, and M. Peshkin, "T-PaD: Tactile pattern display through variable friction reduction," Proceedings - Second Joint EuroHaptics Conference and Symposium on Haptic Interfaces for Virtual Environment and Teleoperator Systems, World Haptics 2007, pp. 421–426, 2007.

[20] E. Mallinckrodt, A. Hughes, and W. Sleator, "Perception by the Skin of Electrically Induced Vibrations," Science, vol. 118, no. 3062, pp. 227–278, 1953. [Online]. Available: https://www.jstor.org/stable/1680528?seq=2

[21] F. Giraud, M. Amberg, and B. Lemaire-Semail, "Merging two tactile stimulation principles: Electrovibration and squeeze film effect," World Haptics Conference, WHC 2013, pp. 199–203, 2013.

[22] C. Shultz, M. Peshkin, and E. Colgate, "Surface Haptics via Electroadhesion: Expanding Electrovibration with Johnsen and Rahbek," IEEE World Haptics Conference, 2015.

[23] O. Bau, I. Poupyrev, A. Israr, and C. Harrison, "TeslaTouch: Electrovibration for touch surfaces," UIST 2010 - 23rd ACM Symposium on User Interface Software and Technology, pp. 283–292, 2010. [Online]. Available: http://tuio.org

[24] C. Basdogan, F. Giraud, V. Levesque, and S. Choi, "A Review of Surface Haptics: Enabling Tactile Effects on Touch Surfaces," pp. 450–470, 7 2020.

[25] A. Costes, F. Danieau, F. Argelaguet, P. Guillotel, and A. Lécuyer, "Towards Haptic Images: A Survey on Touchscreen-Based Surface Haptics," IEEE Transactions on Haptics, vol. 13, no. 3, pp. 530–541, 7 2020.

[26] J. Mullenbach, M. Blommer, M. Peshkin, P. Buttolo, R. Curry, R. Swaminathan, S. Hopkins, J. Greenberg, T. Dalka, and L. Tijerina, "Reducing Driver Distraction with Touchpad Physics," Master's thesis, Northwestern Univ., Evanston, IL, USA, Tech. Rep., 2013. [Online]. Available: https://robotics.northwestern.edu/documents/publications/Mullenbach_Masters_Thesis_Final.pdf

[27] F. Beruscha, W. Krautter, A. Lahmer, and M. Pauly, "An evaluation of the influence of haptic feedback on gaze behavior during in-car interaction with touch screens," in 2017 IEEE World Haptics Conference, WHC 2017. Institute of Electrical and Electronics Engineers Inc., 7 2017, pp. 201–206. [Online]. Available: https://ieeexplore.ieee.org/document/7989901

[28] P. M. Fitts, "The information capacity of the human motor system in controlling the amplitude of movement," Journal of Experimental Psychology, vol. 47, no. 6, pp. 381–391, 1954.

[29] Y. Zhang and C. Harrison, "Quantifying the targeting performance benefit of electrostatic haptic feedback on touchscreens," in Proceedings of the 2015 ACM International Conference on Interactive Tabletops and Surfaces, ITS 2015. Association for Computing Machinery, Inc, 11 2015, pp. 43–46.

[30] S. C. Kim, A. Israr, and I. Poupyrev, "Tactile rendering of 3D features on touch surfaces," UIST 2013 - Proceedings of the 26th Annual ACM Symposium on User Interface Software and Technology, pp. 531–538, 2013. [Online]. Available: http://dx.doi.org/10.1145/2501988.2502020

[31] J. Stewart, R. Minton, and Z. Rafhi, Calculus: Early Transcendentals, international edition, 7th ed. Brooks/Cole Cengage Learning, 2011.

[32] D. S. Ebert, F. K. Musgrave, D. Peachey, K. Perlin, and S. Worley, Texturing & modeling : a procedural approach, 3rd ed. Morgan Kaufmann, 2003.

[33] D. J. Inman, Engineering Vibration International Edition, 4th ed. Pearson, 2014.

[34] R. D. Blevins, Formulas for natural frequency and mode shape. New York: Van nostrand reinhold company, 1979.

[35] G. Casiez, N. Roussel, and D. Vogel, "1€ Filter: A simple Speed-based Low-pass Filter for Noisy Input in Interactive Systems," in CHI'12, the 30th Conference on Human Factors in Computing Systems,, 2012, pp. 2527–2530. [Online]. Available: https://hal.inria.fr/hal-00670496/document

[36] X. Liu, M. J. Carré, Q. Zhang, Z. Lu, S. J. Matcher, and R. Lewis, "Measuring contact area in a sliding human fingerpad contact," Skin Research and Technology, vol. 24, no. 1, pp. 31–44, 2 2018.

[37] SAE, "SAE Operational Definitions of Driving Performance Measures and Statistics," pp. 131–134, 2015.

[38] A. Newell and P. S. Rosenbloom, "Mechanisms of skill acquisition," Cognitive skills and their acquisition, pp. 1–55, 1981.

[39] F. A. Wichmann and F. Jäkel, "Methods in Psychophysics," in Stevens' Handbook of Experimental Psychology and Cognitive Neuroscience. John Wiley & Sons, Ltd, 3 2018, pp. 1–42.

[40] X. Dai, J. E. Colgate, and M. A. Peshkin, "LateralPaD: A Surface-Haptic Device That Produces Lateral Forces on A Bare Finger," in IEEE Haptics Symposium (HAPTICS). IEEE, 2012, pp. 7–14.

[41] J. Mullenbach, M. Peshkin, and J. Edward Colgate, "EShiver: Lateral Force Feedback on Fingertips through Oscillatory Motion of an Electroadhesive Surface," IEEE Transactions on Haptics, vol. 10, no. 3, pp. 358–370, 7 2017.

[42] S. Ghenna, E. Vezzoli, C. Giraud-Audine, F. Giraud, M. Amberg, B. Lemaire-Semail, and F. Giraud, "Enhancing Variable Friction Tactile Display using an ultrasonic travelling wave," IEEE Transactions on Haptics, vol. 10, pp. 296–301, 2016. [Online]. Available: https://ieeexplore.ieee.org/abstract/document/7563434?casa_token=S0OaHa7kTl0AAAAA:Yel_1V3wxaBinB_vPhZbkf0_MolNRl6nT_6bg0lAHQatyoy1syPjgLqluvuAodmyc42yxjK39Q

A

Design Process

The design of the haptic touchscreen has been part of the research assignment[2] by the same author (T.J. Brans) prior to the master thesis project. For completeness sake, and due to the iterations and changes made to the device, the full design process is included in this appendix, though it may share large parts of the report made for the research assignment.

A.1. Design requirements

The design of the haptic touchscreen can be divided in multiple subsystems. This being; finger position sensing, visual rendering and haptic rendering. By splitting up the system, the specific requirements can be easily explained (see Table A.1).

A.1.1. Splitting visual and friction functionalities

The first option is to use the surface of the LCD screen that displays the visuals for rendering the virtual textures. However, when this surface is actuated at ultrasonic frequencies it is unknown how this would influence the electronics. Additionally, it would require more energy because unnecessary mass is actuated, and determining the eigenfrequency and vibration mode would be complex.

As a solution, the system's functionalities are split up by providing a transparent plate above the screen to render the virtual textures. For this transparent plate a piece of borosilicate glass will be used with piezoelectric actuators attached. Applying an oscillating voltage signal to the piezos causes them to

Table A.1: System requirements and final specifications of the prototype

Description		Requirement	Units	Final result
Overall System				
OS-1	Active area	>100x100	mm	155x86
OS-2	Latency between user motion and friction rendering	<5	ms	50
OS-3	Visuals and virtual textures are to be rendered at the same location	-	-	
Finger Position sensing				
FP-1	Accuracy of position sensing	<1	mm	1
FP-2	Scanning frequency	>200	Hz	200
Display system				
DS-1	Ability to display moving images	-	-	
DS-2	Refresh rate	>60	fps	80
DS-3	Resolution	>100	dpi	130
DS-4	Screen viewing area	>100x100	mm	155x86
Actuation system				
AS-1	Vibration frequency	>40	kHz	34.9

deform. By placing the piezos at a specific location and calculating the eigenmode and eigenfrequency of the glass plate the surface will oscillate as well. Borosilicate glass has a high Q-factor (low mechanical loss) and high resistance to abrasion, when compared to other transparent materials, making it a well suited material to use for this application.

Software wise, the haptic and visual feedback is also separated. The haptic feedback needs a high refresh rate due, while the visual feedback can suffice with lower refresh rates. For the visual part of the system a Raspberry Pi is used, together with a 7 inch touchscreen.

A.2. Plate vibrations

Actuating the glass plate in its eigenfrequency is most viable and preferred because its behaviour is most predictable and stable. However, the downside is that at the location of the nodal lines the amplitude of vibrations is less. For the particular case of the haptic touchscreen this is not a significant problem, because the contact area of the finger used to interact with the screen is relatively large. Moreover, the high frequency causes the nodal lines to be close to another. These properties combined will average out the effect of a lower amplitude at the nodal lines.

For the haptic touchscreen horizontal nodal lines are preferred as it makes the amplitude in one dimension constant. This is not the case with a combined mode shape with horizontal and vertical lines. Using only vertical lines could also be considered, but the largest dimension of the screen is horizontal and thus more movement and actions can be performed in this direction.

To determine the dimensions of the plate, such that the required mode shape (horizontal nodal lines) and eigenfrequency are met, an analytical model is presented which is used to optimise the results using MATLAB. These calculations are validated using a finite element model in Comsol.

A.2.1. Analytical determination of mode shapes

For the analytical calculations the plate is assumed to behave as a beam, such that the dimensions of the plate can be calculated using beam dynamics. To achieve a mode shape where the nodal lines are horizontal the width of the plate is taken to be in between two resonance lengths, while a resonance length is used for the length of the plate.

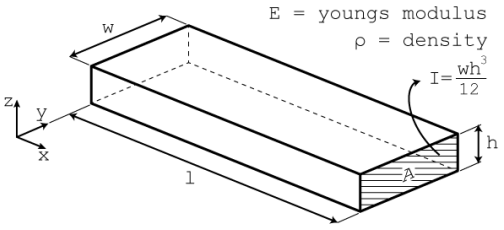

Figure A.1: Rectangular beam with length(l), rectangular cross sectional area ($A = wh$) and area moment of inertia (I)

Starting with a rectangular beam as visualised in Fig. A.1 and using the Bernoulli theory of transverse vibrations, the equation of motion follows as in Eq. A.1 [3], with v being the out of plane deformation in z direction.

$$EI\frac{\partial^4 v}{\partial x^4} + \rho A\frac{\partial^2 v}{\partial t^2} = 0 \tag{A.1}$$

By using separation of variables for the solution, the deformation formula is represented by Eq. A.2. It consists of the mode shape ($\varphi(x)$), and temporal equation ($e^{i\omega t}$). From this general solution the second and fourth order derivatives can be calculated. Substituting these derivatives into Eq. A.1 gives the solution for the equation of motion [3].

$$v(x,t) = \varphi(x)\ e^{i\omega t} \tag{A.2}$$

The second derivative with respect to time of Eq. A.2 is calculated to be Eq. A.3 [3].

$$\frac{\partial^2 v}{\partial t^2} = \varphi(x) \cdot -\omega^2 e^{i\omega t} = -\omega^2 \cdot v(x,t) \tag{A.3}$$

By using $\beta = \frac{2\pi}{\lambda}$ and $\omega = \frac{2\pi}{T}$, the general solution of $\varphi(x)$ can be expressed in the form of Eq. A.4. The fourth order derivative is calculated in Eq. A.5 and rewritten in Eq. A.6 [3].

$$\varphi(x) = A\cos(\beta x) + B\sin(\beta x) + C\cosh(\beta x) + D\sinh(\beta x) \tag{A.4}$$

$$\frac{\partial^4 \varphi}{\partial x^4} = \beta^4 A\cos(\beta x) + \beta^4 B\sin(\beta x) + \beta^4 C\cosh(\beta x) + \beta^4 D\sinh(\beta x) \tag{A.5}$$

$$\frac{\partial^4 \varphi}{\partial x^4} = \beta^4 \varphi(x) \tag{A.6}$$

Substituting the two derivatives of Eq. A.3 and Eq. A.6 into Eq. A.1 results in Eq. A.7. This is simplified to the form as seen in Eq. A.8 [3].

$$\frac{Ewh^3}{12}\frac{d^4\varphi}{dx^4}e^{i\omega t} - \rho\ wh\ \omega^2\varphi(x)e^{i\omega t} = 0 \tag{A.7}$$

$$\frac{Ewh^3}{12}\beta^4 = \rho\ wh\ \omega^2 \tag{A.8}$$

Rewriting the solution in terms of ω and β results in Eq. A.9a and b respectively [3].

$$\omega^2 = \beta^4 \frac{Eh^2}{12\rho} \tag{A.9a}$$

$$\beta = \sqrt[4]{\omega^2 \frac{12\rho}{Eh^2}} \tag{A.9b}$$

Given the so called free-free boundary conditions, meaning that no shear force or bending moment is present on the free edges of the plate or beam (Eq. A.10) the solution can be calculated as presented in Eq. A.11 [3].

$$\left.\frac{d^2\varphi}{dx^2}\right|_{\substack{x=0\\x=l}} = \left.\frac{d^3\varphi}{dx^3}\right|_{\substack{x=0\\x=l}} = 0 \tag{A.10}$$

$$\cos(\beta_n l)\cosh(\beta_n l) - 1 = 0 \tag{A.11}$$

A.2.2. Shape optimization

To provide a graphical overview of the possible resonance lengths a scatter plot is created as seen in Fig. A.2. In this plot a preferred frequency can be chosen for which the resonance lengths follow from Eq. A.11. The final dimensions are constrained by the dimensions of the LCD screen and required space to physically construct the prototype. The length of the plate is taken at a resonance length ($= 149.8$ mm) and the width of the plate is chosen in between two of the resonance lengths ($(160.1 + 170.5)/2 = 165.3$ mm).

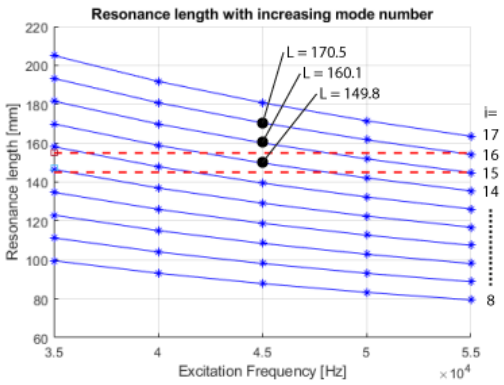

Figure A.2: Scatter plot with the resonance lengths for increasing mode numbers (i). In dashed red lines are the dimensions of the screen (minimum width=155mm and length=145mm of the glass plate)

With the dimensions chosen above, the mode shape can be calculated using the formulas provided by Blevins [4]. With the formula for a free-free beam (Eq. A.12) and mode number 14, from Fig. A.2, the shape can be calculated. The formula gives the shape as fraction of length of the beam, where λ and σ are given by Eq. A.13.

$$\tilde{y}_i\left(\frac{x}{l}\right) = \cosh\frac{\lambda_i x}{l} + \cos\frac{\lambda_i x}{l} - \sigma_i\left(\sinh\frac{\lambda_i x}{l} + \sin\frac{\lambda_i x}{l}\right) \tag{A.12}$$

$$\lambda_i = (2i+1)\frac{\pi}{2}; \quad i > 5 \tag{A.13a}$$

$$\sigma_i \approx 1.0; \quad i > 5 \tag{A.13b}$$

From these formulas the first antinode is extracted and used to indicate the location of the piezos. The center of the piezos are 7.8 mm from the edge of the glass plate. Important to note here is that the system eventually is actuated at a different mode. During the validation progress as explained in Appendix D it is found that the vibration amplitude was higher at mode 12. The same analysis holds for the calculations at mode 12. The same dimensions of the glass plate are kept. This is possible because the wavelength difference between mode 14 and 12 is small.

A.2.3. Determining thickness of the plate

In the calculations above, the thickness of the plate is taken to be 2.0 mm. The thickness however, has a significant influence on different aspects of the vibration. In Eq. A.9a it is already apparent that the thickness (h) influences the eigenfrequency. Furthermore, the thickness also relates to the weight of the plate. When looking at a standard mass-spring-damper system the damping ratio (Eq. A.14) is determined by the damping factor (c) implied by your finger acting as a damper, the mass and the natural frequency.

$$\zeta = \frac{c}{2m\omega_n} \tag{A.14}$$

A under damped system ($\zeta < 1$) is desired, so a higher mass contributes to a lower decay. As a result, a thicker plate will result in a higher mass and a lower decay. However, another factor has to be taken into account. A small distance between the finger and the LCD screen is preferred, as disassociation due to misalignment perceived by the user can otherwise occur. This is mainly a problem if the viewing angle is extremely acute. A thickness of 2 mm of the glass plate is therefore chosen to compromise between these two factors.

Length	$165.3mm$
Width	$149.8mm$
Thickness	$2mm$
Density	$2803kg/m^2$
Young's modulus	$72GPa$
Poisson's ratio	0.17

Table A.2: Dimensions and material properties of the glass plate used in the finite element modelling

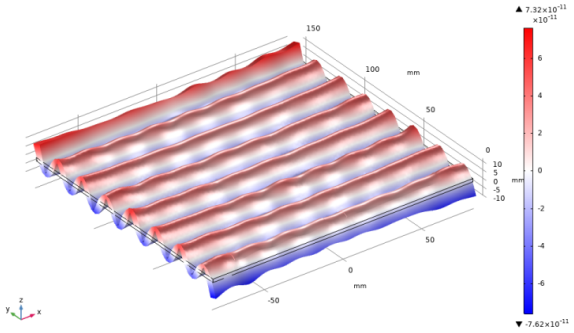

Figure A.3: Displacement field in Z-direction at the eigenfrequency of 42505Hz

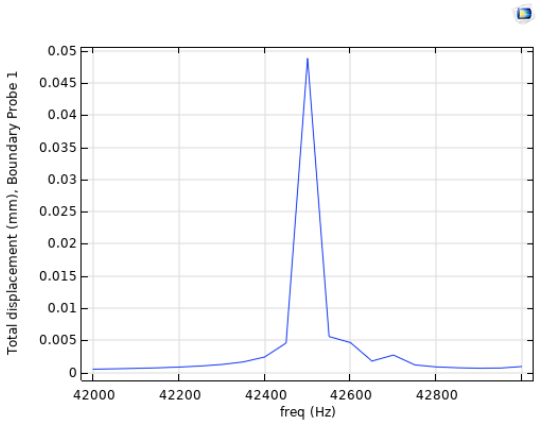

Figure A.4: Total displacement of the top surface for different frequencies

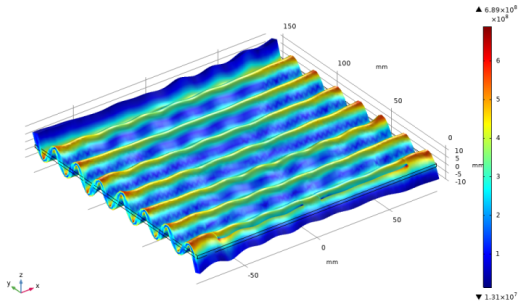

Figure A.5: Von Mises stresses at a frequency of 42500 Hz applied to the piezos

A.2.4. Finite Element Validation

To confirm the results of the analytical calculations a finite element model in COMSOL is used. The plate is modeled with the parameters and material properties given in Table A.2. The piezos are placed on the theoretical first antinode as calculated in Section A.2.2.

Two simulations are performed. The first being an eigenfrequency search around 43000 Hz without taking into account the presence of the piezos. The solution of this study shows an eigenfrequency of 42505 Hz, for which the displacement field is seen in Fig. A.3. Other eigenfrequencies were found around the same frequency with different mode shapes, but those will likely not be present because the piezos will dominate the shape due to their placement on the antinode of the preferred mode shape.

In the second study a piezoelectric frequency sweep is applied to the two piezos. For a range between 42 and 43 kHz with steps of 50 Hz the surface von Mises stress is calculated at each frequency as well as the total displacement of the top surface (Fig. A.4). From this figure it can be seen that the frequency with a dominant spike in displacement is at 42.5 kHz. The corresponding mode shape can be seen in Fig. A.5, which is very similar to the shape calculated in the first study.

A.2.5. Plate fixtures

To properly fixate the vibrating glass plate, fixtures are required that hold the plate in place but still allow for the vibrations to occur. The challenge posed is that the finger of the user will present forces perpendicular to the plate (normal forces), requiring the fixture to be stiff in this direction. However, the vibrations are actually happening in the same direction, and to not dampen the vibrations you also want the fixture to be flexible in this direction.

The plate is modelled with free boundaries on all sides, which means that clamping along the edges is not an option as it will dampen the vibrations and change the eigenfrequencies of the plate. Therefore,

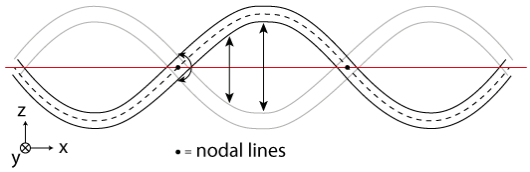

Figure A.6: Exaggerated view of the vibrations of the plate (oriented in the x,y-plane) viewed from the side (x,z-plane).

the best theoretical location for a fixture is on the nodal lines, as no vertical movement is occurring in these locations, thus solving the previous mentioned challenge. As illustrated in Fig. A.6 the nodal lines do not move in x or z direction. A fixture in this location can thus be stiff in x, y and z to withstand the friction forces of the finger (x and y) as well as the normal force (z).

The downside is that this nodal line represents only a single point in the x,z-plane. The surrounding material will still move due to the vibrations. Locally around the nodal line, the material will rotate around this nodal line (y-axis). Therefore, when clamping the material from the top and bottom in this location, it should allow for rotations along this axis.

Four different geometries are designed based on the idea that the translational stiffness in x,y and z directions are high and the rotational stiffness around the y-axis is low (Fig. A.7). All designs are printed on a 3D-printer (ultimaker 2+) in PLA with a layer height of 0.1 mm. Fixture design (a) requires an additional metal set screw with a diameter of 2mm and a tapered contact point. These four fixtures are tested to hold a small aluminium plate, that has been used in a previous haptic device. The plate is actuated using the piezos and the resulting output voltage of a pick-up piezo is measured. As the output voltage, with the use of the short tapered plus, was highest this design is consequently used as a fixture for the haptic surface.

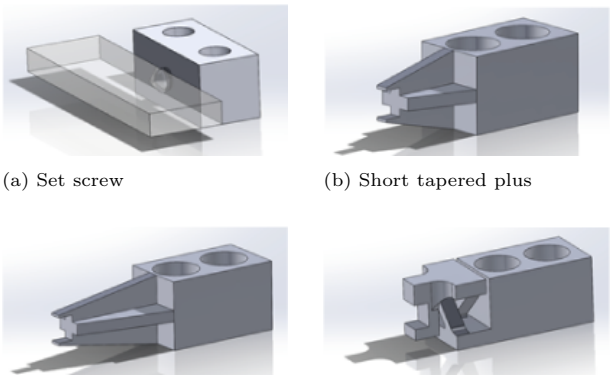

(a) Set screw

(b) Short tapered plus

(c) Long tapered plus

(d) Cross-flexure

Figure A.7: Fixture designs

A.3. Hardware

The hardware and electronics is largely the same as used in the research assignment. Difference being that the ultrasonic signal generation is integrated on a printed circuit board, instead of the use of an external signal generator (Tektronix AFG100). An attempt has been made to also integrate the amplification circuit by using power amplifiers. However, this circuit could not be realised in time due to instability issues. Thus still external amplifiers are used.

As explained, the visual and haptic system is separated for the sake of obtaining high refresh rates in the haptic feedback loop. The global schematic and interaction between the components is seen in Fig. A.8. The visuals are generated on a Raspberry Pi 4B single-board computer, while the haptic driving signal is generated by a Teensy 3.6 micro-controller. The communication between the two sub-systems is done using the USB Human Interface Device protocol, as well as sending Ethernet UDP messages. The position sensing is done using an optical position sensor, which is connected to the micro-controller.

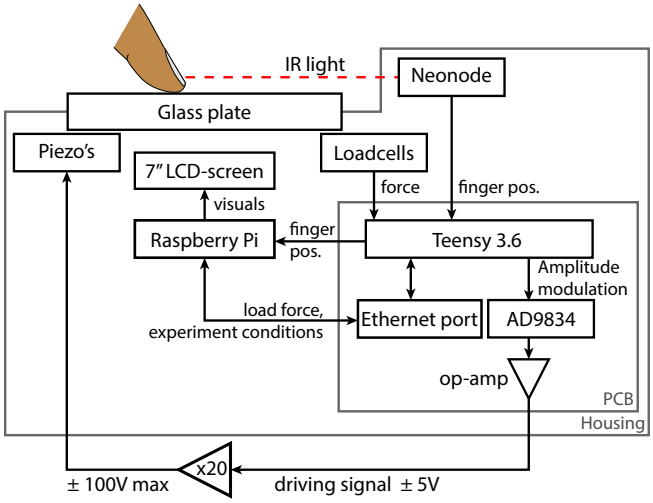

Figure A.8: Schematic overview of the haptic touchscreen prototype.

A.3.1. Position sensing

Although a LCD with capacative touch capability is used as visual feedback, this finger position functionality cannot be used due to the glass plate being placed in front. Therefore the position sensing is managed with the use of a Neonode touch sensor module (NNAMC1581PCEV). This sensor uses an array of infrared light to sense the position of objects, in this case a finger. The device is located at the top of the glass plate, with its active sensing plane just above the glass plate. The position data is sent to the Teensy, using I^2C.

A.3.2. Haptic system

The Teensy 3.6 is a micro-controller, featuring a 32 bit 180MHz ARM Cortex-M4 processor and can be programmed using the Arduino IDE. This makes it well suited for high refresh rates and easy to use. The Teensy is mounted on a custom pcb (circuit diagrams in Appendix B). The Teensy receives the position data from the position sensor and calculates the corresponding vibration amplitude for the glass plate. The ultrasonic signal is generated by an AD9834 chip, of which the frequency is set using a 3-wire serial interface to the Teensy. Hereafter, the ultrasonic signal can be modulated by connecting the full-scale-adjust pin to an analog output of the Teensy. The resulting modulated ultrasonic signal is amplified to $10V_{pp,max}$ using a series of op-amps and sent to two external amplifiers (PiezoDrive PD200). Each of these amplifiers actuates six, parallel connected, piezo-elements (SMPL26W8T07111). These are glued (using 3M Skotch-Weld DP490) to the bottom of the glass plate in two rows of six at the first and last anti-node.

Also included in the design are four loadcells (CZL611CD). The fixtures that hold the glass plate are connected to these loadcells. The electrical signal of these loadcells is amplified by instrumental amplifiers on the pcb. The Teensy measures this signal on the analog inputs, which gives a measure of the applied normal force.

Both the position data and the force data are relaid to the Raspberry Pi. The Teensy is programmed to act as a mouse input device over USB and the force data is sent to the Pi using an Ethernet port (WIZ820io).

A.3.3. Visual system

The Raspberry Pi is programmed using Python and uses a 7 inch display especially made to be connected to a Pi to display the visuals. It is connected through a ribbon DSI cable. The visuals are rendered using PyGame. As far as the Pi concerns, the finger position data is received like regular mouse position data over USB. The remaining communication is accomplished by the Ethernet connection. Here, the force data is received but also the specific haptic conditions that need to be rendered are send back to the Teensy. The Raspberry Pi is powered with 5V supplied by an USB-C cable. This power is distributed to the Teensy over the USB-cable, which also powers the rest of the components on the pcb. The external amplifiers have their own 230V connection.

A.3.4. Housing

The majority of the equipment is housed in a 3D-printed enclosure (Fig. A.9). Only the external amplifiers are located outside this enclosure. The enclosure consists of multiple parts that are screwed together using M3-bolts and threaded inserts. The glass plate and LCD screen are angled at 30 degrees to ease the interaction. In the first prototype the screen was horizontal. To properly interact, people had to lean over the touchscreen or strain their neck, this is solved by angling the touchscreen. The exploded view of the prototype can be seen in Fig. A.10. The power cable and the connections to the external amplifiers are fed through holes in the back of the housing.

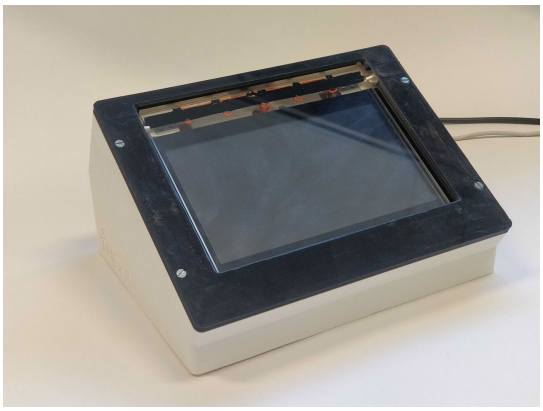

Figure A.9: Picture of the touchscreen prototype, external amplifiers are not visible.

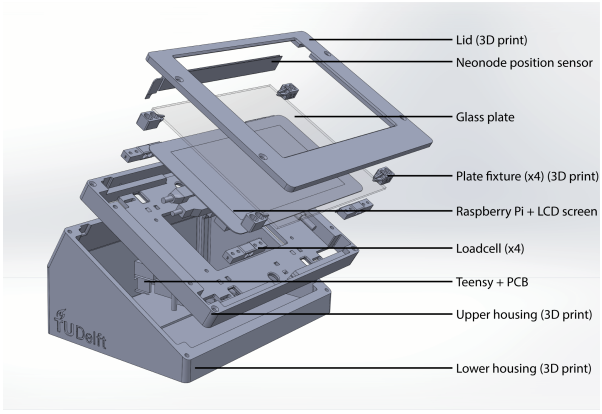

Figure A.10: Exploded view of the touchscreen prototype.

A.3.5. Integrated amplifier circuit

The integration of the amplifiers onto the pcb and removing the need of the external amplifiers has been researched. Due to time limitations however, the external amplifiers are used. The acquired knowledge on this subject is shared in this section.

The external amplifiers are designed to drive a capacitive load with high power. To achieve the same performance of output voltage and current, an oscillating circuit can be utilized. By connecting an inductor in parallel with the capacitive load (piezo's), such an oscillating circuit can be made (Fig. A.11). The inductor value should be selected such that the impedance of the LC-circuit is around zero at the resonating frequency. Because the capacitance and the desired frequency is known, the inductor value is easily found using Eq. A.15.

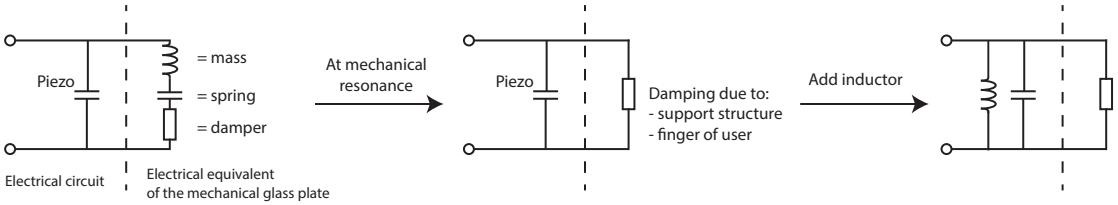

Figure A.11: Explanation of the interaction between the electrical and mechanical circuit.

$$Z = j(L\omega - \frac{1}{\omega C}) + R \tag{A.15}$$

To drive this circuit a Texas Instruments OPA2544 high power amplifier is used, together with a transformer to increase the voltage. The amplifier is connected in a bridge drive configuration as seen in Fig. A.12. The output of this amplification circuit is connected to an 1:10 transformer (Wurth Elektronik 750311486). The output of this transformer is wired to the LC-circuit.

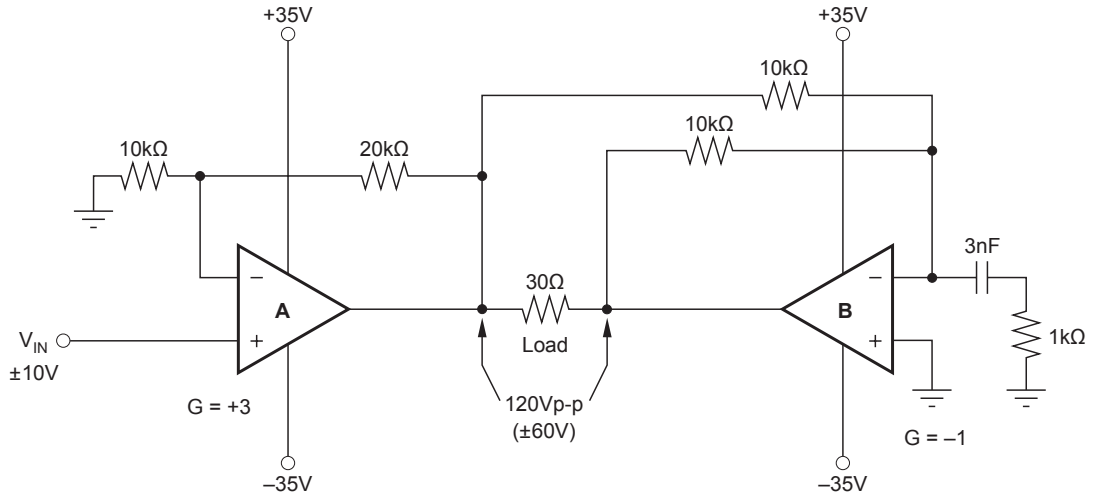

Figure A.12: Bridge drive circuit as illustrated by figure 4 in the TI OPA2544 datasheet

When testing this setup, the amplifier drew a lot of current ($0.2A$ with an input of $1V_{pp}$) and the package became extremely hot. Upon closer inspection on the output signals using an oscilloscope it became apparent that large spikes were present. An in-loop compensation technique, called frequency compensation [5] is implemented in an attempt to solve this issue, but without success.

B

Printed Circuit Board Design

The circuit diagram presented in this appendix is used for the printed circuit board of the haptic system. The micro-processor (Teensy 3.6) is the central unit the design is based around. On the following pages the schematic of the PCB is given. Also included is the bill of materials in Table B.1.

Teensy 3.6

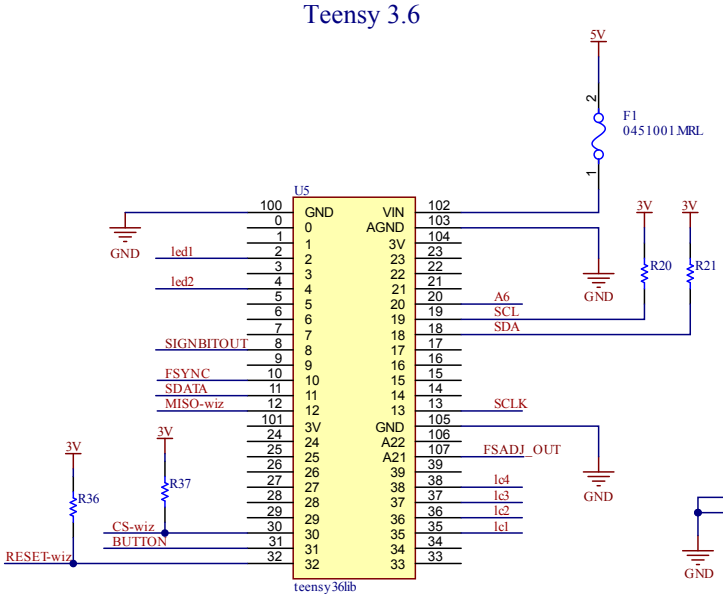

Neonode Connector

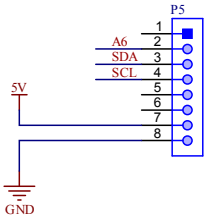

Ethernet module

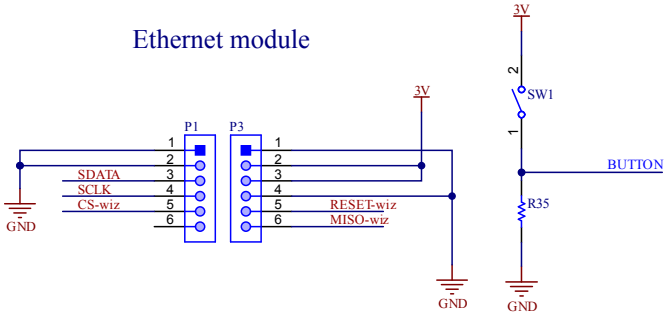

Ultrasonic signal generation and modulation

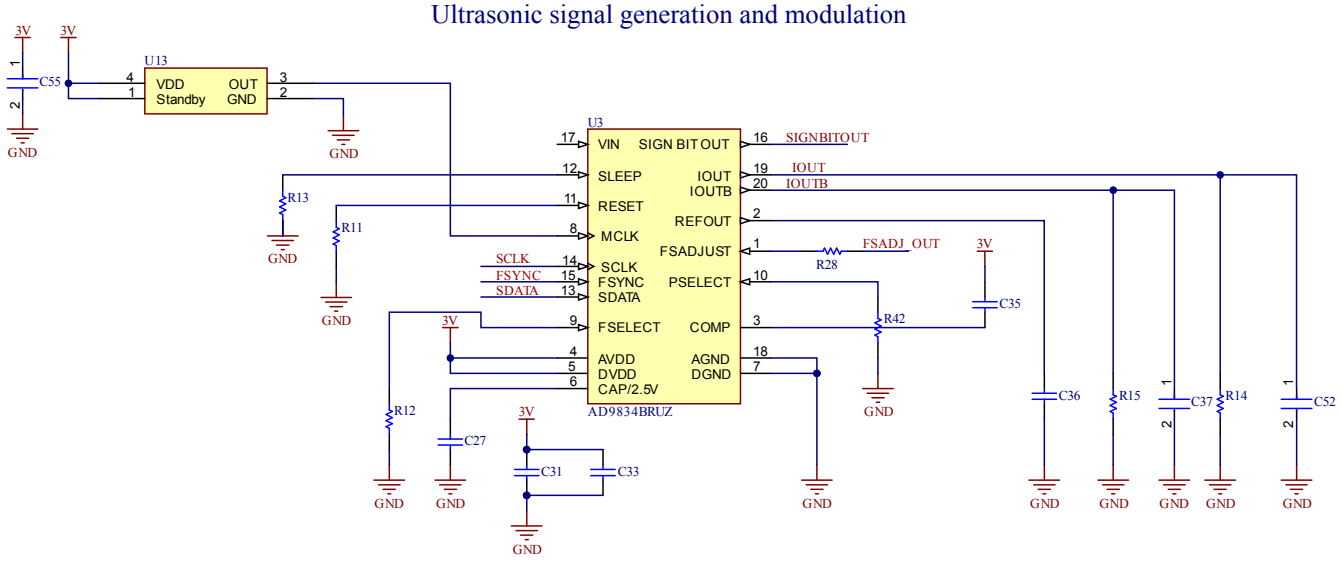

Ultrasonic signal amplification

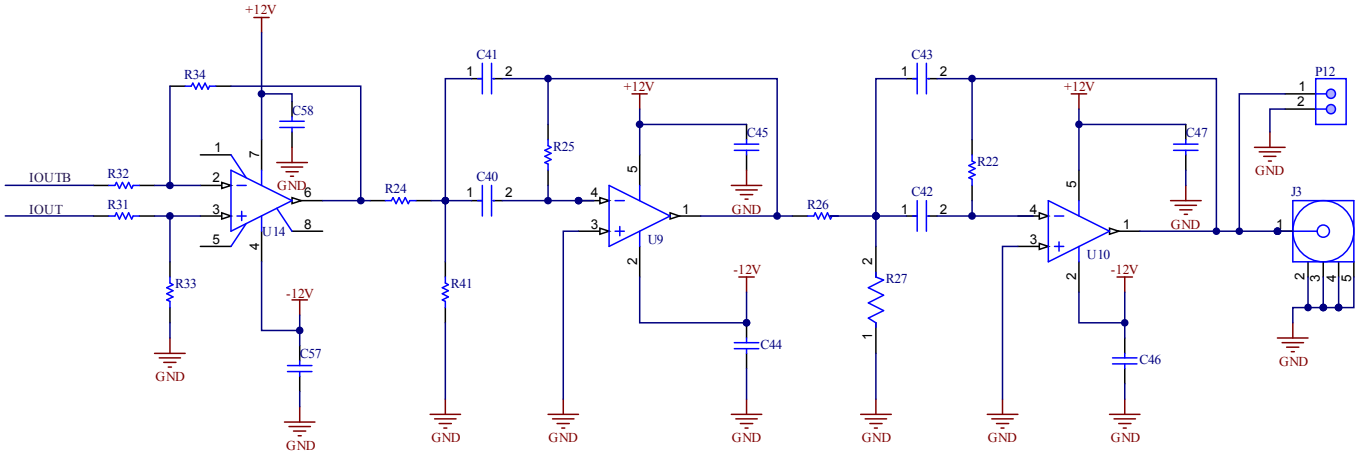

Designed by E. Hoseini

Loadcell connectors & instrumental amplifiers

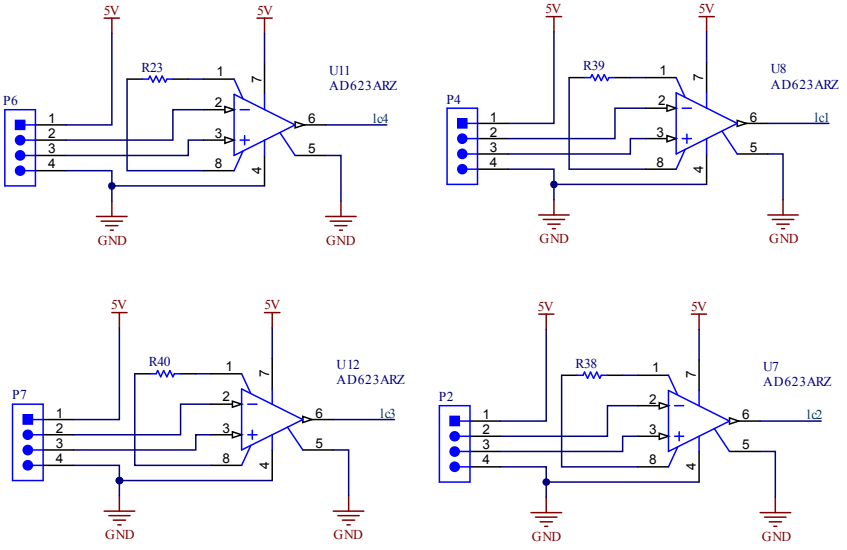

Miscellaneous

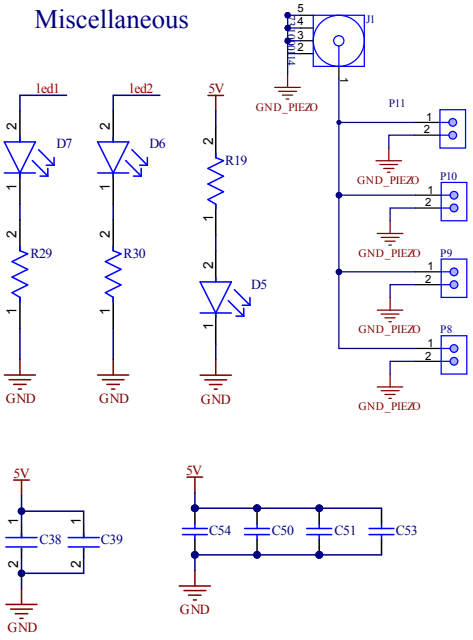

Voltage regulation

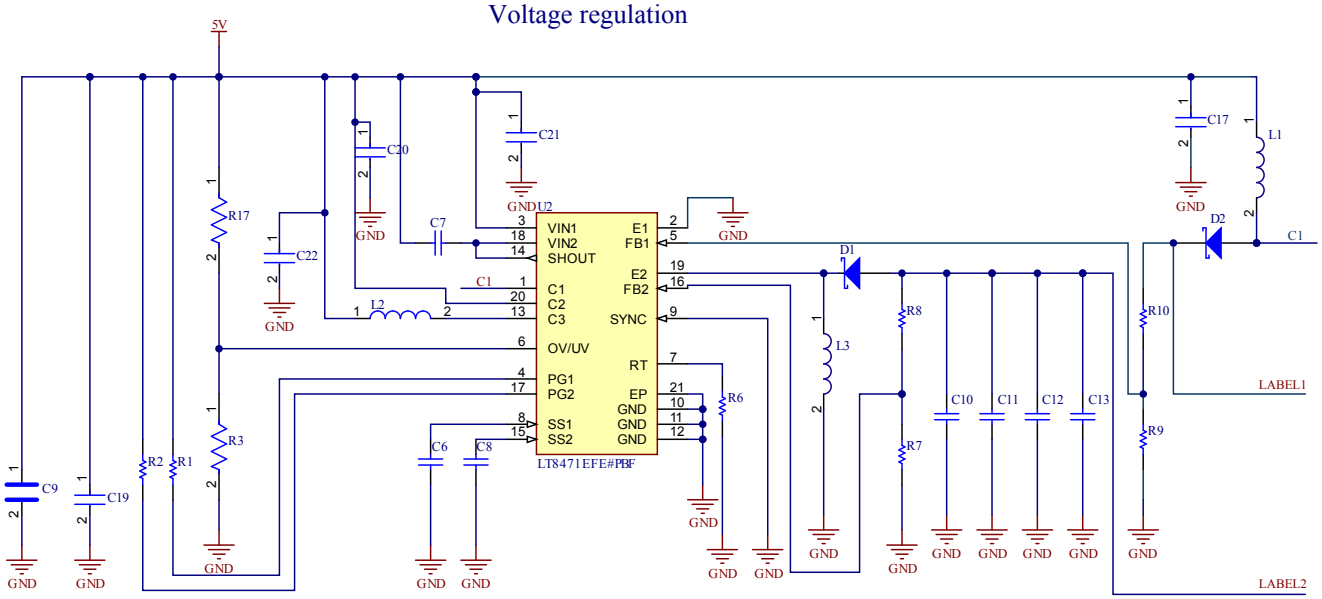

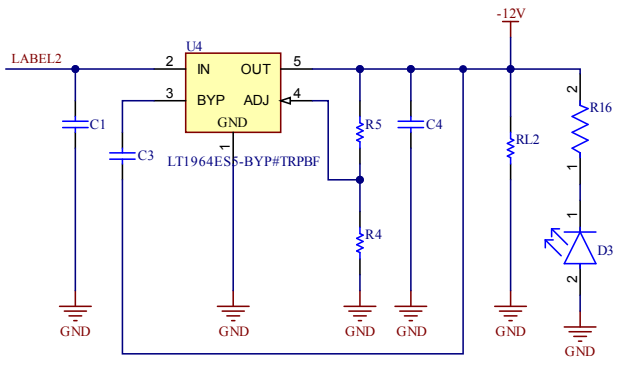

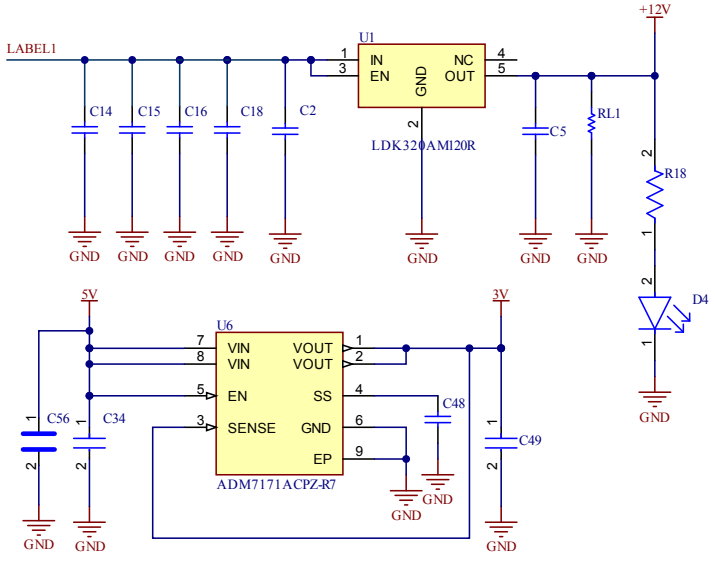

Table B.1: Bill of materials, *DNP = Do Not Populate.

Capacitors(F)		Resistors (Ω)		Diodes/LEDs	
C1	1u	R1	100k	D1	DFLS240L-7
C2	0.1u	R2	100k	D2	DFLS240L-7
C3	0.01u	R3	270k	D5	standard 0603 LED
C4	1u	R4	1.13k	D6	standard 0603 LED
C5	2.2u	R5	10k	D7	standard 0603 LED
C6	0.1u	R6	107k		
C7	1u	R7	10k	Fuses	
C8	0.1u	R8	158k	F1	0451001.MRL
C9	47u	R9	10k		
C10	47u	R10	158k	Connectors/headers	
C11	47u	R11	10k	J1	731000114 (SMA Right-Angle)
C12	47u	R12	10k	J3	731000114 (SMA Right-Angle)
C13	47u	R13	10k	P1	61300611121 (pin header)
C14	47u	R14	200	P2	22-27-2041
C15	47u	R15	200	P3	61300611121 (pin header)
C16	47u	R17	510k	P4	22-27-2041
C17	2.2u	R19	2.2k	P5	22-27-2081
C18	47u	R20	4.7k	P6	22-27-2041
C19	2.2u	R21	4.7k	P7	22-27-2041
C20	2.2u	R22	4.7k	P8	22-27-2021
C21	2.2u	R23	220	P9	22-27-2021
C22	1u	R24	1.62k	P10	22-27-2021
C27	0.1u	R25	4.7k	P11	22-27-2021
C31	0.1u	R26	1.6k	P12	22-27-2021
C33	0.1u	R27	229		
C34	4.7u	R28	6.8k	Inductors	
C35	0.01u	R29	2.2k	L1	74437324100
C36	0.1u	R30	2.2k	L2	744025150
C37	20p	R31	220	L3	74437324100
C38	2.2u	R32	220		
C39	0.1u	R33	2.2k	Buttons	
C40	3300p	R34	2.2k	SW1	FSMSM Push Button Switch
C41	3300p	R35	1k		
C42	5100p	R36	4.7k	Packages	
C43	5100p	R37	4.7k	U1	L4931ABD120TR
C44	1u	R38	220	U2	LT8471
C45	1u	R39	220	U3	AD9834
C46	1u	R40	220	U4	LT1964ES5-BY
C47	1u	R41	232	U5	Teensy pin headers
C48	1n	R42	10k	U6	ADM7171ACPZ-R7
C49	4.7u			U7	AD623ARZ
C50	0.1u			U8	AD623ARZ
C51	0.1u			U9	ADA4004-1ARJZ-R2
C52	20p			U10	ADA4004-1ARJZ-R2
C53	0.1u			U11	AD623ARZ
C54	0.1u			U12	AD623ARZ
C55	0.01u			U13	75MHz
C56	DNP* (47u)			U14	LM7171
C57	1u				
C58	1u				

C

Manufacturing

Detailed information on the manufacturing of the haptic touchscreen prototype is given in this appendix. The device is assembled in house and uses several off-the-shelf components, as well as custom made components.

C.1. Housing

The housing of the haptic touchscreen is 3D-printed on an Ultimaker 2+. The housing consists of 3 parts, each printed in PLA with a layer height of 0.15mm and 20% infill. Threaded inserts are placed in pre-modelled holes using a soldering iron. The three separate parts are held together using M3 bolts.

The housing has several features such that the electronic hardware can be easily connected to the housing using screws. The glass plate is made to specifications by glass workshop Saillart and held in place by four 3D-printed fixtures. These fixtures are connected to the loadcells, which are in turn connected to the housing.

C.2. Attachment of piezo's

The piezo's are placed on the glass plate, along the anti-nodes of the calculated mode shape. By glueing the piezo's to the glass plate a strong connection can be achieved. However only one side of the piezo will remain accessible after glueing. To reach the electrode on the side of the glass plate a 0.07 mm thick piece of copper tape (Velleman copper foil adhesive tape[1]) is soldered to the piezo first.

On both the piezo and the copper tape, a little bit of solder (STEMiNC SMAGLF32OZ1[2]) is applied (Fig. C.1a). Special care is taken to not apply too much solder, because this will add to the total added thickness. Next, the tape is placed on the piezo and is heated with the soldering iron on the adhesive side of the tape (Fig. C.1b). The excess solder is pushed away from underneath the copper foil using the soldering iron.

The placement of the piezos is marked on the glass plate and two part epoxy (3M Scotch-Weld Epoxy Adhesive DP490[3]) is used to attach the prepared piezos. The glue is mixed in a mixing cup and applied to the glass plate (Fig. C.2a). Adding too much glue, will result in a thick layer between the piezo and and glass plate as well as a lot of squeeze out. However, applying to little will result in voids which can cause the piezo to detach during use. After placing the piezo on the glue, the assembly is clamped together with small clamps (Fig. C.2b). Wax paper is placed in between the clamps and the piezo to prevent accidental glueing of the clamps. The glue is allowed to cure for at least 24 hours before handling. Hereafter the piezos are soldered in parallel, while making sure not to heat up the piezos for more than 2 seconds (Fig. C.2c).

[1] https://www.velleman.eu/products/view/?id=439240
[2] https://www.steminc.com/PZT/en/lead-free-no-clean-flux-core-silver-solder
[3] https://www.3m.co.uk/3M/en_GB/p/d/b40066473/

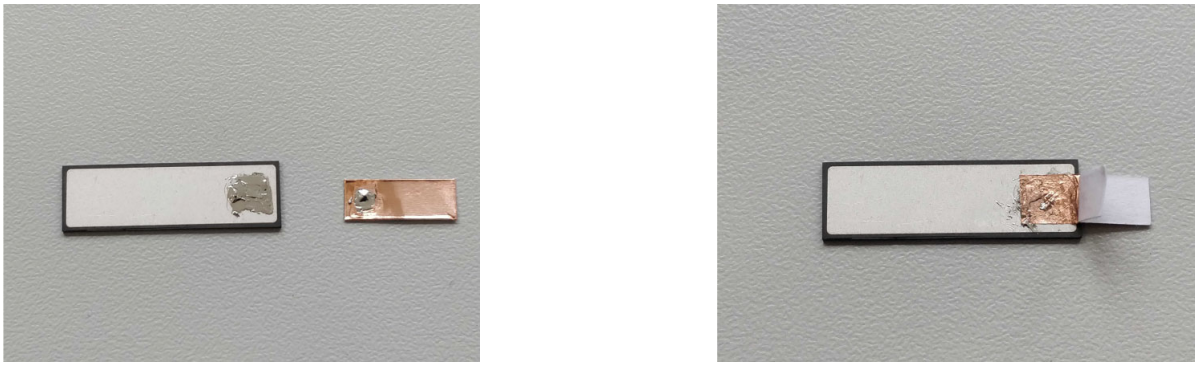

(a) Applying solder to both the tape and piezo

(b) Soldering the tape to the piezo

Figure C.1: Soldering copper foil tape to the piezo electrode

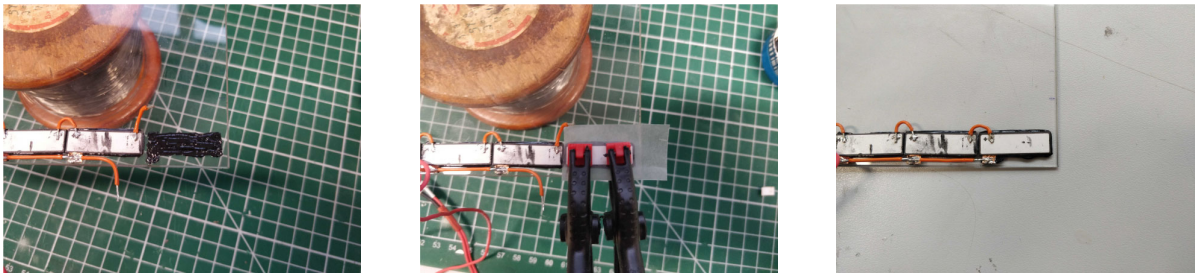

(a) Applying epoxy glue

(b) Clamping the piezos

(c) Soldering wires to the piezos

Figure C.2: Attaching the piezos to the glass plate.

C.3. Glue selection

For the particular application of attaching the piezo's to a glass plate to excite the antinode of a bending mode, the glue has to have certain properties. With the application of a voltage the piezo's will expand and contract, thus a high shear strength of the bond is required. Due to this expansion and contraction the bending mode of the glass plate is excited thus also a high peel strength is necessary (Fig. C.3). Lastly, a high Young's modulus is prerequisite. If the glue is too flexible the deformation of the piezos will not be transferred to the glass plate, resulting in a low Q factor.

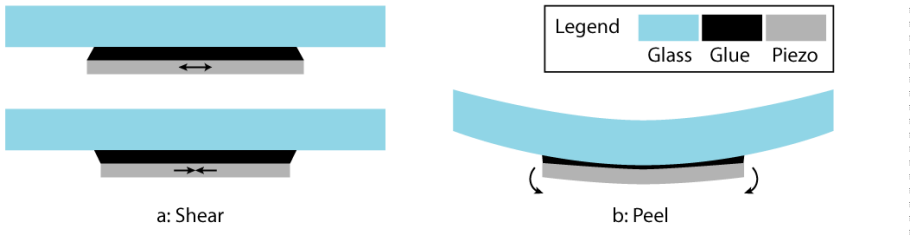

Figure C.3: Schematic representation of the glass-glue-piezo assembly, stressing the need for (a) high shear strength and (b) high peel strength.

The impact of the type of glue became clear during the design process. First the epoxy glue DP105[4] was used to attach the piezo's. However, the preferred amplitudes of the glass plate could not be reached after which the DP490 epoxy was used. Using the new glue improved the amplitudes significantly. The mechanical properties of these glues could unfortunately not be compared properly, because information was not specified in the datasheets Table C.1. Detailed figures on the influence of the glue on the vibration amplitude are given in Appendix D.

[4]https://www.3m.co.uk/3M/en_GB/p/d/b40066495/

Table C.1: Mechanical data of epoxy glue

	Key features	Optical	Floating roller peal $[N/cm]$	Overlap Shear $[MPa]$	Shore D hardness	Tensile strength $[N/mm^2]$
dp105	Very Flexible	clear	89	14	39	4.2
dp490	Tough&Durable	black	60	31	Na	Na

C.4. Electronic hardware

The visual system uses an off-the-shelf Raspberry Pi 4B, connected to a 7 inch touchscreen display. The screen is connected with a flat DSI cable and jumper wires are soldered between the Raspberry Pi and the touchscreen control board to connect 5V and ground. The system is powered with 5 Volt via a USB-C cable, connected to the mains through an adapter.

The haptic system uses the Teensy 3.6, mounted on a custom printed circuit board. The detailed connections of this circuit are explained in Appendix B and the resulting pcb is depicted in Fig. C.4. The Neonode position sensor is connected to this pcb via the supplied control board. The position sensor itself is mounted in a slot at the top side of the glass plate. It is held in place by two small set screws.

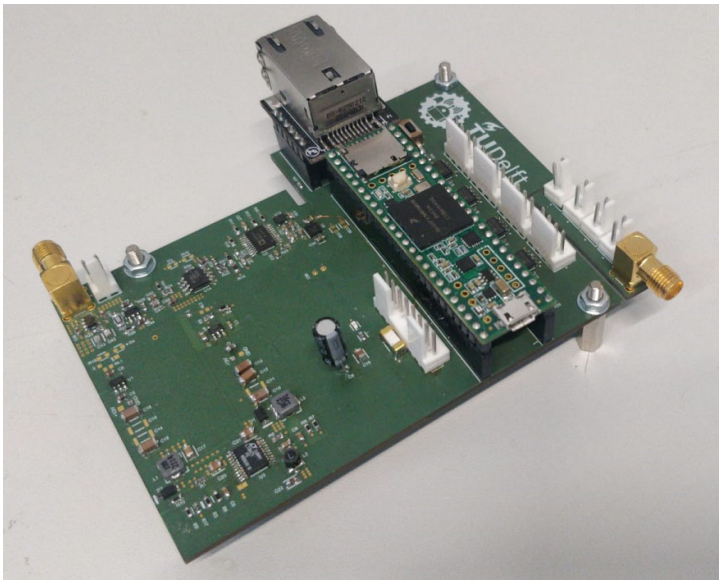

Figure C.4: Picture of the assembled pcb

D

Plate Characterisation

The dynamics of the glass plate are characterised to provide reference values to other surface-haptic devices. The most important metrics being; the vibration amplitude and frequency at which the plate is actuated. As stated in Appendix C, the selection of the glue had considerable influence on the final vibration amplitude. The results of several tests, using a laser interferometer (OFV505, Polytec) to measure the displacements, are shared in this appendix.

D.1. Glue comparison

The glues in question are used to attach the piezo-electric plates to the glass plate. A stiff connection is needed to couple the deformation of the piezos to that of the glass plate. It is preferred that as much electrical energy as possible ends up in deforming the glass plate. Essentially, the glue layer can be seen as an additional spring-damper between the piezo and the glass plate. Using the incorrect glue results in big energy losses at this interface. This effect is clearly visible in Fig. D.1. A driving signal, with an amplitude of 100 Volt is sent to the piezo-electric actuators as a chirp of 5 seconds. The displacement is measured using the laser interferometer. The resulting frequency response shows that the DP490 glue has a more prominent peak than the DP105 glue. The glue selection increased the maximum vibration amplitude with a factor 3. In hindsight, the initial glue selection (DP105) was incorrect, because it is highly flexible. Nonetheless, this emphasises the importance of this part of the system.

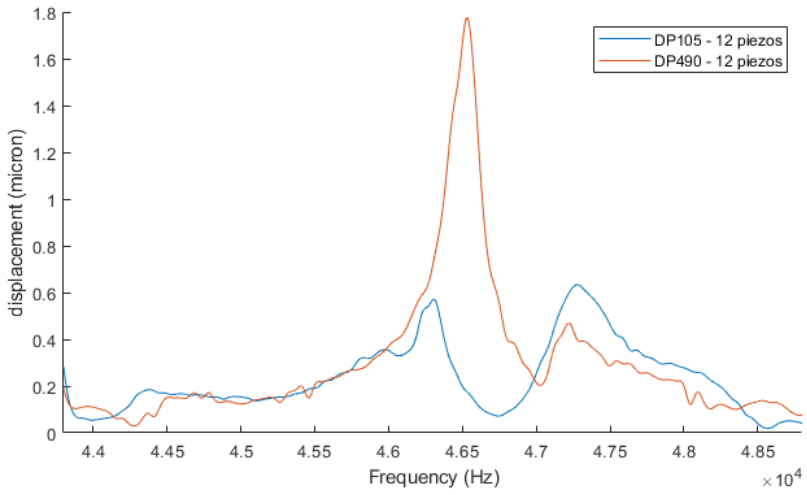

Figure D.1: Frequency response of two different kinds of glue (used to attach the piezos to the glass plate).

D.2. Frequency response

The eigenfrequency is checked by sending a chirp signal (25kHz to 70kHz in 30 seconds at an amplitude of 20V) to the actuators using a function generator (Tektronix AFG 1062). The amplitude response (see Fig. D.2) is showing several local maxima corresponding to different eigenmodes. The eigenmodes are confirmed by actuation of the system at said frequency and placing fine grained salt on the glass plate. The nodal lines, that become visible due to accumulation of the salt, are counted to find the mode number. The zoomed in figures are then acquired by using another sweep signal with lower range. The highest vibration amplitude of the glass plate is found at mode 12, with an eigenfrequency of 34.9kHz. Consequently, the system is actuated at this frequency to have the preferred banded mode shape and highest amplitude.

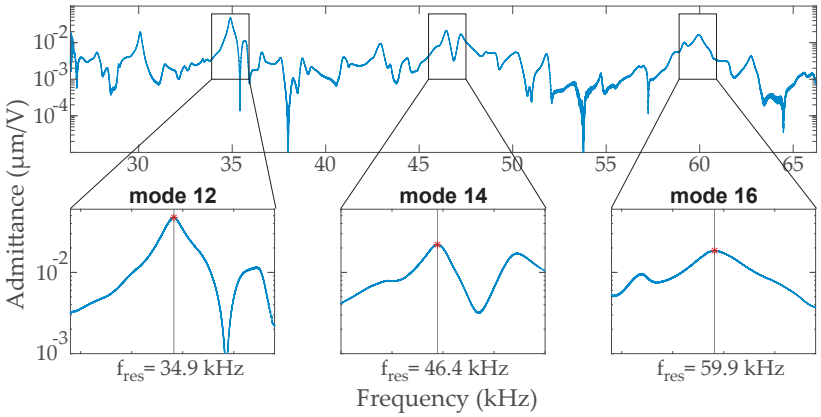

Figure D.2: Frequency response of the glass plate. Driving signal: chirp of 30 seconds at 20V amplitude for the full frequency range. Zoomed in figures are with a chirp of 5 seconds across the corresponding frequency range.

D.3. Maximum amplitude

The experiment is followed by the actuation of the system using a modulating ramp-up and -down (from 0V to 100V and back in 5 seconds) signal. This is used to confirm the linearity of the system and to find the peak vibration amplitude. Fig. D.3 shows that a maximum displacement amplitude of 5 micron is measured at the maximum actuation amplitude of 100V. The figure also shows that no saturation occurs and the actuation is within the linear regime of the piezo's.

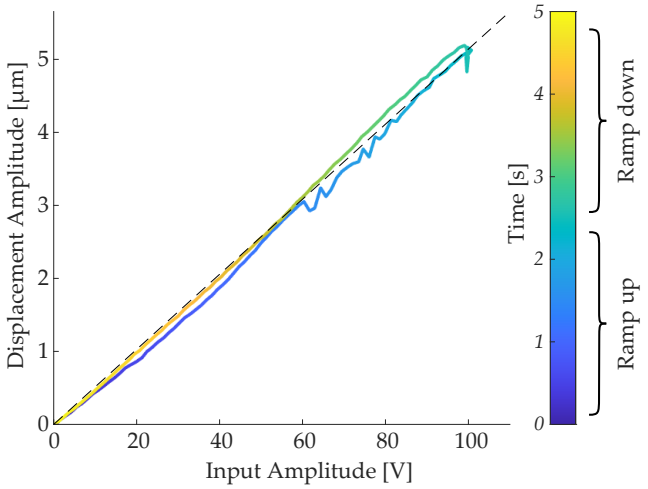

Figure D.3: Displacement amplitude measured at the second anti-node of the glass plate with a ramp-up and -down driving signal. The linear fit is represented with a dashed line.

D.4. Step response

With the last validation experiment the glass plate and its components are connected in the final setup. A step-up and -down signal is initiated by the micro-controller and the amplitude response is measured. The resulting graphs (Fig. D.4) show a 5%-rise time of 6.3 ms and a 5%-fall time of 7.6 ms for the glass plate. An additional visualisation is given in red, of the driving signal that is sent to the piezo-electric actuators. The settling time for this signal is 3.0 ms and 2.2 ms for the step-up and -down respectively.

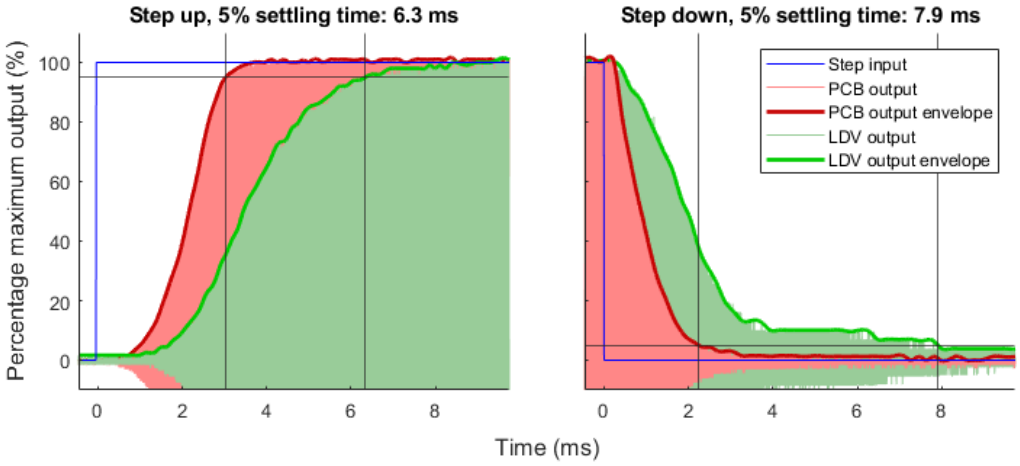

Figure D.4: Response of the piezo driving (voltage) signal and the displacement of the plate after a step-up and -down input. Vertical lines show the 5%-settling time.

D.5. Stress calculations

To confirm the safe operation of the system an analytical calculation is done to calculate the maximum stress. Concerns were raised by the safety manager that the glass might break due to actuation in its eigenfrequency like what would happen when a singer holds a specific tone next to a wine glass, and it shatters. Ideally this is included in the design process, but because the true deformations of the glass plate were known with the measurement, the stresses can be calculated according to the known deformations.

From the deformation measurements using a Laser Doppler Vibrometer (LDV), The maximum deformation is measured to be 5 micrometer. Using the approximation that the plate is deforming in a sinusoidal pattern, the displacement can be described using the following formula.

$$y = \mathrm{A}\sin(kx), \text{ with } k = \frac{2\pi}{\lambda} \tag{D.1}$$

The wavelength (λ) is 24 millimeters with the mode shape of $n = 12$. Taking the second derivative of the deformation gives the curvature of the glass plate.

$$\frac{d^2y}{dx^2} = \frac{1}{\rho} = -Ak^2\sin(kx) \tag{D.2}$$

The maximum curvature of the plate can then be calculated followed by the maximum stress at this location.

$$\max\left(\frac{1}{\rho}\right) = Ak^2 = A\left(\frac{2\pi}{\lambda}\right)^2 \tag{D.3}$$

$$\sigma = E\varepsilon = E\frac{t/2}{\rho} = E\frac{t}{2}A\left(\frac{2\pi}{\lambda}\right)^2 \tag{D.4}$$

With a Youngs modulus of $E = 64\text{GPa}$[1] and a thickness of $t = 2\ \text{mm}$, the maximum stress in the material is 22MPa.

$$\delta = 64 \cdot 10^9 \cdot \frac{0.002}{2} \cdot 5 \cdot 10^{-6} \cdot \left(\frac{2\pi}{0.024}\right)^2 = 22\text{MPa} \tag{D.5}$$

This is well below the maximum bending stress of 150 MPa[1]. With a safety factor of 5 the limit will not be exceeded. Additionally, while the finger is in contact with the glass plate, the vibrations will be damped meaning that the maximum amplitude of 5 micron will not be reached while the participants are touching the haptic touchscreen

[1]The mechanical properties are from the manufacturer website: https://www.schott.com/en-si/products/borofloat/downloads

E

Haptic Rendering Method

Unlike other tactile effects generally employed on a touchscreen the pseudo-potential field rendering method takes the direction of movement into account as well as the position of the finger. This results in a continuous feedback principle where not only confirmatory feedback is given. This appendix gives further details on the construction of these potential fields.

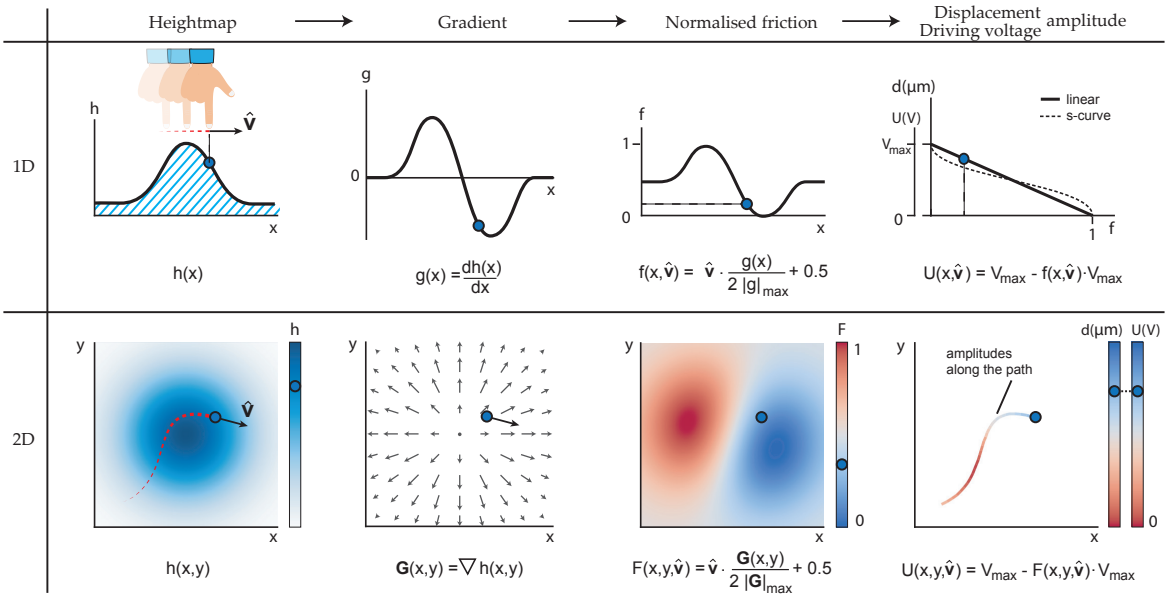

Figure E.1: Visualisation of the pseudo-potential haptic rendering method, for an one- and two-dimensional case. The unit velocity vector is multiplied by the gradient at that position. Normalising this to the driving signal range results in the rendering of a pseudo-potential field.

As explained in the paper, the pseudo-potential field rendering method would result in more possibilities in interaction design than position-based friction modulation. This intuitively makes sense, because an extra variable (movement direction) is taken into account. The experiments with target acquisition use the position-based rendering method [6][7]. In these experiments the target acquisition task was always executed in one dimension and the targets were known to the user. However, if a target has to be found on a two dimensional touchscreen it is expected that the position-based rendering method would lack in the provided feedback. The user would have to explore the whole surface in a searching pattern to find a single area of high friction. It would be more intuitive if the user would be guided to the target, by making it easy to move towards and harder to move away from the target. This can be achieved by taking the direction of movement into account when modulating the friction. Movement towards the target would be rendered as low friction and movement away from the target as high friction. In

theory, this will provide the user with directional cues, and provide that not the whole screen has to be explored to find the target.

The specific calculations of this rendering method are provided in the paper, and the visualisation of this method is seen in Fig. E.1 for reference.

E.1. Experiment conditions

The pseudo-potential field that is used in the human factors experiment is a result of a number of pilot experiments (Appendix I). The final interaction design is governed by a combined potential field, consisting of a path attractor and a point attractor (Eq. E.1). The point attractor is modelled as an upside-down cone heightmap, with the target at the lowest point (Eq. E.2). The path attractor is given by the absolute of an arc tangent function, as in Eq. E.3. This results in a flat bottomed valley at the path location. The constant a is a scaling factor which is set to $\frac{1}{5}$. This value is determined such that the pseudo-potential field method has a similar maximum spatial change in friction as the position-based method. The vertical position of the valley is determined by y_{path}. This is one of the three possible path locations determined by the polynomial in Eq. E.4. The paths all start at the vertical center ($y = 240px$) and end at one of the target positions.

$$Z(x,y) = \frac{1}{2} \cdot Z_{path}(x,y) + \frac{1}{2} \cdot Z_{cone}(x,y) \tag{E.1}$$

$$Z_{\text{cone}}(x,y) = \sqrt{\left(x - x_{\text{target}}\right)^2 + \left(y - y_{\text{target}}\right)^2} \tag{E.2}$$

$$Z_{\text{path}}(x,y) = \left| \frac{1}{a} \cdot tan^{-1}(a \cdot (y - y_{\text{path}}(x))) - (y - y_{\text{path}}(x)) \right| \tag{E.3}$$

$$y_{path}(x) = \frac{-2 \cdot +T}{L^3}(x-100)^3 + \frac{3 \cdot +T}{L^2}(x-100)^2 + 240 \quad \text{for } x = [100 : 700],\ T = [-200 \text{ or } 0 \text{ or } 200],\ L = 600 \tag{E.4}$$

E.2. Gradient normalisation

For the pseudo-potential field rendering method to work, the gradient of the potential field has to be normalised to the possible vibration amplitude range of the device. Remember that the apparent frictional coefficient of the touch surface can only be reduced and not increased. For this reason, the 'neutral' friction should be at 50% of the vibration amplitude range. This way, the friction compared to the neutral point can be both increased and decreased. The gradient function is mapped to a range of $[-0.5, 0.5]$ using Eq. E.5. After multiplication with the unit velocity a constant of 0.5 is added to end up with a normalised friction range between 0 and 1. This range corresponds to the max vibration amplitude to no vibrations.

$$\mathbf{G}_{norm}(x,y) = \frac{\mathbf{G}(x,y)}{2|\mathbf{G}|_{max}} \tag{E.5}$$

F

Pseudo Code

The experiment is initialised by generating the array of trial data. This includes the randomised target positions, friction conditions and haptic strengths. This data is used in the main visual loop to communicate to the Teensy and to display the correct visuals. In algorithm 1 the pseudo-code on the Raspberry Pi is given. During the whole of the experiment, the while loop executes at 80 Hertz. In this loop the finger position is read from USB and the trial conditions are sent to the Teensy over UDP. A UDP message is send back with the normal force data. Continuously, the timestamps, finger position and force data is saved to a log. When a trial is finished, the summary data is also saved to a log file. The interaction of the different software functions and data streams are visualised in Fig. F.1.

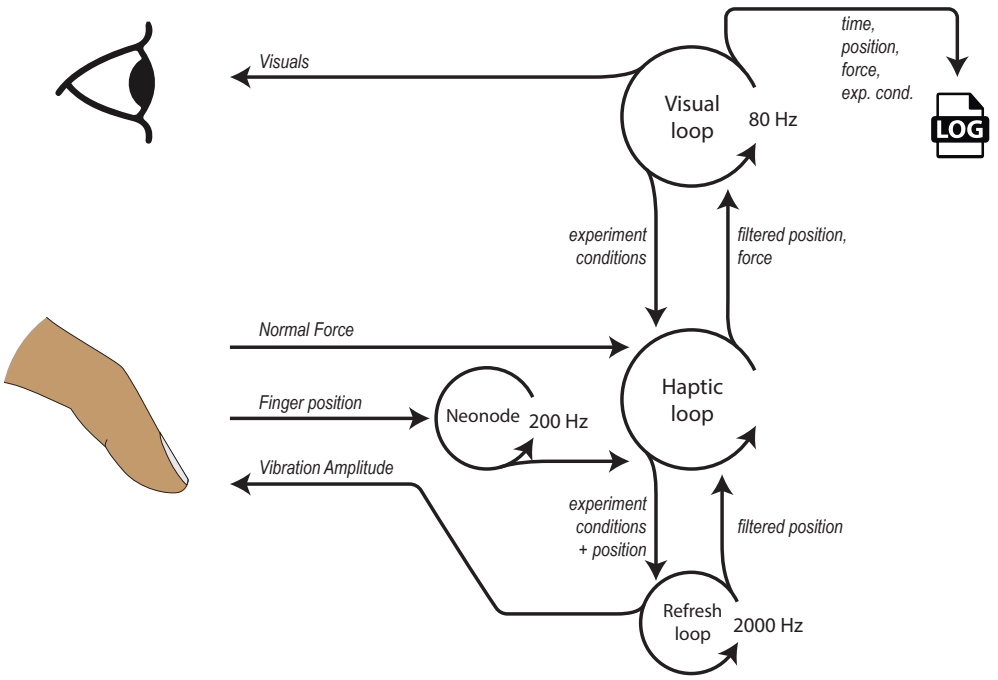

Figure F.1: Visualisation of the different software functions and data streams.

Algorithm 1 Visual Loop

```
target_pos[1 : 180] ← (top, middle or bottom)          % Predefined trial conditions
haptic_strength[1 : 180] ← (33, 66, or 100%)
friction_cond[1 : 180] ← (heightmap or frictionmap)
t ← 1                                                  % Trial Number
time ← 0
start_time ← 0
while t ≤ 180 do
    time ← get_system_time()
    x, y ← get_usb_mouse_position()
    sent_udp_data(target_pos[t], haptic_strength[t], friction_cond[t])
    force ← recieve_udp_data()
    detail_log ← csv_write(time, x, y, force)
    if x > 700 then
        trial_finished ← true
        crossing_pos ← y
        movement_time ← time − start_time
    end if
    if trial_finished then
        summary_log ← csv_write( movement_time, target_pos[t], crossing_pos, …
                                 friction_cond[t], haptic_strength[t])
        t ← t + 1
        trial_finished ← false
        start_time ← time
    end if
    display_update()
    wait(80fps)
end while
```

The main loop on the Teensy is given in algorithm 2. Here, the position data is sent over USB, the UDP data is read and the loadcell readings are send over ethernet. Also included are two interrupt functions. These are either activated externally by the neonode or internally by the teensy at 2000Hz. For the external interrupt (algorithm 3) the neonode position sensor indicates that data is ready to be read out. This is done in this function and the data needed for the extrapolation of the position data is recalculated. The extrapolation and filtering is done in the internal interrupt function (algorithm 4). The position data is first extrapolated and then filtered using an 1€-filter [8]. The algorithm and tuning of the filter is explained in detail in Appendix G. The unit velocity vector is also given by the filter function. The velocity vector is multiplied with the pre-calculated normalised gradient values (according to the haptic condition and target position) at the current position. This gives the modulation value when the system is requested to run at the full range. If the haptic strength is required to be lower, the output value is mapped to this requested range.

Algorithm 2 Haptic Loop

```
while true do
    if since_mouse_update > 3ms then                          % update mouse posittion
        since_mouse_update ← since_mouse_update − 3
        usb_mouse_moveto(x_filt, y_filt)
    end if
    if udp available then                                     % receive UDP data
        target_pos, haptic_strength, friction_cond ← recieve_udp_data()
    end if
    if since_Loadcell_update > 30ms then                      % Read and sent loadcell reading
        since_Loadcell_update ← since_Loadcell_update − 30
        load ← sum(read_analog_pins[1 : 4])
        load_mN ← 1.0712 · load · 9.81                        % convert to mN
        total ← total − buffer[idx]                           % use circular buffer
        buffer[idx] ← load_mN
        total ← total + buffer[idx]
        idx ← idx + 1
        if idx ≥ 5 then
            idx ← 0
        end if
        average ← total/5                                     % average over last 5 entries
        sent_udp_data(average)
    end if
    if external_neonode_interrupt then                        % approx. 200Hz
        read_position()
    end if
    if internal_interrupt then                                % set to 2000 Hz
        refresh_function()
    end if
end while
```

Algorithm 3 Interrupt: read_position()

```
x, y ← read_data_neonode()                                    % receive data over I²C
Ztime ← micros()                                              % get time since start program [micro sec]
deltaZtime ← Ztime − lastZtime
lastZtime ← Ztime
dx_raw ← x − x_last
dy_raw ← y − y_last
x_last ← x
y_last ← y
idx_extrapol = 0                                              % reset extrapolation index
```

Algorithm 4 Internal Interrupt: refresh_function()

```
Constants: sampletime ← 500micros
x_extrapol ← x + idx_extrapol * dx_raw/deltaZtime * sampletime
y_extrapol ← x + idx_extrapol * dy_raw/deltaZtime * sampletime
idx_extrapol ← idx_extrapol + 1
x_filt, dx_unit ← eurofilter(x_extrapol)
y_filt, dy_unit ← eurofilter(y_extrapol)
Gvalx, Gvaly ← read_gradient_value(friction_cond, target_pos, x_filt, y_filt)
output ← (dx_unit · Gvalx + dy_unit · Gvaly) + 0.5
output ← map_value_to_range(output, haptic_strength)
analogWrite(output)
```

G

1 Euro Filter design and tuning

The position measurements from the infrared position sensor (Neonode touch sensor module[1]) are noisy, resulting in unstable cursor positions. These noisy values are harder to interpret and makes target acquisition more difficult [9]. Because the position sensor itself cannot be changed to provide more precision in the measurements a filter is added to remove the jitter. However, by adding a filter lag will inherently be introduced. The 1-euro filter is used to tackle both the jitter and latency [8]. The algorithm uses a first order low-pass filter with an adaptive cutoff frequency. The value for cutoff frequency is changed according to the velocity. At high speeds the cutoff frequency is increased in order to reduce the lag, at the expense of more jitter. Vise versa for low speeds [8].

Before filtering the position data, the values are linearly extrapolated. The raw data is sampled at 200 Hz and two consecutive measurements are linearly extrapolated at a rate of 2kHz. As shown in Fig. G.1 the extrapolation captures the data well when moving at constant velocity but creates spikes, when the velocity changes. These spikes are filtered out using the filter.

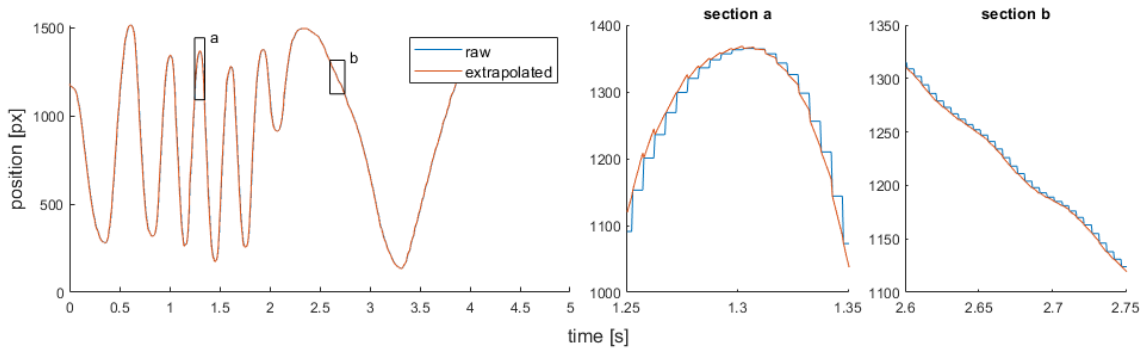

Figure G.1: Raw horizontal position data (blue) and the linearly extrapolated values (red).

The extrapolated position data (x_i) together with the previous filtered position ($\hat{x}_{i-1}$) is fed into the 1 euro filter algorithm. For completeness sake the outline and equations as described by Casiez et. al. [8] are included in this appendix.

[1] https://www.neonode.com/products-and-solutions/touch-sensor-modules/

At each timestep the filtered position ($\hat{x}_i$) is returned according to Eq. G.1. This is the discrete time realization of a first order low-pass filter, where α is the smoothing factor.

$$\hat{x}_i = \alpha_i \cdot x_i + (1 - \alpha_i) \cdot \hat{x}_{i-1} \tag{G.1}$$

This alpha value (α_i), traditionally fixed for low pass filter design, is dynamically adapted according to Eq. G.2 and Eq. G.3. Here the time constant τ_i is dependent on the cutoff frequency $f_{c,i}$. Included in these equations is the refresh rate ($f_r = 2kHz$).

$$\alpha_i = \frac{1}{1 + (\tau_i \cdot f_r)} \tag{G.2}$$

$$\tau_i = \frac{1}{2\pi f_{c,i}} \tag{G.3}$$

The cutoff frequency is determined according to a linear relationship with the absolute speed, as in Eq. G.4. The values introduced here; the minimum cutoff frequency ($f_{c,min}$) and the slope (β) are to be tuned by the designer.

$$f_c = f_{c,min} + \beta \cdot |\hat{dx}| \tag{G.4}$$

The derivative of the position (i.e. velocity) is computed by taking the difference between the last filtered position and the current raw position, as in Eq. G.5 and filtering this value using a low pass filter (Eq. G.6).

$$dx_i = (x_i - \hat{x}_{i-1}) \cdot f_r \tag{G.5}$$

$$\hat{dx}_i = \alpha \cdot dx_i + (1 - \alpha) \cdot \hat{dx}_{i-1} \tag{G.6}$$

Here the value for alpha is not changed dynamically, but rather has a fixed value. This is calculated as in Eq. G.2 and Eq. G.3 but with a fixed cutoff frequency of $f_{c,dx} = 1Hz$.

According to Casiez et. al. the resulting values that need manual tuning are: $f_{c,min}$ and β [8]. However, in their work the cutoff frequency for the derivative values is set to a fixed value of $f_{c,dx} = 1Hz$. Inspecting the recorded position data together with the velocities (Fig. G.2) it would not be correct to adopt the same cutoff frequency. Clearly visible in the velocity graph is the large lag.

Contrary to the tuning procedure as described by Casiez et. al.[8], first the cutoff frequency for the derivative is tuned to reduce the lag. To ease the tuning process a single data sequence is recorded on the Teensy, after which the tuning is done in Matlab. The derivative cutoff frequency is slowly increased while observing the resulting figures. With a value of $f_{c,dx} = 25Hz$ the filtered velocity is in better agreement with the raw velocity (Fig. G.3). However, a large disagreement still exists with the actual data, when comparing the position data and velocity data in section a. Here the velocity has the same phase as the raw and extrapolated position data, which is incorrect.

From here the same tuning process as described by Casiez et. al. [8] is picked up on. The minimum cutoff frequency $f_{c,min}$ is increased to adjust for the large lag. With a value of $f_{c,min} = 20Hz$ the lag is reduced and the phase difference between position and velocity is correct (Fig. G.4).

The final step of the tuning is done by slowly increasing β. With the final values of the tuning process being $f_{c,min} = 20Hz$, $\beta = 0.0004$ and $f_{c,dx} = 25Hz$ the extrapolated position values are filtered nicely without introducing to much lag (Fig. G.5). The tuned filter values are implemented in the Arduino program for both the x and y position. As a final check the two conditions (with and without filter) are visually compared when using the touchscreen.

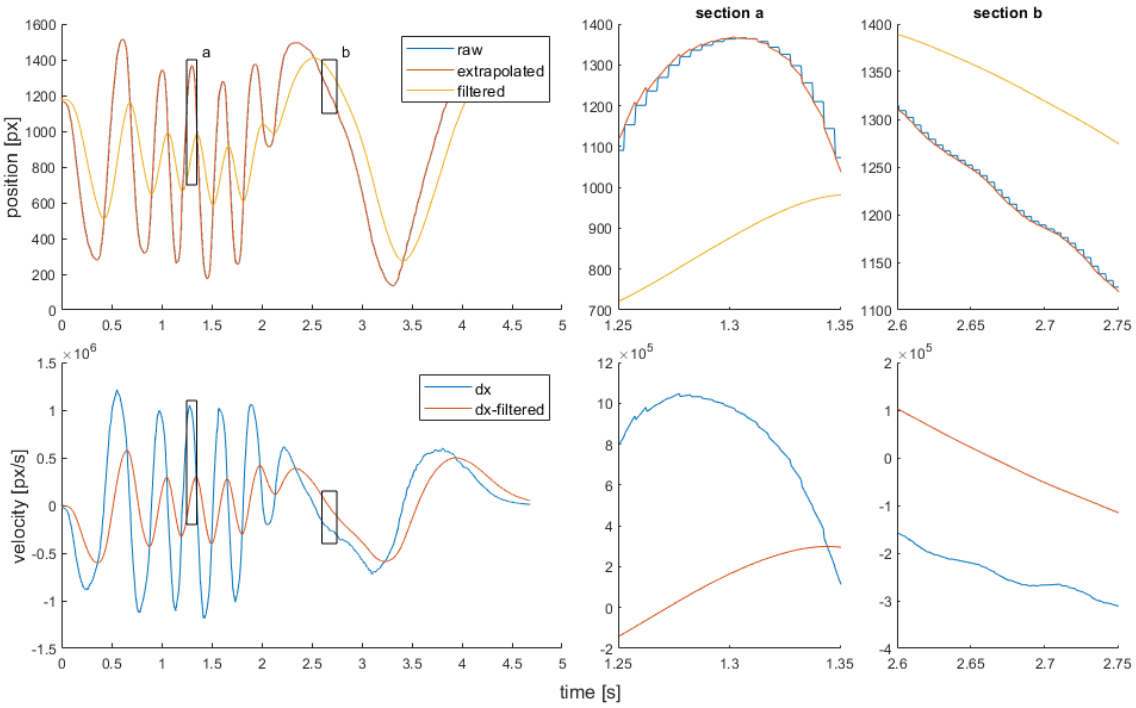

Figure G.2: Position and velocity data for the starting values for tuning: $f_{c,min} = 1Hz$, $\beta = 0$ and $f_{c,dx} = 1Hz$

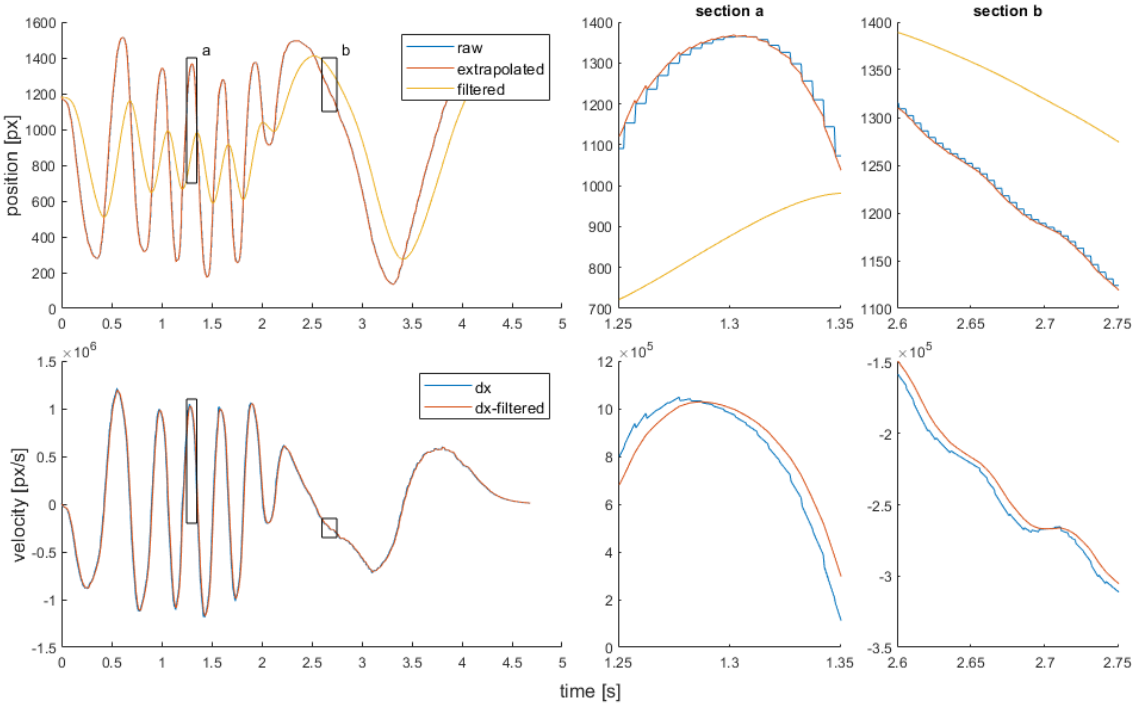

Figure G.3: Position and velocity data for the filter values: $f_{c,min} = 1Hz$, $\beta = 0$ and $f_{c,dx} = 25Hz$

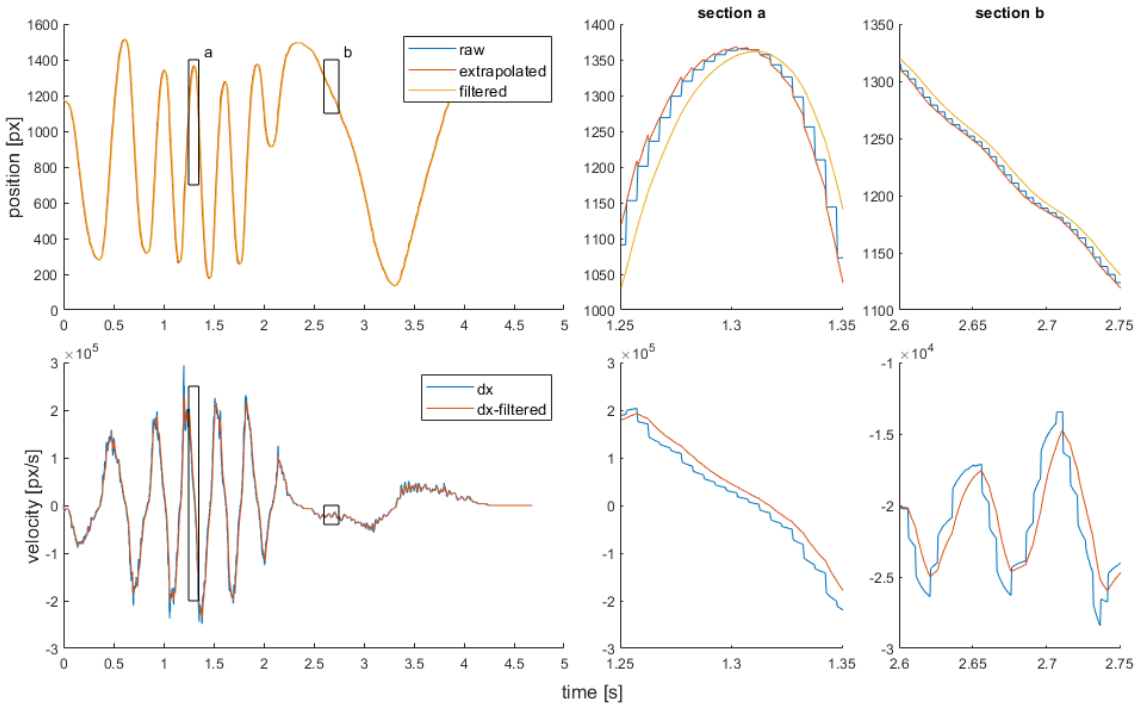

Figure G.4: Position and velocity data for the filter values: $f_{c,min} = 20Hz$, $\beta = 0$ and $f_{c,dx} = 25Hz$

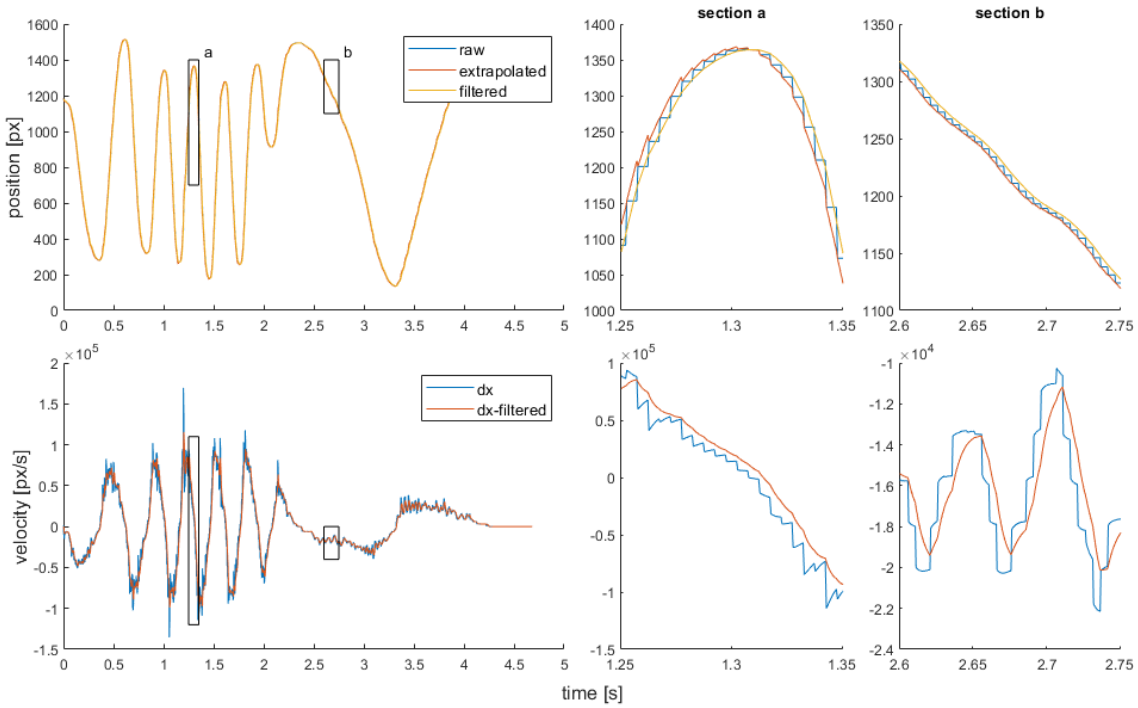

Figure G.5: Position and velocity data for the filter values: $f_{c,min} = 20Hz$, $\beta = 0.0004$ and $f_{c,dx} = 25Hz$

Safety and Ethics

To ensure the safety of the participants as well as the secure processing of their personal data, several procedures are followed.

An inspection report (page 50) is written by the author, which provides the general working principles of the haptic touchscreen and lists any potential hazards, together with their mitigation measures. This document is inspected, together with the physical setup of the experiment, by the safety manager of the faculty of mechanical engineering at the TU Delft.

A data management plan is constructed as well, to provide the safe storage of the personal data of the participants. The study includes the collection of the participants' age, gender and handedness. This personal data, as well as the experiment data is stored with only a participant number as reference. The participant name is only written on the consent form, which is not linked to any participant number. The participant itself holds their own participant number as a key, should a request of data removal be filed. The consent form (page 57) is signed by the participant before the experiment, to make sure that it is understood what the experiment entails, what the risks are, how the data is used and what the procedure of withdrawal is.

An additional checklist (page 58) for the ethics review is composed. This includes a small summary of the research and a risk assessment checklist. This document is sent to the ethics committee, together with the inspection report, data management plan, participant information letter and consent form. The procedure of the experiment is approved by the Human Research Ethics Committee on 21-01-2022 with ID 1980.

Delft University of Technology
INSPECTION REPORT FOR DEVICES TO BE USED IN CONNECTION WITH HUMAN SUBJECT RESEARCH

This report should be completed for every experimental device that is to be used in interaction with humans and that is not CE certified or used in a setting where the CE certification no longer applies[1].

The first part of the report has to be completed by the researcher and/or a responsible technician.

Then, the safety officer (Heath, Security and Environment advisor) of the faculty responsible for the device has to inspect the device and fill in the second part of this form. An actual list of safety-officers is provided on this webpage.

Note that in addition to this, all experiments that involve human subjects have to be approved by the Human Research Ethics Committee of TU Delft. Information on ethics topics, including the application process, is provided on the HREC website.

Device identification (name, location): Haptic touchscreen, Cognitive Robotics lab (TU Delft, 3me, 34-F-0-470)

Configurations inspected[2]: NA

Type of experiment to be carried out on the device:[3] Human factors experiment where participants have to find a way through a maze using a touchscreen that provides haptic feedback via friction modulation.

Name(s) of applicants(s): Dr. Michaël Wiertlewski

Job title(s) of applicants(s): Assistant professor

(Please note that the inspection report should be filled in by a TU Delft employee. In case of a BSc/MSc thesis project, the responsible supervisor has to fill in and sign the inspection report.)

Date: 02/12/2021

Signature(s): 

1 Modified, altered, used for a purpose not reasonably foreseen in the CE certification

2 If the devices can be used in multiple configurations, otherwise insert NA

3 e.g. driving, flying, VR navigation, physical exercise, ...

Setup summary

The experimental device pictured below (Fig. 1) will be used to test the hypothesis, whether a haptic shared control principle can be applied on a friction modulated touchscreen. Participants will be interacting with the device by moving their index finger across a glass plate mounted above an LCD screen.

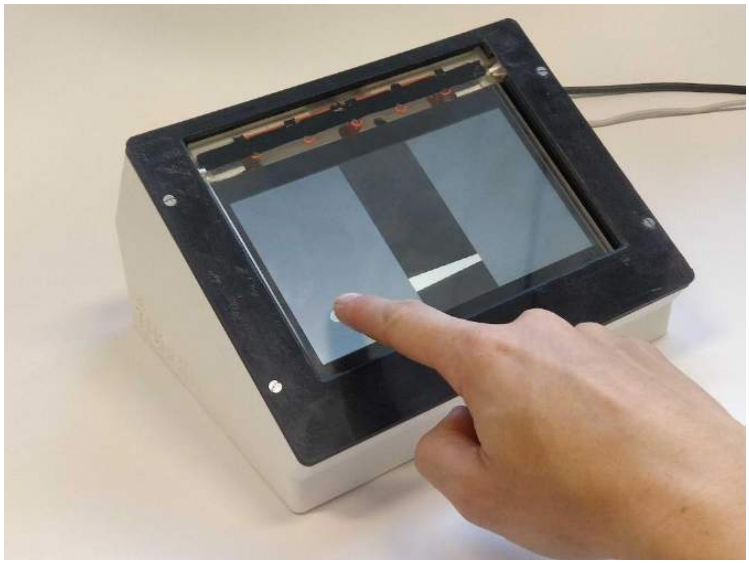

Figure 1: Haptic Touchscreen.

While exploring and interacting with the device, participants will feel changing friction forces. The modulation of friction force is controlled by ultrasonic lubrication. To achieve lubrication, the glass plate is actuated at an ultrasonic frequency, which levitates the skin slightly above the plate (Fig 2a and b). This levitation reduces the effective friction between the user's finger and the glass plate. By combining the modulation of the friction with the visuals presented on the LCD screen placed below this surface (Fig 2c) a multi-modal interaction can be achieved.

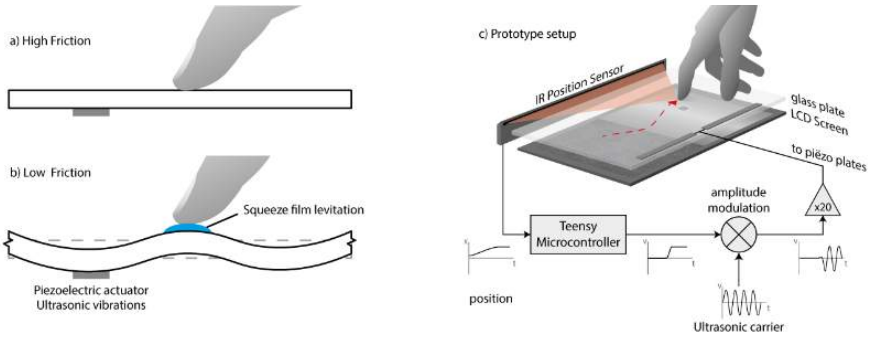

Figure 2: Schematic overview of the working principles of the haptic touchscreen.

Friction Modulation

The friction at the object-fingertip interface can be decreased by vibrating the glass plate at ultrasonic frequencies. Due to squeeze film levitation and intermittent contact the friction is reduced. In this particular device, the 2mm-thick glass plate is actuated by 12 piezoelectric actuators, glued to the underside of the glass plate and not accessible to the participant. The driving signal is an amplitude modulated sinewave of 35kHz with 200Vpp. The signal is fed to the piezoelectric actuators which excite the resonance of the plate and control the amplitude of the vibrations in a range of [0, 5] µm. This results in a wide range of friction coefficients that can be controlled, during the use of the touchscreen.

The frequency at which the glass plate is actuated is chosen such that a mode shape with only horizontal nodal lines is excited. This results in the most uniform profile across the interactive area. This eigenfrequency is around 34.8kHz and corresponds to mode shape (0,12), as seen in Fig. 3.

The piezoelectric actuators (STEMiNC, SMPL26W8T07111) are placed in two rows of six on the far ends of the glass plate, all on the underside of the surface. The placement is such that the actuators are at an antinode to provide optimal power transfer from the electrical domain to the mechanical domain.

The glass plate is held in place by four 3D-printed fixtures. These are placed at the antinodes, where the vibration amplitudes are minimal. The fixtures are friction fitted around the glass edge.

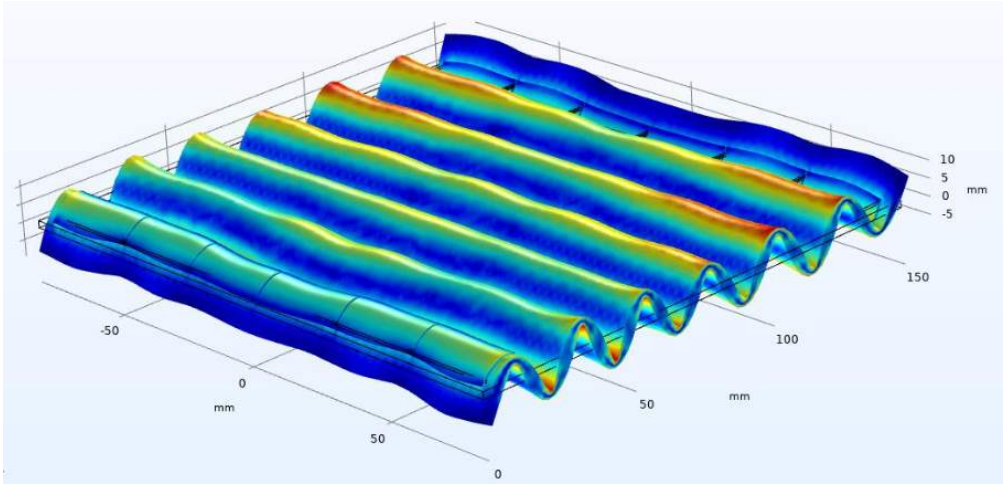

Figure 3: FEM of the glass plate with piezoelectric actuators showing the mode shape.

Visuals

The visual feedback is provided by a LCD screen placed below the glass plate. This screen is connected to a Raspberry Pi, running a python script which provides the required visuals.

Electrical circuit

A teensy 3.6 microcontroller is used as a central processing unit which ties the individual components together. This microcontroller provides the haptic feedback, and reports the finger position to the Raspberry Pi. An overview of all connections between the different components can be seen in figure 4 and will be further explained below.

Neonode position sensor

A Neonode position sensor is used to measure the location of the user's finger. This sensor is placed near the top edge of the glass plate and uses infrared light emitters and detectors embedded in a thin strip. The array emits short pulses of light just above the glass plate. Any objects in the light path cause intensity shifts in the received light. This information is used to track any object and reports its position to the microcontroller using I^2C. In the case of the experimental setup the object being the participant's index finger.

Loadcells

For the friction modulation to work optimally, users should not exert to much force on the glass plate. The force is measured using four strain gauge loadcells (Phidgets, CZL616C) located at each corner of the glass plate, directly below the 3D-printed plate fixtures. The measurements are summed and provided as visual feedback to the participant.

Custom PCB

The electrical components are connected to a custom PCB tying all components and connections together. The output of this PCB is an amplitude modulated signal, with a maximum amplitude of 5V.

Amplifier

The driving signal (output of the PCB) is split into two and amplified by a set of low noise linear amplifier (PiezoDrive PD200) with an amplification factor of x20. The maximum output of these devices is a signal with an amplitude of 100V. The output of the amplifiers is fed back into the case and is connected to the piezoelectric actuators. Each amplifier actuates one row of piezo of six piezoelectric actuators.

Data Acquisition

The position data is stored using the Python script on the Raspberry Pi. During the experiment this data is stored locally on the raspberry pi using .csv files. These can be accessed and analyzed by the researches after the experiment.

Case

The case is 3D printed and houses all electronics, except for the two linear amplifiers. The casing isolates the electronic circuits. The connections going to and from the linear amplifiers are done by using coaxial BNC cables. None of the electronic connections can be touched by the participant or experimenter during the experiments, including the piezoelectric actuators.

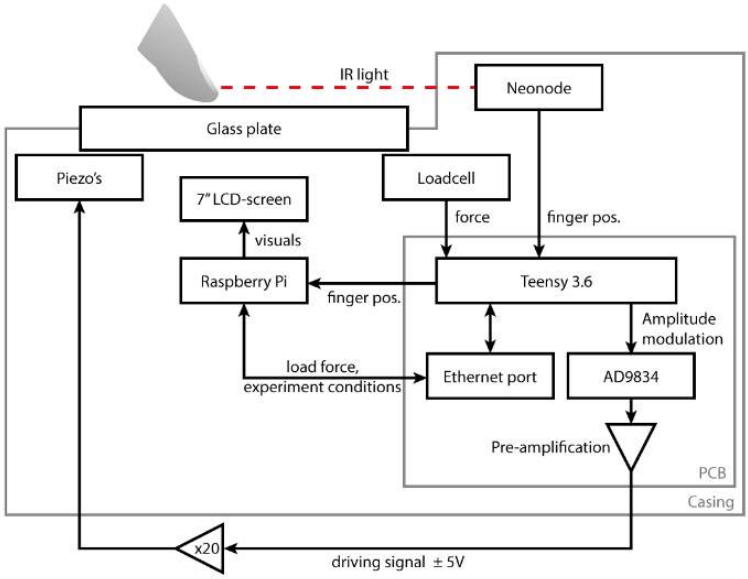

Figure 4 schematic overview of the haptic touchscreen

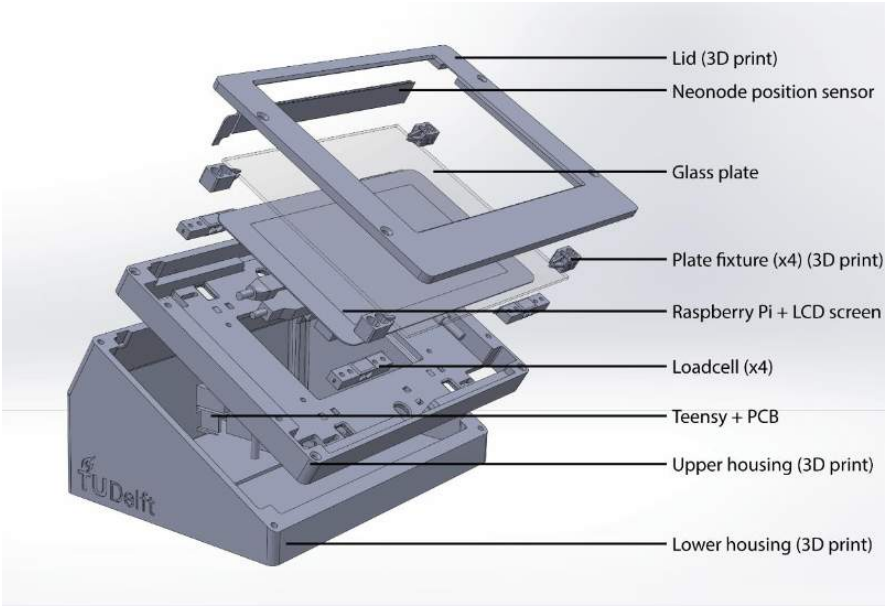

Figure 5 exploded view of the haptic touchscreen

Risk checklist

Please fill in the following checklist and consider these hazards that are typically present in many research setups. If a hazard is present, please describe how it is dealt with.

Also, mention any other hazards that are present.

Hazard type	Present	Hazard source	Mitigation measures
Mechanical (sharp edges, moving equipment, etc.)	No		
Electrical	Yes	High voltage (max ±150V) driving signal for piezoelectric actuators	Isolation of the electrical circuits to avoid contact with participants and researchers.
Structural failure	No		
Touch Temperature	Yes	Possibility of gradual heating through the glass due to heat produced by the piezoelectric actuators	Allow for unobstructed reaction reflexes
Electromagnetic radiation	No		
Ionizing radiation	No		
(Near-)optical radiation (lasers, IR-, UV-, bright visible light sources)	Yes	Low power IR emitted by the neonode zForce position sensor	Low power source is non-hazardous according to manufacturer.
Noise exposure	Yes	Audible frequencies can be excited due to nonlinearities	Wearing noise-cancelling headphones
Materials (flammability, offgassing, etc.)	No		
Chemical processes	No		
Fall risk	No		
Other:			
Other:			
Other:			

Device inspection

(to be filled in by the AMA advisor of the corresponding faculty)

Name: Peter Kohne

Faculty: 3mE/IO

The device and its surroundings described above have been inspected. During this inspection I could not detect any extraordinary risks.

(Briefly describe what components have been inspected and to what extent (i.e. visually, mechanical testing, measurements for electrical safety etc.)

Zelf ondervonden hoe het apparaat veilig werkt.

Date: 11-01-2022

Signature: 

Inspection valid until[4]:

Note: changes to the device or set-up, or use of the device for an experiment type that it was not inspected for require a renewed inspection

4 Indicate validity of the inspection, with a maximum of 3 years

– CONSENT FORM –

Effect of haptic feedback, using ultrasonic friction modulation, on the use of a touchscreen

Please tick the appropriate boxes	Yes	No
Taking part in the study		
I have read and understood the study information dated __/__/____, or it has been read to me. I have been able to ask questions about the study and my questions have been answered to my satisfaction.	○	○
I consent voluntarily to be a participant in this study and understand that I can refuse to answer questions and I can withdraw from the study at any time, without having to give a reason.	○	○
I understand that taking part in the study involves: - Indicating your name, age, gender and handedness. - Interacting with a touchscreen interface while finger position, applied forces and object vibrations are acquired using dedicated measuring equipment.	○	○
Risks associated with participating in the study		
I understand that taking part in the study involves the following risks: a low risk of an electrical shock and possible muscle fatigue.	○	○
Use of the information in the study		
I understand that information I provide will be used for reports, publications, and courses in-line with the original research purpose for which data is collected.	○	○
I understand that personal information collected about me that can identify me, such my name, will not be shared beyond the study team.	○	○
Future use and reuse of the information by others		
I give permission for the **non-personal** data that I provide to be archived in 4TU.ResearchData so it can be used for future research and learning.	○	○

Signatures

_____	_____	_____
Name of Participant	Signature	Date

I have accurately read out the information sheet to the potential participant and, to the best of my ability, ensured that the participant understands to what they are freely consenting.

_____	_____	_____
Researcher name	Signature	Date

Study contact details for further information: Tammo Brans, +31 6 18458259, t.j.brans@student.tudelft.nl

Delft University of Technology
ETHICS REVIEW CHECKLIST FOR HUMAN RESEARCH
(Version 12.03.2021)

*This checklist should be completed for every research study that involves human participants and should be submitted **before** potential participants are approached to take part in your research study.*

All submissions from students doing their Master's thesis need approval from their research supervisor (responsible researcher) who indicates their approval of the content and quality of the submission through signing and dating this form (or providing approval via email).

Additional elements of research compliance:
There are various aspects of human research compliance which fall outside the remit of the HREC as follows:

1) **The Data Steward of your faculty and/or the TUD Privacy Team** privacy-tud@tudelft.nl can help you with any issues related to the protection of personal data – including how data are processed and stored, and the informed consent that is required for legal compliance with GDPR.
2) **Research related to medical questions/health may require special attention**. See also the website of the CCMO before contacting the HREC.
3) **Your faculty HSE representative** should provide advice on any health, safety and environmental requirements including non-CE certified experimental devices, covid regulations, liability and insurance etc
4) **Your faculty/departmental contract managers** may also provide advice on, eg: procurement and working with third parties
5) **Professional standards/best practice** – there may be professional standards determined within different research disciplines with which you are expected to comply.

Submission and additional Information:
You can find more instructions and additional information on your application here.

IMPORTANT NOTICES:
*1: Please ensure that this form is properly signed and dated **by the responsible researcher** before submission. In the case of a student research project the responsible researcher must be the project supervisor.*
*2: Please note that incomplete submissions (either in terms of documentation or the information provided therein) will be returned for completion **prior to any assessment by the HREC.***
3: Please note that participants should always direct queries and complaints regarding their participation to the responsible researcher(s) and not the HREC. Please therefore do not list HREC as a point of contact for participants in your research documentation (e.g., informed consent form).

I. Table 1: Basic Data

Project title:	Effect of haptic feedback, using ultrasonic friction reduction, on the use of a touchscreen.
Research period (planning):	April 2021 – March 2022
Faculty:	3ME
Department:	CoR
Level of the research project:	Masters

Eg: Masters, PhD, Postdoc, Tenure Track, Permanent Researcher, Organisational	
Funder of research: Eg: EU, NWO, TUD, other (in which case please elaborate)	TUD
Name of corresponding researcher (if different from the responsible researcher):	Tammo Brans
E-mail corresponding researcher (if different from the responsible researcher):	t.j.brans@student.tudelft.nl
Position of corresponding researcher: Eg: Masters, PhD, Postdoc, Professor	Masters
Name of responsible researcher: Note: all student work must have a named supervisor who must approve, sign and submit this application	Michaël Wiertlewski
E-mail of responsible researcher: This must be an institutional email address (ie: not google etc)	M.Wiertlewski@tudelft.nl
Position of responsible researcher : Eg: PhD, Posdoc, Professor	Professor

II. Summary Research

With ultrasonic friction modulation a haptic effect can be generated on a flat touchscreen interface. The friction at the touchsreen-fingertip interface can be changed by modulating the vibration amplitude of the glass plate at ultrasonic frequencies. Due to squeeze film levitation and intermittent contact the friction is reduced. By combining the haptic feedback with visuals on the touchscreen a multi-modal interaction is achieved.

By presenting a virtual haptic heightmap the finger is effectively assisted in the movement towards valleys and restricted in moving uphill. It is tested whether this principle of haptic feedback can assist people in navigating paths and mazes with their finger. The research question "*Can friction modulation assist people in the interaction with a touchscreen"* will be tested using an in-house built touchscreen with friction modulation capabilities.

Healthy adult participants will be invited to interact with the touchscreen for no longer than a hour. The exact number of participants will be determined after conducting a pilot experiment, which will be conducted after the approval of the HREC. The amount of participants will not exceed 30.

III. Table 2: Risk Assessment Checklist

Potential Risk	Yes	No
1. Does the study involve participants who are particularly vulnerable or unable to give informed consent? (e.g., children, people with learning difficulties, patients, people receiving counselling, people living in care or nursing homes, people recruited through self-help groups).		x
2. Are the participants, outside the context of the research, in a dependent or subordinate position to the investigator (such as own children or own students)?[1]		x
3. Will it be necessary for participants to take part in the study without their knowledge and consent at the time? (e.g., covert observation of people in non-public places).		x

[1] **Important note concerning questions 1 and 2.** Some intended studies involve research subjects who are particularly vulnerable or unable to give informed consent. This includes research involving participants who are in a dependent or unequal relationship with the researcher or research supervisor (e.g., the researcher's or research supervisor's students or staff). If your study involves such participants, it is essential that you safeguard against possible adverse consequences of this situation (e.g., allowing a student's failure to complete their participation to your satisfaction to affect your evaluation of their coursework). This can be achieved by ensuring that participants remain anonymous to the individuals concerned (e.g., you do not seek names of students taking part in your study). Please ensure that you include such risks – and how you will mitigate against them in your risk section.

Potential Risk	Yes	No
4. Will the study involve actively deceiving the participants? (For example, will participants be deliberately falsely informed, will information be withheld from them or will they be misled in such a way that they are likely to object or show unease when debriefed about the study).		x
5. Will the study involve discussion or collection of personal sensitive data (e.g., financial data, location data, data relating to children or other vulnerable groups)? Definitions of sensitive personal data, and special cases are provided on the TUD Privacy Team website.		x
6. Will drugs, placebos, or other substances (e.g., drinks, foods, food or drink constituents, dietary supplements) be administered to the study participants? *If yes see here to determine whether medical ethical approval is required*		x
7. Will blood or tissue samples be obtained from participants? *If yes see here to determine whether medical ethical approval is required*		x
8. Is pain or more than mild discomfort likely to result from the study?		x
9. Does the study risk causing psychological stress or anxiety or other harm or negative consequences beyond that normally encountered by the participants in their life outside research?		x
10. Will you be offering any financial, or other, inducement (such as reasonable expenses and compensation for time) to participants?		x
Important: if you answered 'yes' to any of the questions mentioned above, you **MAY** be asked to submit a full Research Ethics Application.		
11. Will the experiment collect and store any personally identifiable information (PII) including name, email address, videos, pictures, or other identifiable data of human subjects? [2]	x	
12. Will the experiment involve the use of devices that are not 'CE' certified? *Only, if 'yes': continue with the following questions:*	x	
➢ Was the device built in-house?	x	
➢ Was it inspected by a safety expert at TU Delft? (*Please provide a signed device report*)	x	
➢ If it was not built in house and not CE-certified, was it inspected by some other, qualified authority in safety and approved? *(Please provide records of the inspection).*		x
13. Has this research been approved by a research ethics committee other than this one? *If yes, please provide a copy of the approval and summarise any key points in your Risk Management section below.*		x
14. Is this research dependent on a Data Transfer Agreement with a collaborating partner or third party supplier? *If yes please provide as a copy of the signed DTA and summarise any key points in your Risk Management section below.*		x

[2] Note: You have to ensure that collected data is safeguarded physically and will not be accessible to anyone outside the study. Furthermore, the data has to be de-identified if possible and has to be destroyed after a scientifically appropriate period of time. Also ask explicitly for consent if anonymised data will be published as open data.

IV. **Risk management and Informed Consent**

A: Risk management

Collection and storing of personal data: (question 11 risk assesment)

Data collected from participants concerns their age, gender and left/right-handedness. The forms will be stored in a locked cabinet and are de-identified for the use of the study. The consent to publish anonymised data will be included in the consent form. Participants will be asked to sign this form before the start of the experiment. If no consent is given the collection of data will not take place.

Risk management of the in-house built device: (question 12 risk assesment)

The device uses high voltage piezoelectric transducers to induce ultrasonic vibrations of a glass plate. Contact with the electrical circuit driving these actuators can result in electrical shock. These electrical circuits are properly isolated to avoid any contact and electrical shock. The device is inspected by the safety manager and the signed device report is included as an eclosure.

Risks regarding SARS-COV-2:

The setup is touched by the participants and will be disinfected before and after the experiment using isopropyl alcohol to limit the spread of any virus. Participants are also asked to wash their hands before starting the experiment. The distance between participant and researcher can be maintained to be larger than 1.5 meters. Any current covid-related measures endorsed by the RIVM or TU Delft at the time of the experiment will be implemented (e.g. wearing face masks covering nose and mouth). Participants are instructed to refrain from participating, and stay at home, if they have coronavirus symptoms. The same holds for when the experimenter has coronavirus symptoms.

B: Informed Consent

The participant information letter as well as the informed consent form is presented to the participant before the experiment starts. It includes the information on what the study entails, what the potential risks are and what mitigation measures are taken against those risks.
The Informed Consent form is included as enclosure in this application.

Please note that by signing this checklist list as the sole/responsible researcher you are providing approval of the content and quality of the submission, as well as confirming alignment between GDPR, Data Management and Informed Consent requirements.

V. **Signature/s**

Name of corresponding researcher (if different from the responsible researcher)
Tammo Brans

Signature of corresponding researcher: 

Date: 14 jan 2022

Name of responsible researcher
Michaël Wiertlewski

Signature (or upload consent by mail) responsible researcher: 

Date: 14/01/2022

VI. Additional enclosures

Please, tick the checkboxes for any additional submitted enclosures as follows:

- A data management plan reviewed by a data-steward.
- (If requested by the HREC) a full research ethics application
- An Informed Consent form
- A signed, up-to-date device report
- Submission details to an external research ethics committee, and a copy of their approval if available.
- An approved Data Transfer Agreement with a third party
- Specific advice/approval from a Data Steward or TU Delft Privacy Team regarding eg: a Data Privacy Impact Assessment – or (where data are potentially sensitive and Privacy Team advice has been sought) confirmation that no DPIA is required
- Specific advice/approval from an HSE representative regarding a specific experimental set-up.
- Other – please explain in the table below:

Document name	Brief description

Pilot Experiments

Before starting the main experiment, two different pilot experiments are executed with several iterations. These pilot experiments provided valuable insights in the working principles and limitations of the haptic touchscreen. The pilot experiments are explained below, together with the main findings. This also includes valuable comments from the participants in these pilot studies, which are noted down by the experimenter during and after the trials.

I.1. Pilot A - Steering law

The primary idea of this experiment originated from the the extension of Fitts' law [10] experiments conducted by Levesque et. al. [7] and Casiez et. al. [6] showing the added benefit of haptic friction feedback on target acquisition tasks. The question was raised whether this principle could be extended to the steering law [1] as well. A feedback modality that improves on the metrics in the steering law related tasks would be helpful for shared control tasks, where the user is guided by the intentions of the computer during the execution of a command.

During this pilot, 1 participant (male, right handed) was invited to partake in the experiment. During the trials the participant was asked to start at the left side of the screen and move to the right, across a highlighted path (an example of this visual feedback is seen in Fig. I.1). This straight horizontal path varied in length and the width at both the start and end, resulting in different Indexes of difficulty. While navigating this path, the haptic feedback consisted of 1 of three conditions: Converging, Diverging or Neutral. In the converging condition the path is located on a virtual valley, where high friction is rendered when moving away from the center line and low friction when moving towards the center line, essentially assisting the user to stay on track. Vice versa for the diverging condition, hindering the user in staying on track. In the neutral condition the amplitude of the vibrations was set to 50 percent to provide a reference without haptic feedback.

Figure I.1: Visual representation of a single trial. Path is in white and at the position of the finger, a circle is rendered as a cursor.

The independent variables consisted of the following:

- Tunnel length, $L = [200, 400, 500, 600]px$
- Width start, $W_{start} = [20, 40, 60]px$
- Width end, $W_{end} = [20]px$
- Haptic condition, [Converging, Diverging, Neutral]

The haptic heightmap is calculated using the formula:

$$H = \left| width(x) \cdot \arctan\left(\frac{1}{width(x)} \cdot (y - y_{center})\right) - (y - y_{center}) \right| \tag{I.1}$$

Where the width is a linear interpolation between the width at the start and end of the path. The lowest point of the heightmap is located at the vertical center of the screen, hence the required offset of $y_{center} = 240$. This specific formula is chosen, because the slope approaches 1 and -1, has a flat bottom at the center of the path and is continuous throughout its range. This ensures that the gradient is easily calculated. The resulting heightmap and gradient can be seen in Fig. I.2. These calculations result in the heightmap associated with the converging haptic condition. The gradient values needed for the diverging conditions can be easily calculated by multiplying the gradient by -1. This makes the calculations straightforward without the need of calculating an individual heightmap for this condition.

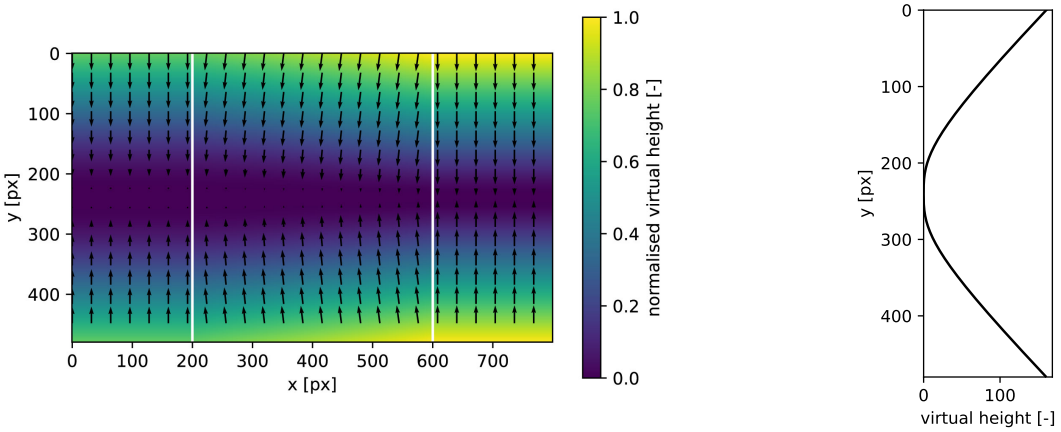

(a) The x coordinates of the start and end of the path are visualised by two white lines. The resulting 2 dimensional gradient is visualised by the quivers.

(b) Heightmap cross section view at the start of the path, x = 200

Figure I.2: Virtual heightmap of a presented path with $W_{start} = 60$, $W_{end} = 20$, $L = 400$ and the converging haptic condition. This corresponds to the visual feedback as in Fig. I.1

According to the steering law formula (Eq. I.2), the different path dimensions result in 12 Indexes of Difficulty. Together with the three friction conditions a total of 36 unique trials are presented in random order. These trials are presented in 2 sets such that the full experiment exists of 72 trials.

$$ID = \frac{L \cdot (\ln|W_{end}| - \ln|W_{\text{start}}|)}{W_{end} - W_{start}} \tag{I.2}$$

It is hypothesised that the trials conform to the steering law, where the converging feedback will help the participants execute the task faster. On top of that, the hypothesis that the converging haptic feedback will result in less deviation from the center line is tested.

I.1.1. Results

Fig. I.3 shows the movement time per index of difficulty. According to the fits law, this should follow a linear relationship as follows $t_{movement} = a + b \cdot ID$. As seen in the graph the general trend seems to

follow this linear relationship. However there seems to be a large spread in each condition, resulting in low R-squared values.

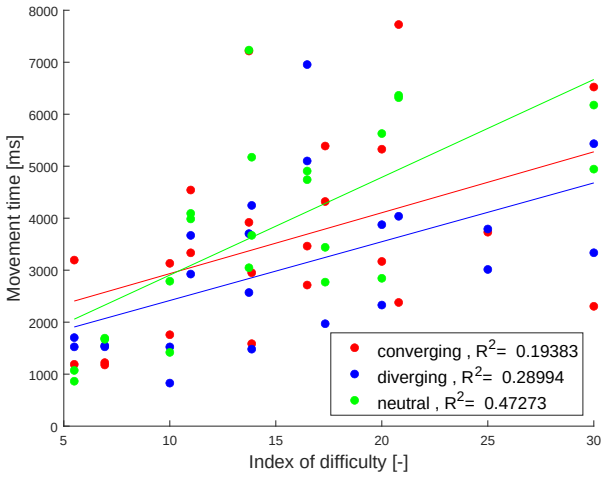

Figure I.3: Time in milliseconds spend plotted against the Index of Difficulty. A linear fit is visualised for each haptic condition

In Fig. I.4 the histogram of the velocity vectors is plotted for all trials. It can be seen here that the movement of the participant is mainly in the x-direction and not many deviations in y-direction are observed. Though the feedback is only effective when there is movement in y-direction.

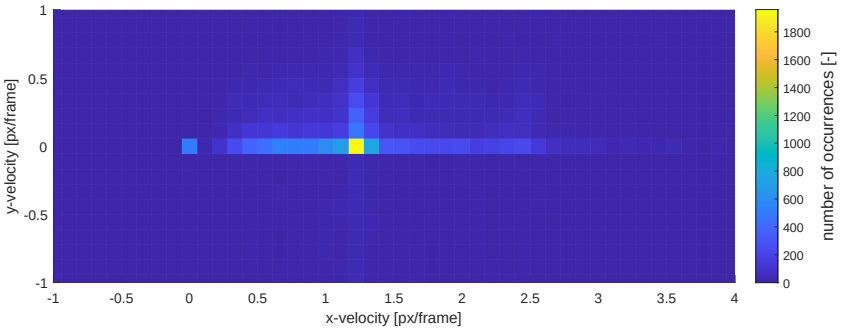

Figure I.4: Histogram of the velocity vectors during execution of the trials.

I.1.2. Written notes

During the experiment written notes are made by the experimenter. The observations and comments from the participant include:

- Position errors occur resulting in jittery movement of the cursor
- The visual feedback provided during the trial results in a ballistic movement.
- The amplitude of the vibrations might not be high enough to provide adequate haptic feedback

I.1.3. Findings

Visual feedback and ballistic movement seem to dominate the resulting finger paths. The haptic feedback is not strong enough to provide any substantial feedback to the user to improve the task or make the task easier. The amplitudes of the ultrasonic vibrations in the glass plate are not large enough. The finger position readings from the optical position sensor are noisy. This causes a jittering motion of the mouse cursor. Extrapolating and smoothing finger position measurements might improve the interaction, both visually and haptically.

I.2. Pilot B - Steering law

The following pilot experiment was conducted in a similar fashion to that of Pilot A. The main research idea was the same. Several paths with different Indexes of Difficulty were displayed, while varying the haptic conditions. Before the experiment, several improvements and changes were implemented. First of all, the amplitude of the vibrations in the glass plate was increased. This was done by increasing the number of piëzo's as well as using a different glue to attach them. The glue made a significant impact as the amplitude was tripled by using a the different glue. Secondly, the 1-euro filter is implemented to make the position measurements more smooth. Thirdly, the visual feedback of the location and geometry of the path is removed once the participant entered the path in an attempt to make the participant rely more on the haptic feedback. The path of each trial was also assigned a random vertical position. Previously the optimal path position was always at the same y-coordinate, resulting in a repeating ballistic movement. The randomised positions were limited to a finite number of predefined positions, such that the center of each path is located at a theoretical anti nodal line. Lastly the haptic heightmap was converted to a more narrow valley by scaling. The formula is changed to:

$$H = \left| \frac{width(x)}{s} \cdot \arctan\left(\frac{s}{width(x)} \cdot (y - y_{center})\right) - (y - y_{center}) \right| \tag{I.3}$$

Where previously the scale (s) was set to 1, in the new experiment a value of 10 is used. A comparison of the cross sections between the two scales can be seen in Fig. I.5. This essentially increases the contrast in haptic feedback when crossing the path perpendicularly. Also a larger range of amplitudes will be utilised because the gradient is higher, close to the center of the path. This change was included because it was observed that the variation in y-position was relatively low in the previous pilot experiment.

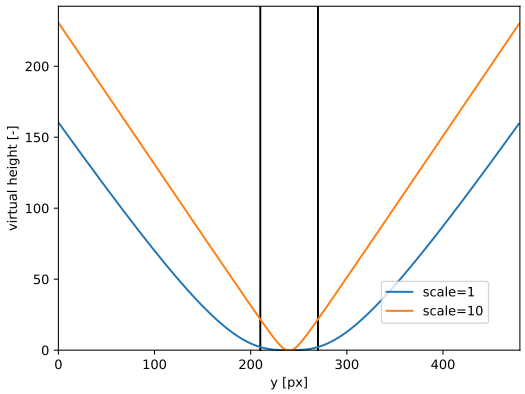

Figure I.5: Comparison between the new and old virtual height. Vertical black lines represent the width of the path as visually presented.

This pilot experiment is performed by 1 participant (male, right handed) and was given the same instructions as previously. After performing the trials, the comment was made that the visual cursor (circle in Fig. I.1) was distracting. Hereafter, the same participant repeated the same experiment but this time with the cursor removed completely.

The independent variables where also changed slightly to have more repetitions per Index of difficulty, they consisted of the following:

- Tunnel length, $L = [200, 300, 400, 500, 600]px$
- Width start, $W_{start} = [20]px$ (constant)
- Width end, $W_{end} = [20]px$ (constant)
- Haptic condition, [Converging, Diverging, Neutral]

This resulted in 15 unique trials, which are repeated 4 times throughout the full experiment. Thus 60 trials are performed by the participant.

I.2.1. Results

As before, the movement time versus the Index of Difficulty is analysed. As seen in Fig. I.6, again no large differences between haptic conditions can be observed.

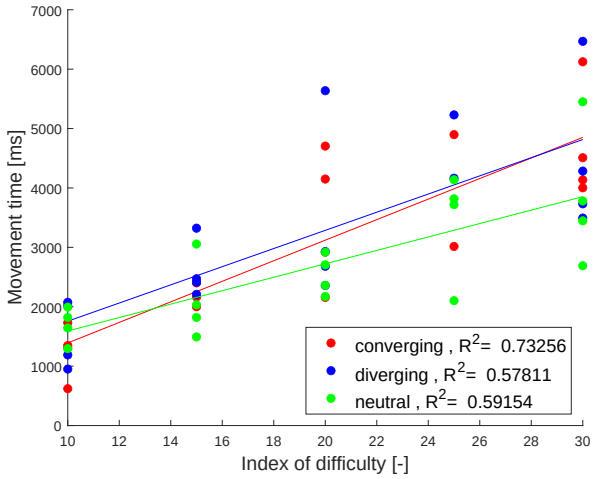

Figure I.6: Time in milliseconds spend plotted against the Index of Difficulty. A linear fit is visualised for each haptic condition

Also upon investigation of the finger movement during the experiment, no significant effects are observed in standard deviation between the haptic conditions. This is depicted in Fig. I.7 where all position data is normalised to a length of 500 pixels.

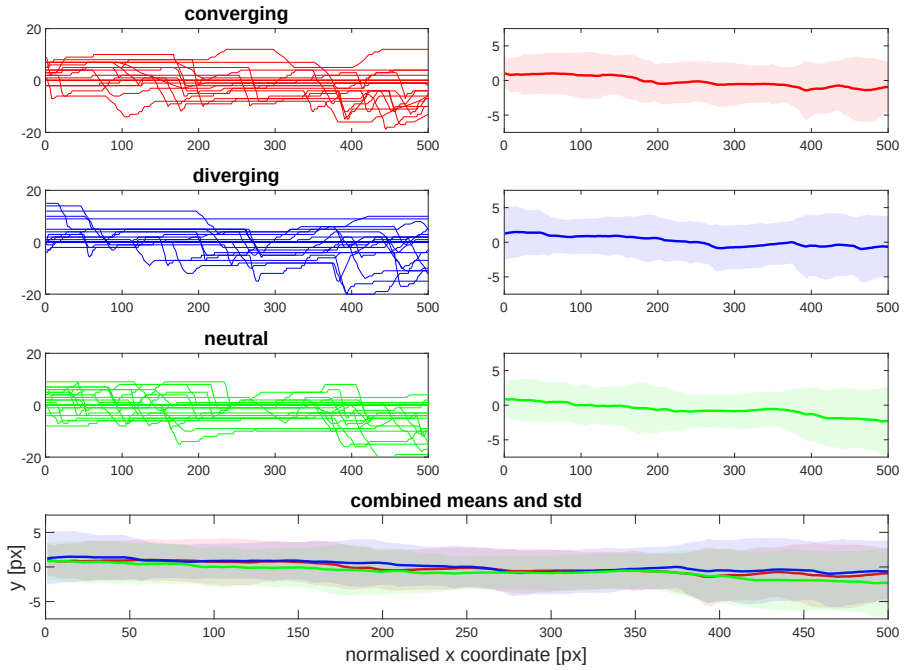

Figure I.7: Individual position data on the left and their corresponding mean and standard deviation for the normalised path length of 500 pixels. Bottom graph shows the same plots as on the right, but overlaid.

I.2.2. Written notes

- Remove visual cursor because it draws the user to focus more on the visual aspect
- Add a progress bar to inform users at what trial they are
- Include normal force feedback to inform users not exert to much force

I.2.3. Findings

From the results of this experiment it was concluded that during the execution of this task, the variation in y-direction is not that large. However, due to the nature of using friction modulation as haptic feedback the finger has to move in the direction of (or opposite to) the feedback direction for the feedback to work. The assumed variation in y during execution of this task is too low/not present for the feedback to assist during this task.

I.3. Pilot C - Target finder

In light of the findings of the steering law experiments, it was decided to move to a task where more exploration by the participant is required. Naturally, this also means that more movements in the feedback direction will occur. In order to validate that people can comprehend the heightmap feedback principle a trial is constructed where one of three paths has to be chosen according to the haptic feedback that is felt. The visual feedback, as in Fig. I.8, shows the three possible paths and resulting targets on the right of the screen. The decision by the participant is made by crossing the right border, after which visual feedback is given in order to show if the chosen target is indeed the correct target.

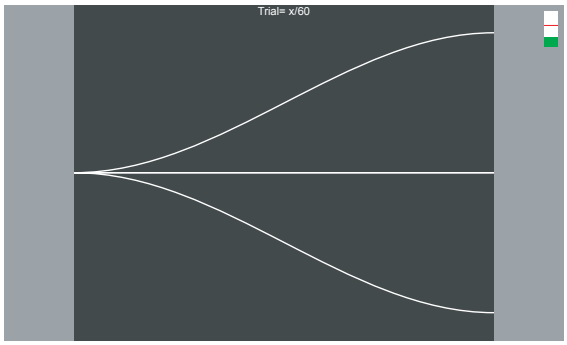

(a) Visuals as presented to the participant during a trial. Trial number is presented at the top and force feedback is provided by a bar on the top right.

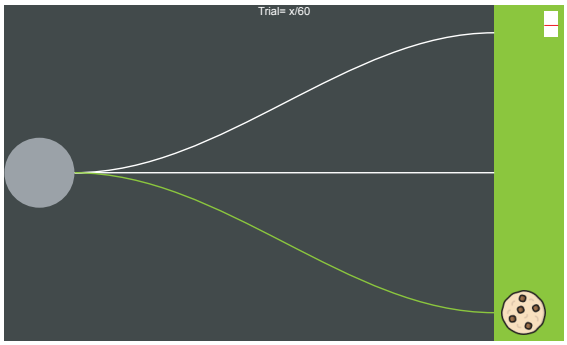

(b) Visuals as presented to the participant once a trial is finished. The correct path is highlighted in green and the right section is colored either green or red according to the correctness of the answer provided

Figure I.8: Visual feedback during Pilot C

The presented haptic feedback is similar to the previous experiments where the virtual height is calculated according Eq. I.4, with a fixed width of 20px and scale of 10. This results in the following formula:

$$H = \left| 2 \cdot \arctan\left(\frac{1}{2} \cdot (y - y_{center}(x))\right) - (y - y_{center}(x)) \right| \tag{I.4}$$

The center of the virtual valley follows one of the three paths. The middle path being a straight line and the others a spline curve that is represented by the following cubic polynomial:

$$y_{center}(x) = \frac{-2 \cdot \pm 200}{600^3}(x - 100)^3 + \frac{3 \cdot \pm 200}{600^2}(x - 100)^2 + 240, \text{ D: } x = [100, 700] \tag{I.5}$$

This results in the virtual heightmap presented in Fig. I.9. The haptic feedback is designed in such a way that it always assists the user in finding the correct path, contrary to pilot A and B. The three target positions are randomly presented to the participant, each condition being repeated 20 times, resulting in 60 trials in total.

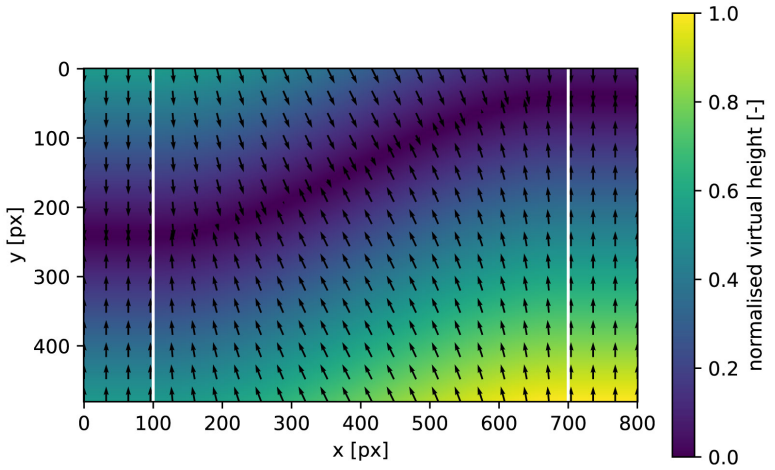

Figure I.9: Virtual heightmap guiding the user to the top path. The x coordinates of the start and end of the path are visualised by two white lines. The resulting 2 dimensional gradient is visualised by the quivers.

This pilot experiment is performed by 3 participants (2 male / 1 female, all right handed) who were instructed to start each trial at the left side of the screen. It is clarified that they are free to explore the whole touchscreen at their own pace. Once the participant is confident that they found the target path they would cross to the right section, locking in their decision. There was no possibility to skip a trial or not to give an answer, drawing its analog to a two-alternative forced choice experiment [11]. After each trial the participant is visually informed if the answer was correct and a new trial could be initiated by moving to a 'reset-circle' on the left of the screen, see Fig. I.8b.

The hypothesis tested during this experiment is formulated as follows: users are able to find the correct target with a hit rate higher than chance (1/3).

I.3.1. Results

For each of the correct answers given by the participant the score increases by 1. In Fig. I.10 the correct answers are visualised for each participant, as well as the maximum possible score and the probability based purely on chance (1/3 for each trial). It is clear that each participant is able to score higher than the average chance of 20 out of 60. However, due to the limited amount of participants little can be said about whether the participants truly perceived the haptic feedback properly. The null hypothesis is tested that the results of the three participants comes from a normally distributed population with a mean of 20 by using an one sided student's t-test. This results in a p-value of 0.076. With a significance level of 0.05, this means that the null hypothesis can not be rejected.

Further analysis of the data includes a confusion matrix as seen in Fig. I.11. This again shows that the average of correct responses is around 50 percent, but more interestingly it also shows that the top target is more often correctly identified than the middle and bottom targets.

The movement time needed for each trial is also recorded for each participant. In Fig. I.12 the individual movement times for each participant are plotted. The distinction is made for trials that were correct and incorrect. From the difference within the participants little conclusions can be drawn. It is clear however, that a large variability exists between participants. Additionally, the distribution of datapoints is skewed. The assumption of normally distributed data might not be correct.

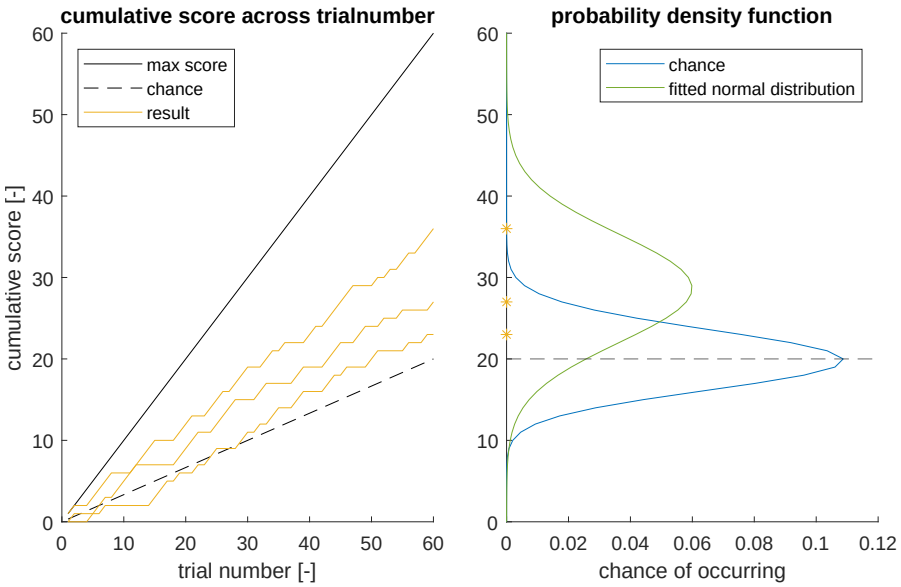

Figure I.10: Results of the 3 participants during pilot C. The left figure shows the cumulative score across the trials. On the right the final scores are visualised, as well as a probability function based on chance.

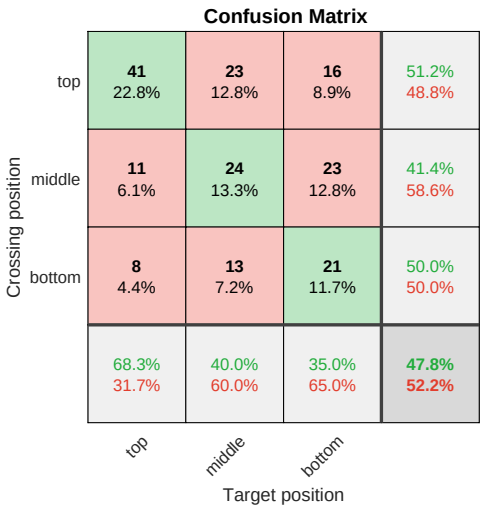

Figure I.11: Confusion matrix of all three participants combined. The values in the bins indicate the total amount, as well as the percentage, of the responses. Horizontally are the target positions and vertically the responses of the participants.

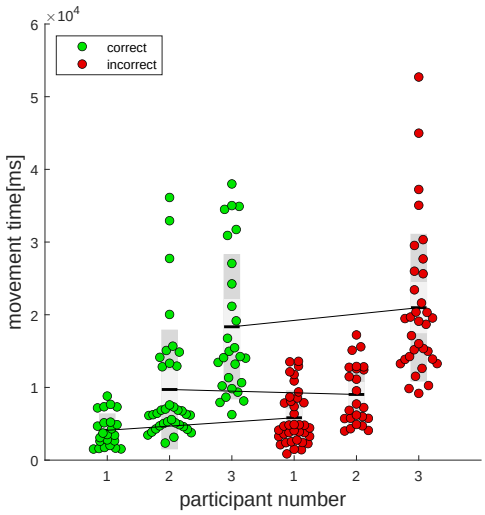

Figure I.12: Movement time for each trial. Sorted per participant and whether the answer is correct. A solid black line is drawn between the two means for each participant.

I.3.2. Written notes

- Add a forced break in between the trials, participants do not tend to initiate a break themselves.
- Sometimes another finger is inside the field of view of the position sensor, causing a error in the position reading.
- More trials would be possible.
- Screen makes quite some noise, participant indicates that the choices where influenced by the noises they hear.
- Glass plate moves up and down, fixture redesign needed.

I.3.3. Findings

From the results and the notes taken during this pilot it is clear that some tweaks on the experimental design are needed. First of all, it is promising to see that participants seem to be able to perceive the haptic feedback properly (although the p-value is not significant due to a low amount of participants). To further improve the experimental design it would be beneficial to compare the haptic feedback principle of potential fields to another haptic rendering method instead of comparing it to chance only. Also the noise coming from the touchscreen needs to be lowered next to the other small tweaks mentioned in the written notes.

I.4. Pilot D - Target finder

The last pilot before the main experiment build on the previous pilot. The main difference being that another haptic rendering method is introduced in order to make a comparison. Also the strength of the haptic feedback is varied in order to acquire an estimate of the psychometric curves.

The new haptic rendering method is based on having a slippery path with high friction surroundings. This method only takes into account the position of the user's finger. When the participants position their finger on the targeted path, the vibrations in the glass plate increase. This renders a haptic feeling of a slippery path, confirming to the users that this is the target. To avoid a sharp transition in amplitude when entering or exiting the targeted path, a smooth transition zone is introduced in this frictionmap. The amplitude of the driving signal is described by the second-order smoothstep function [12], which has zero first- and second-order derivatives at the boundaries. The generalised form of the smoothstep function is described in Eq. I.6. Here, the smoothed step function ranges from 0 to 1. This is scaled such that the smoothstep function ranges over 20 pixels. The width of the path is set to 20 pixels as well after which a similar smooth step down is calculated with the same feather size.

$$S_{up}(y) = \begin{cases} 0 & y \leq 0 \\ 6y^5 - 15y^4 + 10y^3 & 0 \leq y \leq 1 \\ 1 & 1 \leq y \end{cases} \tag{I.6}$$

The function described by the smoothstep functions are shifted such that the centerline of the path is on the earlier presented formula Eq. I.5. This results in the frictionmap as depicted in Fig. I.13. Here the path has low friction, which smoothly transitions into a high friction surrounding.

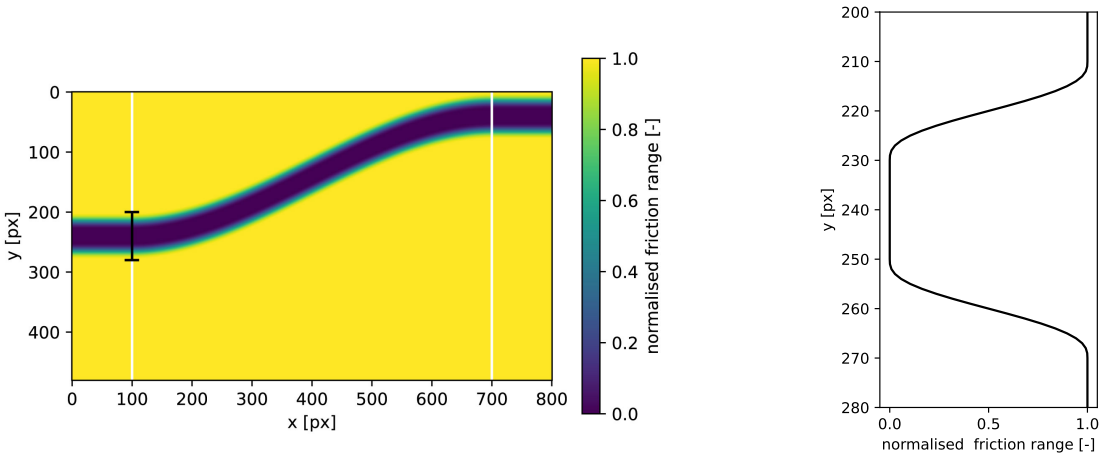

(a) Normalised frictionmap, designed to guide the user to the top path. The x coordinates of the start and end of the path are visualised by two white lines. Black indicator lines represent the cross section visualised on the right.

(b) Cross section view of the normalised friction at the start of the path.

Figure I.13: Visual representation of the frictionmap.

The heightmap condition is also changed, in an attempt to make the haptic feedback to the user more clear. In the heightmap used in pilot C, the gradient only points towards the path. However, the target as explained to the user also includes the endpoint. In some situations this results in confusing feedback when the user moves towards the correct endpoint, but the gradient only points towards the path. To correct for this, an additional attracting point (sink) is introduced. This sink is modelled as a heightmap as well. This is simply described by an upside down cone (Eq. I.7). The resulting heightmap is seen in Fig. I.14a. This is then added with equal weights to the already existing path attractor heightmap, resulting in the heightmap visualised in Fig. I.14b.

$$Z_{\text{cone}} = \sqrt{\left(x - x_{\text{target}}\right)^2 + \left(y - y_{\text{target}}\right)^2} \tag{I.7}$$

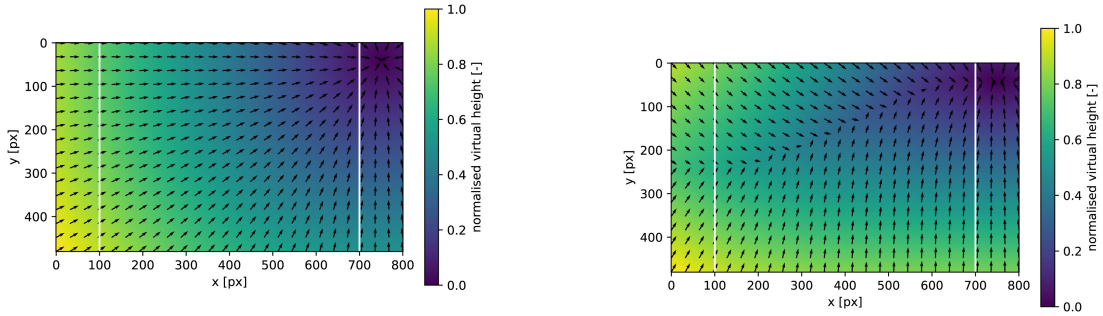

(a) Heightmap described by an upside down cone with its low point at the target position.

(b) Combined heightmap with a path- and point attractor.

Figure I.14: Virtual heightmap generation for guiding the user to the top target.

From the previous pilot study it was already seen that the haptic heightmap condition was difficult to perceive. In the effort to extract more information on what the limits of perception are in these conditions, different haptic strength levels are tested. With this information, psychometric curves can be fitted and extrapolated. The different strength levels, or amplitudes of the vibrations, are set to [100, 66, 33] percent. The amplitude is scaled with respect to the 50 percent reference point. This means that not only the maximum amplitude is lowered, but also the minimum amplitude is increased. Examples of the maximum possible modulation signals are given in Fig. I.15. From pilot C, it is estimated that the heightmap feedback principle would be in the lower part of this curve, but established theories can help extrapolate this data.

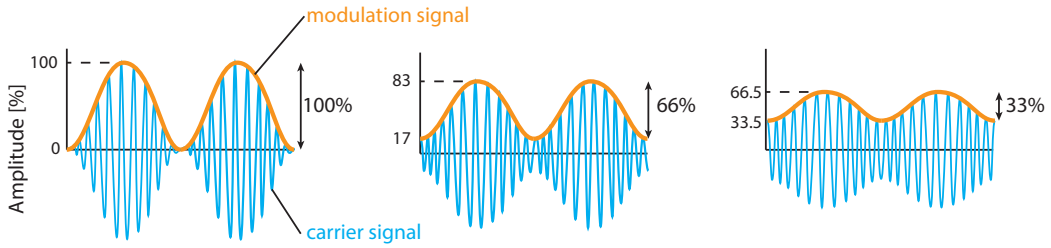

Figure I.15: Scaling of the amplitude modulation signal. Maximum ranges are, from left to right, 100 percent, 66 percent and 33 percent.

Several other small changes compared to the previous pilot include a change in the visual feedback given at the end of the experiment. This visual feedback after finishing a trial is changed to a visual representation of the haptic feedback, instead of just highlighting the correct path. This is implemented for both the heightmap and the frictionmap, as seen in Fig. I.16. The visual feedback during the trial is the same as before, showing the 3 possible target paths with 3 white lines on a dark grey background.

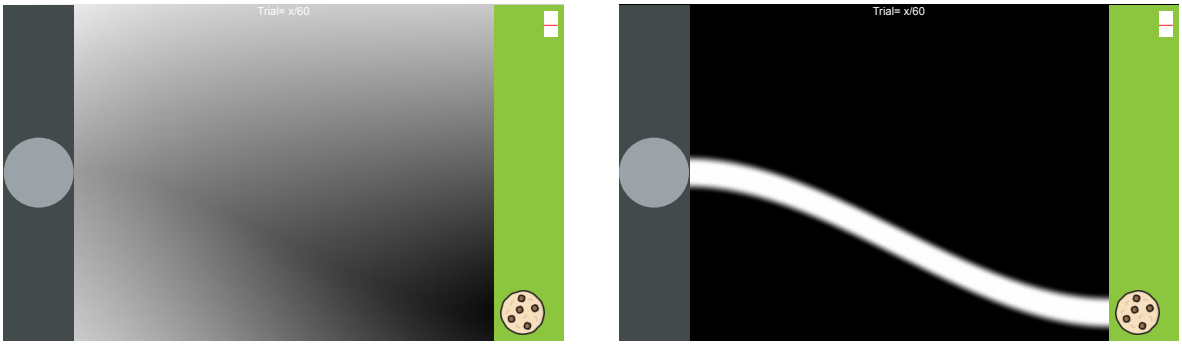

(a) Heightmap (b) Frictionmap

Figure I.16: Visual feedback as presented to the participant, after a target is selected by the user. Both conditions show an example of guidance to the bottom target.

Two participants (1 male / 1 female, both right handed) were asked to participate in the experiment. The first participant was first presented with all frictionmap conditions and the heightmap conditions afterwards. For the second participant the order was reversed. Within these conditions, the target positions (top, middle, bottom) and haptic strengths (100, 66, 33 percent) were presented in random order. Each unique combination was shown 10 times throughout the experiment. This resulted in a total of (2x3x3x10=) 180 trials. After 45 consecutive trials a pause screen was automatically introduced such that the participant could take a break before continuing. The participants were free to explore the screen freely, just like the previous pilot.

During the experiment the participants wore an active noise cancelling headphone (Bose QuietComfort 35). Pink noise was playing on these headphones in order to mask the sound coming from the touchscreen.

The hypothesis is tested whether the participants can achieve a higher hit-rate with the heightmap condition than the friction condition. This is done by analysing the psychometric curves. Additionally the hypothesis is tested whether participants are faster in making the correct decision.

I.4.1. Results

Because in the previous pilot it became clear that not all of the target positions were identified equally often the confusion matrix of both conditions was analysed first. Where previously the top position was identified correctly most often, no clear bias is seen in Fig. I.17.

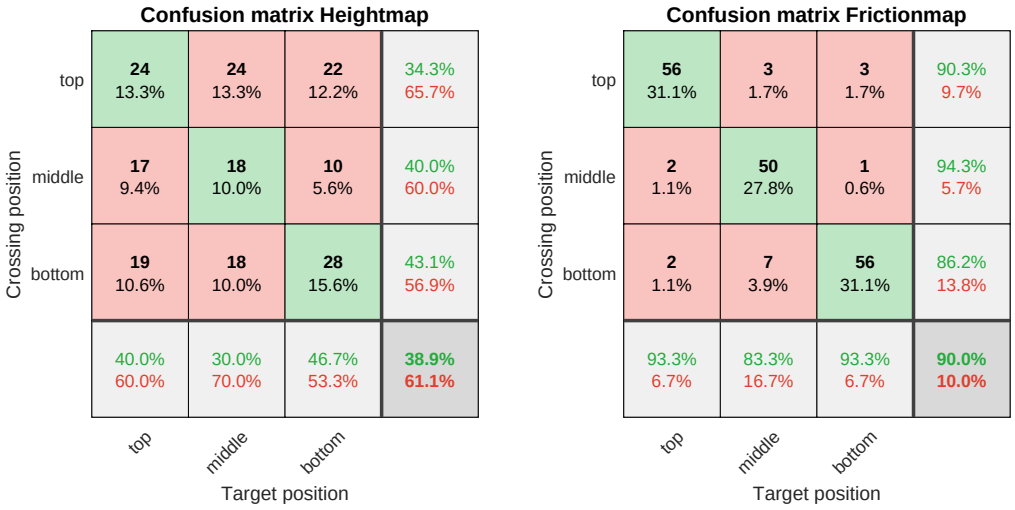

Figure I.17: Combined confusion matrices for the two haptic feedback conditions.

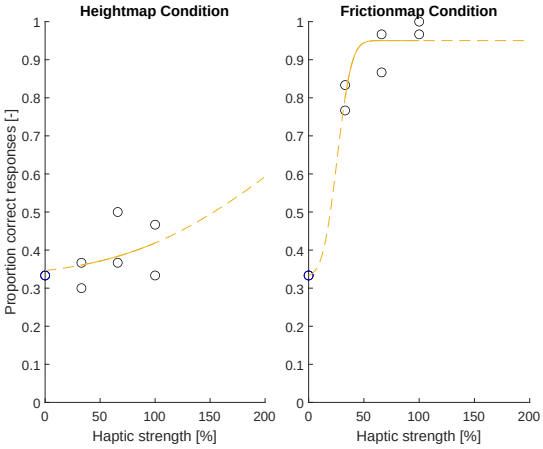

Figure I.18: Fit of the psychometric curves on the hit rates per haptic strength and haptic feedback condition. Extrapolated curves are visualised with broken lines.

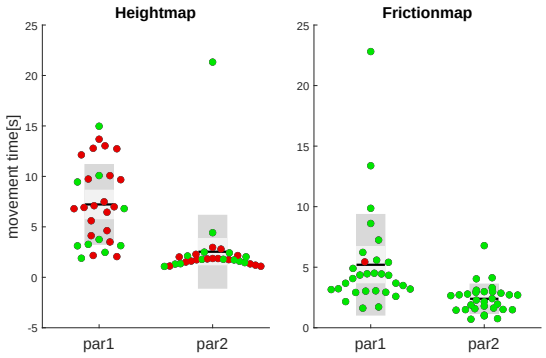

Figure I.19: Movement time for both haptic conditions (at 100%) for each participant. Correct answers are green, incorrect answers are red. Lightgrey box indicates the Standard Error of the Mean, darkgrey box indicates the standard deviation.

The hit rates of both participants are plotted in Fig. I.18. Each of the data points represents the hit rate over 30 trials. For both the haptic feedback conditions, a psychometric curve is plotted according to the method described by Wichmann and Hill [13]. This method takes into account both the guess rate and lapse rate when plotting these S-curves. It is already clear that a big difference between the conditions exists and that the frictionmap condition outperforms the heightmap condition in terms of hit rate.

Also the movement time to complete each trial is recorded. This is defined as the time difference between first leaving the left start area and entering the finish area on the right. For both participants, the time needed to complete the trials with 100 percent feedback strength are plotted in Fig. I.19. Again the difference in hit rate is evident as indicated by the colors, but also the time taken by the participant shows a clear difference between conditions. Also recognised in this figure is the difference between the participants. Here participant 1 spent more time executing the trials than participant 2 in both feedback conditions.

I.4.2. Written notes

- Sound is still a big issue, maybe even worse than before. Just playing noise does not help, the transients in the sound from the touchscreen could still be heard.
- Both participants stated that their choice was heavily influenced by the auditory feedback.
- Check if the comparison between frictionmap and heightmap are fair.

I.4.3. Findings

As indicated by both participants the results may be heavily influenced by the auditory feedback. This difference in sound level might be more evident in the frictionmap condition, because a more intense transient in sound is observed when moving your finger across the screen. This could explain the difference in the observed hit rate and movement times as well, other than just a difference in haptic feedback. That being said, the results of this pilot, with limited amount of participants, indicates that the frictionmap is preferred over the heightmap in terms of both hit rate and movement time.

To resolve the influence of the auditory feedback during the main experiment, industrial headphones are used. During testing white noise is played on these headphones while interacting with the touchscreen. This was already a mayor improvement over the headphones used previously, but the transients in the sound coming from the touchscreen could still be faintly heard. Hence, a combination of white noise and music is played on the headphones. This proved to be very effective with a small test asking whether the touchscreen could be heard.

After this pilot experiment the question was raised if the comparison between the conditions is fair. This mainly concerns the quite harsh transition between high and low friction during the frictionmap

condition. Despite the smoothing effect added to the path, the vibration amplitude of the glass plate changes rapidly when moving across this path. To analyse this phenomenon, the amplitude is plotted for when a user would move vertically across the screen at x=400 (Fig. I.21). The slope of this amplitude is different for the two conditions. The frictionmap condition has a higher rate of change than the heightmap condition. To make a more fair comparison between the conditions the maximum derivative of amplitude will be matched. This then results in the figures seen in Fig. I.22. The maximum amplitude change of the path attractor is matched to that of the frictionmap. This shows that the conditions are more comparable. This setup is also used in the final experiment. In the end, the frictionmap still benefits from the use of the full range, where the heightmap does not, because the full amplitude range has to be divided over the full 360 degrees of movement direction. This is a limitation of the heightmap and the frictionmap will not be altered to match this as well, because this is a fundamental difference in the interaction.

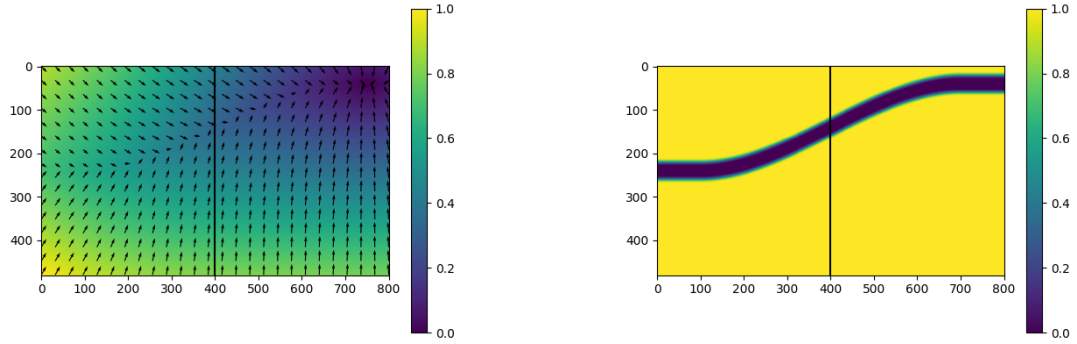

Figure I.20: Location at which the two conditions are compared, indicated by the vertical line (x=400).

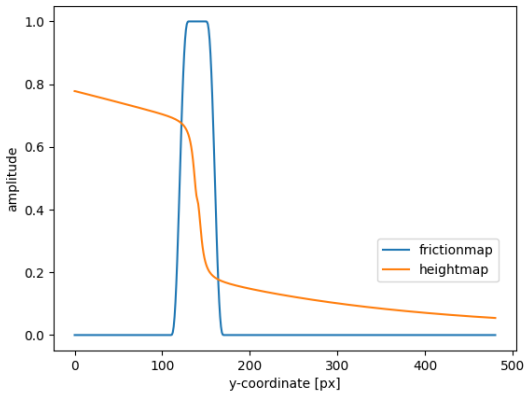

Figure I.21: Vibration amplitudes as they would be rendered if a user is moving vertically across the screen, from top to bottom at x=400 (location as visualised in Fig. I.20).

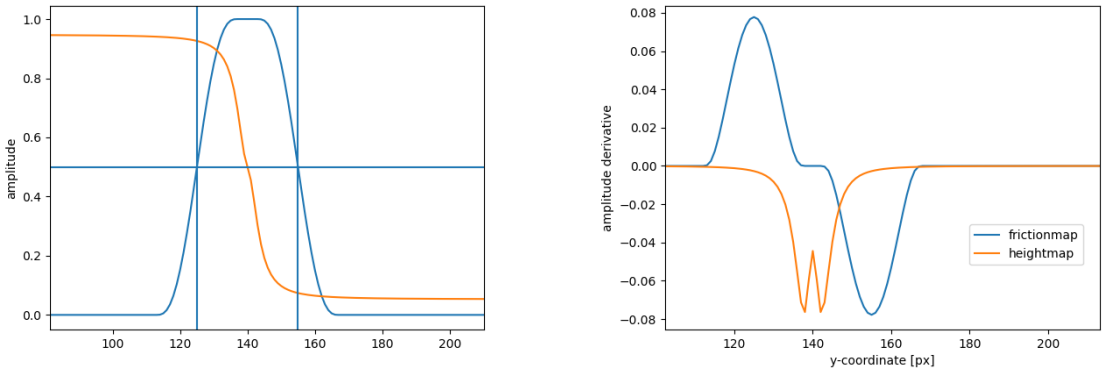

Figure I.22: Vibration amplitude and derivative of the vibration amplitude after the conditions are matched.

J

Experimental Procedure

Participants are recruited by contacting friends, family and fellow students with sending a text message, shortly explaining the research. Included in this message was a teaser image, similar to the one on the cover page. Before the experiment, an information letter was sent to each participant. This included the detailed explanation of the experiment and stated the potential risks. This letter was also read to, or by, the participant just before the start of the experiment. The full participant information letter is given on page 79 in this appendix. Any remaining questions of the participant were answered by the experimenter, without providing any information that might have influenced the results. Any questions or comments are noted down and given in Appendix K.

In total 22 participants, voluntarily took place in the study. The distribution of this population is given in Fig. J.1. The participants are alternately assigned to either the heightmap of the frictionmap first. This resulted in equal distribution in terms of gender and handedness, as well as similar age distribution between the two conditions.

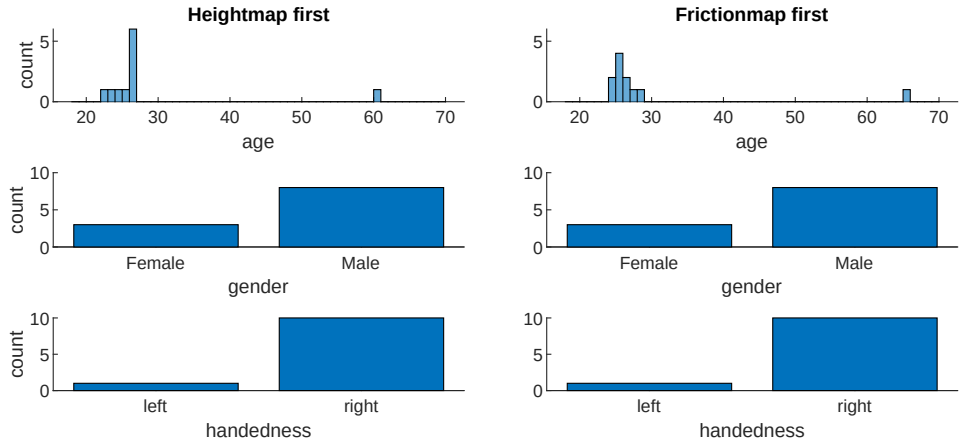

Figure J.1: Distribution of the participants between the two counterbalanced conditions.

During the procedure the participants wear industrial headphones. On these headphones a mixture of white noise and music is playing. The music in question is royalty free music from the website Pixabay. The full list of the songs is given in Table J.1. These songs are combined in one single mp3 file of 1 hour and 6 minutes and are mixed with white noise, using the program Audacity.

A checklist (Table J.2) is used by the experimenter to make sure that every experiment is performed the same, and no parts of the setup or explanation process are skipped. This includes the full process from setting up the experiment to shutting everything down at the end of the experiment. The corresponding boxes are checked before moving on.

At the end of the experiment the participant is thanked for their time and effort. A chocolate chip cookie is gifted to each participant as a thank you. Participants did not know prior to the experiment that any compensation was at place.

Table J.1: List of songs, played during the experiment.

	song	artist	duration	link
1	Chillout 96	1tamara2	11.33	pixabay.com/music/beats-chillout-96-4200/
2	Chillout 112	1tamara2	8.32	pixabay.com/music/beats-chillout-112-4739/
3	Chillout 68	1tamara2	9.25	pixabay.com/music/beats-chillout-68-3140/
4	TelefsizFon Muziki	tgokyigit	11.34	pixabay.com/music/electronic-telifsiz-fon-muzigi-3344/
5	Chillout 14	1tamara2	13.16	pixabay.com/music/beats-chillout-14-953/
6	Chillout 60	1tamara2	12.24	pixabay.com/music/beats-chillout-60-2650/
7	Chillout 98	1tamara2	9.52	pixabay.com/music/beats-chillout-98-4202/
8	Happy Corporate Project Long	ZakharValaha	8.05	pixabay.com/music/corporate-happy-project-long-10242
9	The Dove	Tattooed Preacher	12.21	pixabay.com/music/ambient-the-dove-8563/

Table J.2: Checklist as used by the experimenter. The real list extends to the right to include more participant numbers.

		Participant Nr.				
		1	2	3	4	...
Before Arrival						
	Print participant information letter					
	Print informed consent form					
	Connect all BNC's for experiment					
	Clean glass plate with alcohol					
	Turn on RPi					
	Turn on headphones (set volume to 25%)					
Before Experiment						
	Have participant read the info letter					
	Sign the informed consent					
	Have participant wash + dry hands					
	Turn on amplifiers (x2)					
	Turn on oscilloscope					
	Start Python program					
Demo Screen						
	Write down participant info					
	Explain demo screen, show bumpmap					
	Show repres. of height/slip-map					
	Ask if there are any questions					
After						
	Turn off RPi					
	Turn off amplifiers (x2)					
	Turn off oscilloscope					
	Turn off headphones					

– PARTICIPANT INFORMATION LETTER –
Effect of haptic feedback, using ultrasonic friction modulation, on the use of a touchscreen

Date:

Dear Sir / Madam,

You have been invited to participate in a research study titled “Effect of haptic feedback, using ultrasonic friction modulation, on the use of a touchscreen”. This research is done by Tammo Brans, with his main supervisor Michaël Wiertlewski from the TU Delft. We would like to thank you for the interest in participating. In this letter you will find information about the research. If you have any questions, please contact the person listed at the bottom of this letter. A photo of the experimental setup can be seen on the right.

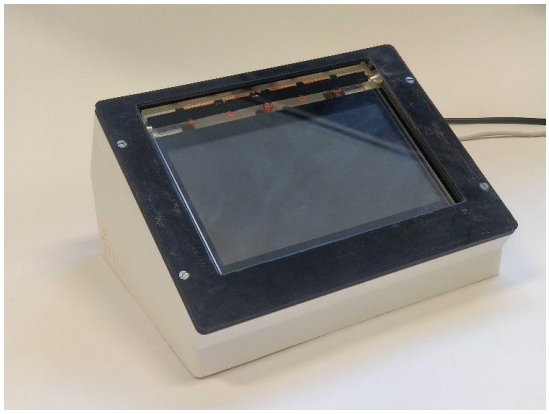

Purpose of the research

The purpose of this research is to better understand the human interaction with touchscreens and ultimately improve the experience and performance when using such devices. The use of touchscreens brings many advantages, mainly being able to dynamically change what the touchscreen displays and how it reacts. With the shift to using touchscreens in vehicles, an important aspect of the interaction is lost. This being the sense of touch. Where before you could feel buttons and knobs on the dashboard while still maintaining focus on the road, touchscreens do not have this kind of interaction.
With this research we investigate whether rich haptic feedback on touchscreens can improve the performance of navigating your finger across a touchscreen.

Experimental procedure

For the trials during the experiment, you will be asked to casually interact with the touchscreen placed in front of you, using your index finger. Throughout the experiment you will be asked to wear headphones to limit any auditory feedback. For the whole of the experiment it is not needed to put more effort into interacting with the touchscreen than you would with using a regular tablet or smartphone. Please try to limit the force you exert on the glass plate. In case you do apply excessive force you will be notified with a visual indicator on the top right corner of the screen.

Familiarization:

To familiarize yourself with the touchscreen and its working principles, you are first presented with a demonstration screen. Here you can feel the glass plate on the touchscreen and compare the two different feedback conditions: Heightmap and Frictionmap (will be explained further).

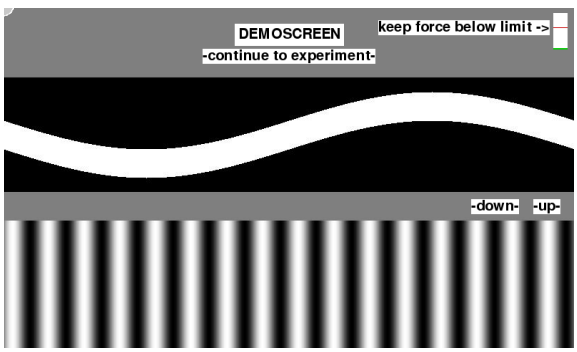

During the familiarization phase you also have access to several 3D printed models. These physical parts represent the haptic feedback principles presented by the touchscreen. The interaction with the touchscreen and physical models will give you a feeling on what the system is trying to replicate.

Trials:
After the familiarization phase the experiment starts. This consists of 180 trials and will take approximately 30 minutes to complete. During a trial you are asked to start in the left area (Start Zone) and move to the right area (End Zone). During this movement you may choose one of the three displayed paths. With the haptic effect you are drawn to one of these paths.
You are encouraged to explore the surface and make your decision based on what you feel during this exploration. Once crossing into the End Zone you receive visual feedback on the haptic effect that was displayed and whether your decision is correct. There are no consequences when the action you provided is incorrect, but you are encouraged to find as many "cookies" as possible.

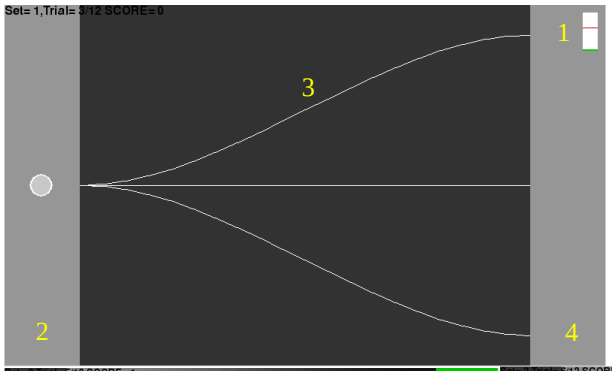

1) Force indicator
2) Start Zone
3) Possible paths
4) End Zone

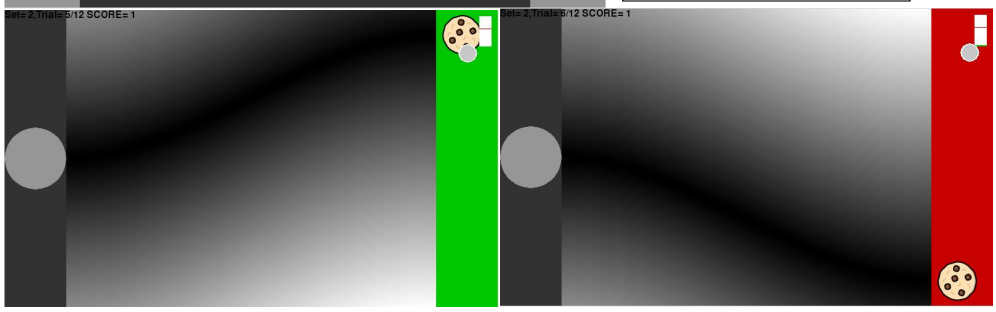

Crossed at the top: Correct

Crossed at the top: Incorrect

When you have finished a trial, you are asked to move your index finger back to the starting position, indicated by the light grey circle on the left. Once in this circle, the system will reset and you will be presented by a new randomised trial.
The experiment consists of 2 conditions. The first 90 trials will be with the one condition (heightmap or frictionmap) and the last 90 trials with the other. The researcher will indicate what condition will be presented first.

Heightmap: The correct path will be located in valley. Moving towards the correct path will be easier, while moving away will be restricted.
Frictionmap: The correct path is slippery (low friction), while the rest has high friction.

The system will always try to help you find the correct path, there are **no** catch trials, where the system deliberately provides the wrong information. The haptic strength however, will be varied throughout the experiment. So sometimes you will feel the effect more easily than other times.
Mind that there is never a need to rush. So start and finish the tasks at your own pace. Feel free to request a pause when you need some time before starting the next trial. The researcher is happy to pause the measurements and facilitate a break.

If anything is unclear about the protocol please indicate this to the researchers before starting the experiments. Please don't refrain from requesting a break if anything is unclear during the experiments as well.

Additional measures against coronavirus
To limit the spread of the coronavirus, some additional measures are taken. The basic rules as determined by the RIVM have to be observed. Therefore, you are kindly asked to:

- Wash and dry your hands before starting the experiment (facilities are provided)
- Stay at home if you have any coronavirus symptoms. Please contact the research team in case you are prevented from participating in the experiment.

The experimental setup will be carefully disinfected by the research team before and after your participation.

Benefits and risks of participating
By participating in this experiment you will be able to interact with a cutting-edge haptic interface technology and experience how it is to feel 3D textures on a flat touchscreen. The touchscreen is a non-CE but expert-tested device.
Risks of participating:

- Low risk of electrical shock upon unlikely contact with electrical circuits embedded in the touchscreen
- Muscle fatigue due to prolonged use of the touchscreen

You are always free to stop the experiment or take a break when it becomes uncomfortable to continue.

Procedures for withdrawal from the study
Your participation in this study is entirely voluntary and you can withdraw at any time. If you give consent to this research you have the freedom to come back on this decision at any time. You can request access to and rectification or erasure of personal data. No explanation has to be given for your decision. You do this by contacting Tammo Brans via t.j.brans@student.tudelft.nl or Michaël Wiertlewski via M.Wiertlewski@tudelft.nl. If you request erasure of your data, it will be removed from the dataset (if technically feasible), unless the data has already been used in scientific publications such as peer-reviewed scientific journals, conference proceedings or archived in a data archive.

Confidentiality of data
This study requires the following personal data to be collected and used: gender, age and handedness (being left or right handed). To safeguard and maintain confidentiality of your personal data, necessary security steps will be taken. The data will be stored in a secure storage environment at the TU Delft. The data will only be accessible to the research team. All data will be processed confidentially and stored using a participant number only.
Your personal data will be retained for a maximum of years to extract anonymised non-personal data, after which the personal data will be destroyed.
The results of the study will be published in possible future publications. Your participant number, name, gender, age and handedness will never be shared in these publications.

Contact information
This project is carried out by the Cognitive Robotics department of the faculty 3ME at the Technical University Delft. For further information or filling a complaint, please contact Tammo Brans (t.j.brans@student.tudelft.nl).
If you have any complaints regarding confidentiality of your personal data, you can contact the TU Delft data protection officer via privacy-tud@tudelft.nl or the Dutch Data Protection Authority (Autoriteit Persoonsgegevens).

Thank you in advance for your possible cooperation,

Tammo Brans

K

Experiment Notes

During the experiments, notes are made by the experimenter. This includes timestamps with observations of the experimenter and also the remarks of participants. The remarks made by the participants were their own, without guiding questions from the experimenter. The comments are written in quotation marks, but are not direct quotes. The comments are translated from Dutch into English and the wording is slightly changed to use the same terms as used in the report.

Participant 1

29-3-2022	
10:00	Explanation
10:12	Start experiment (Frictionmap)
	Observed some errors in the position, explained to the participant that only 1 finger should be in the sensor area
	”Bottom target is difficult to identify”
	The force sensor exhibits drift behaviour.
10:32	Start second half experiment (Heightmap)
	More searching is required, mainly in criss-cross patterns
	”Sometimes stick slip is evident when applying to much force”
	”The glass plate seems to heat up during the experiment”
10:54	End experiment, time = 42 min

Participant 2

12:00	Explanation
12:11	Start experiment (Heightmap)
	Participant often identifies the bottom target correctly
	Participant chooses the middle path less often
10:25	Start second half experiment (Frictionmap)
	Very different tactic than before, more fast movements up and down the paths
	Way faster in making a decision
	Participant seems to loose interest in executing the trials at the end of the experiment
10:35	End experiment, time = 24 min

Participant 3

14:55	Explanation
15:08	Start experiment (Frictionmap)
	Relaxed slow movements
	Possible sensor errors in trial 24 and 25?
	Excellent in finding the correct targets
	Force sensor seems to have some upward drift, maybe due to temperature rise?
15:31	Start second half experiment (Heightmap)
	Participant flexes fingers/hand often and takes breaks more often
	”At the left side I can feel it better, but further to the right I lose the haptic sensation”
	Above comment may be due to visual bias; at the left side the paths start at the same position thus the feedback in each trial is very similar.
15:54	End experiment, time = 46 min

Participant 4

30-3-2022	
14:00	Explanation
14:15	Start experiment (Heightmap)
	”I’m not very good at this” (trial 6)
	”Difficult to feel the effect when moving up. Finger gets stuck”
14:40	Start second half experiment (Frictionmap)
	Drift in force sensor is present again.
	”I react more to the vibrations than I feel change in friction”
15:02	End experiment, time = 47 min

Participant 5

15:13	Explanation
15:20	Start experiment (Frictionmap)
	”I’m feeling confident in making a descision, some trials are more difficult though”
	”If my answer was wrong, I often had some doubt as well”
14:40	Start second half experiment (Heightmap)
	Searching for information to the right of the screen, more than in previous condition
	”This is difficult, I did not find a nice tactic yet”
	”I do like the competitive element to find as many targets as possible”
16:14	End experiment, time = 54 min

Participant 6

31-3-2022	
10:05	Explanation
10:14	Start experiment (Heightmap)
	Participant is very quick in making a descision
	Tactic is to use very quick movements
10:27	Start second half experiment (Frictionmap)
	”Oh, I had the heightmap in the first half”
	Different tactic; more up and down movements
10:43	End experiment, time = 29 min

Participant 7

12:06	Explanation
12:16	Start experiment (Frictionmap)
	”Sometimes I hear a little bit of noise from the screen, not always”
12:28	Start second half experiment (Heightmap)
	”Sometimes it is really difficult to feel the effect”
	”I think it is nice to be guided to a specific goal, instead of a strong on/off-option. Maybe the system will work better with a steeper, less wide valley”
12:40	End experiment, time = 24 min

Participant 8

14:02	Explanation
14:13	Start experiment (Heightmap)
	Some sensor errors at the beginning? The noise from the device seems to have increased.
	”Sometimes the effect is really clear and other times I do not feel it at all”
14:35	Start second half experiment (Frictionmap)
	”I guess this one will be easier?” (before trials, question not answered by experimenter)
	”yes, this is definitely easier, I have to retrace less”
14:47	End experiment, time = 34 min

Participant 9

16:32	Explanation
16:44	Start experiment (Frictionmap)
	”It is a little bit fatiqueing to keep arm raised”
	”I notice when applying less force, the effect is stronger”
	”On the edge of a path you feel a ’shock’ (sudden change in friction), this mainly indicates the correct path”
16:58	Start second half experiment (Heightmap)
	”In some trials, I followed a certain path and did not notice a change in friction, but the answer was incorrect. Maybe this path was on a part of the heightmap were little change in height is present.”
17:10	End experiment, time = 26 min

Participant 10

1-4-2022	
12:29	Explanation
12:38	Start experiment (Heightmap)
	Takes a lot of time to select a target
	”Middle path is difficult to distinquish”
	Only makes movements on the path
	”Can I also explore vertically?” (trial 45, answered: yes, you are free to explore the screen as you wish)
	”Sometimes it is really clear, but most of the time it is difficult to feel a distinction”
13:15	Start second half experiment (Frictionmap)
	”Headphones are a bit loud” (volume not changed)
	Tactic mainly consists of slow vertical movements
	”This condition is way easier. I was aiming for the best possible score”
13:32	End experiment, time = 54 min

Participant 11

13:43	Explanation
13:54	Start experiment (Frictionmap)
	”This is very doable, only sometimes I have to search a lot”
14:14	Start second half experiment (Heightmap)
	Participant seems to struggle to find the correct targets
	”Moving vertically provides me more information”
14:37	End experiment, time = 43 min

Participant 12

14:41	Explanation
14:50	Start experiment (Heightmap)
	Participant does not search a lot in the beginning, mainly just follows a single path. Later in the experiment the participant searches more
	”I am trying to not think to much about it”
15:05	Start second half experiment (Frictionmap)
	”You will find a clear difference between the two conditions, this went way better”
15:15	End experiment, time = 25 min

Participant 13

4-4-2022	
11:00	Explanation
11:12	Start experiment (Frictionmap)
	Participant has long nails; this might cause a mismatch in true finger position and infrared sensor readings.
	”This is really nice, you feel the feedback clearly”
11:25	Start second half experiment (Heightmap)
	With this condition the participant moves slower across the screen
	”This is more difficult”
	”If the haptic feedback is strong, it is super clear”
11:45	End experiment, time = 33 min

Participant 14

12:15	Explanation
12:24	Start experiment (Heightmap)
	”Does this work with airpressure?” (answered: it works with ultrasonic vibrations)
	Participant moves finger up and down on a path. This case the friction changes due to the change in direction. However the participant might feel that something is changing around this path. As a result the participant chooses this path, might be a confirmation bias at play.
	”Do I need to execute the task faster?” (answered: It is totally up to you, take the time you think you need to make a descision)
	”I could really feel changes in friction, but sometimes I interpret it wrongly”
12:47	Start second half experiment (Frictionmap)
	”This can be felt way better”
	”In the heightmap condition, I could feel the slopes but it was difficult to know where it pointed to”
12:58	End experiment, time = 34 min

Participant 15

15:15	Explanation
15:24	Start experiment (Frictionmap)
	"This system works really nicely"
	"The sound on the headphones works well, I don't hear the screen"
	"If I excert a lot of force it becomes more difficult"
15:40	Start second half experiment (Heightmap)
	"I'm curious on how difficult this condition is"
	"It's difficult, I don't have a clear method to find the correct target"
15:59	End experiment, time = 34 min
	"Sometimes I closed by eyes to not be distracted by the visual lines"
	"Should you really provide the red/green feedback at the end? This could be demativating."

Participant 16

16:00	Explanation
16:07	Start experiment (Heightmap)
	Participant uses many small vertical movements
	Noise from the plate seems to have reduced
	"Sometimes I feel it very clearly. Sometimes I have to compare a lot"
16:46	Start second half experiment (Frictionmap)
	"In several trials, while searching, I easily glided to the correct target"
17:06	End experiment, time = 59 min
	"Second condition was way easier"

Participant 17

7-4-2022	
10:00	Explanation
10:16	Start experiment (Frictionmap)
	Participant is lefthanded, movements to the right seem to exhibit stick-slip behaviour.
10:35	Start second half experiment (Heightmap)
	Mainly follows the paths, sometimes up and down
10:?	End experiment, time = ? min (end time not written down)

Participant 18

11:30	Explanation
11:41	Start experiment (Heightmap)
	Mainly uses vertical movements, combined with small deviations around the paths
	"Top path is easiest to identify"
	"I choose the middle target if I'm not sure"
	"Sometimes I do feel something, but I still choose the wrong target"
12:06	Start second half experiment (Frictionmap)
	"Way easier than previous condition"
	"I'm motivated to improve my score"
12:24	End experiment, time = 43 min

Participant 19

13:33	Explanation "Is there a time limit?" (answered: No, you can make your descision once you are confident in your choice.)
13:41	Start experiment (Frictionmap) Participant sometime wipes the index finger with his thumb after a trial. The finger movements are mainly vertical stroking movements. The finger is lifted up when moving up.
14:09	Start second half experiment (Heightmap) "Can I switch fingers?" (answered: Preferably no. Initiated a small break) Participant mainly feels halfway the paths where there is more seperation "This condition is more difficult"
14:45	End experiment, time = 64 min

Participant 20

16:50	Explanation
16.58	Start experiment (Heightmap) "Is it always one of these three targets?" (answered: Yes) "The feedback is more subtle than expected" "The middle target was hard to find. Only hit around 3 times"
17:18	Start second half experiment (Frictionmap) "I have the feeling that I am doing better in this condition"
17:29	End experiment, time = 31 min

Participant 21

8-4-2022	
9:09	Explanation
9:20	Start experiment (Frictionmap) Low battery warning on the headphones. Batteries replaced and experiment continued Participant uses long vertical movements and quickly descides
9:34	Start second half experiment (Heightmap) In the first trials the participant closed his eyes. "I would expect that it is difficult to sample the movement direction real time." "This is quite difficult"
9:54	End experiment, time = 34 min

Participant 22

13-4-2022	
14:12	Explanation
14:33	Start experiment (Heightmap) ”Does it matter how I position my finger?” (answered: No, but be aware of how the position sensor works: don’t place other fingers in the field of view) ”I have the feeling that the force sensor might give away the correct position. Low normal force means the target is at that point” (This extra information does not seem to help the participant much) ”Higher friction would mean that you apply more normal force as well. This is an indicator to if you are correct” ”I apparently have a bias for the bottom position”
15:01	Start second half experiment (Frictionmap) ”I am way more confident in chosing a target, even without comparing to other paths” ”First condition required more cognitive load”
15:10	End experiment, time = 37 min

Results per Participant

For an indication of the intra- and inter-subject variability the raw data per participant is visualised on the following pages. The figures that are presented in the paper are also plotted for one participant only. Fig. L.1 provides the legend for each graph. The colors in each graph is kept consistent; Frictionmap (position-based) and Heightmap (position & velocity-based) are visualised in red and blue respectively.

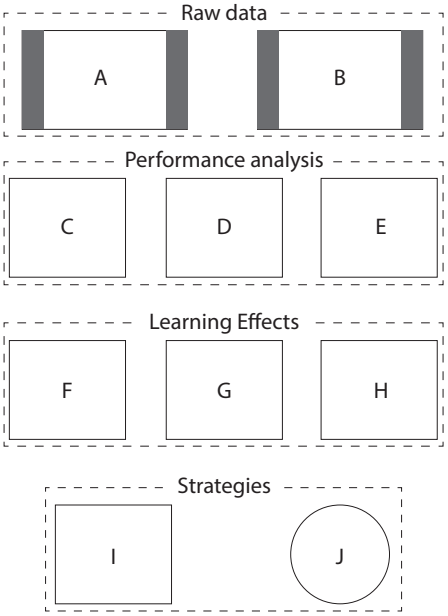

Figure L.1: Legend of the data visualisation per participant. Participant number is given in each legend on the following pages

- A: Raw data paths of all frictionmap trials. The trial numbers corresponding to this data is given in the title. Trials resulting in a correct answer are visualised in green, while incorrect answers are in red.
- B: Raw data paths for all heightmap trials. The trial numbers corresponding to this data is given in the title. Trials resulting in a correct answer are visualised in green, while incorrect answers are in red.
- C: Hit-rate plotted against the vibration amplitude (strength of haptic feedback). Individual datapoints of fig. 11 from the paper.
- D: Movement times for each correctly answered trial at the three free-air vibration amplitudes. Individual datapoints of fig. 12 from the paper.
- E: Amount of direction changes for each correctly answered trial at the three free-air vibration amplitudes. Individual datapoints of fig. 13 from the paper.
- F: Proportion of correct responses for each block of 45 trials. Individual datapoints of fig. 15 from the paper.
- G: Moving average of the movement times (with a window of 10 trials). Individual lines of fig. 15 from the paper.
- H: Moving average of the number of direction changes (with a window of 10 trials). Graph not in the paper.
- I: Total absolute movement in x and y direction for each trial, adjusted for the minimum required distance to select the target. Datapoint size represents the free-air vibration amplitude [1.65, 3.3, 5]
- J: Normalised histogram of the movement angle of all trials. The dashed lines indicate the main angles of the three possible paths. Similar to fig 14 in the paper.

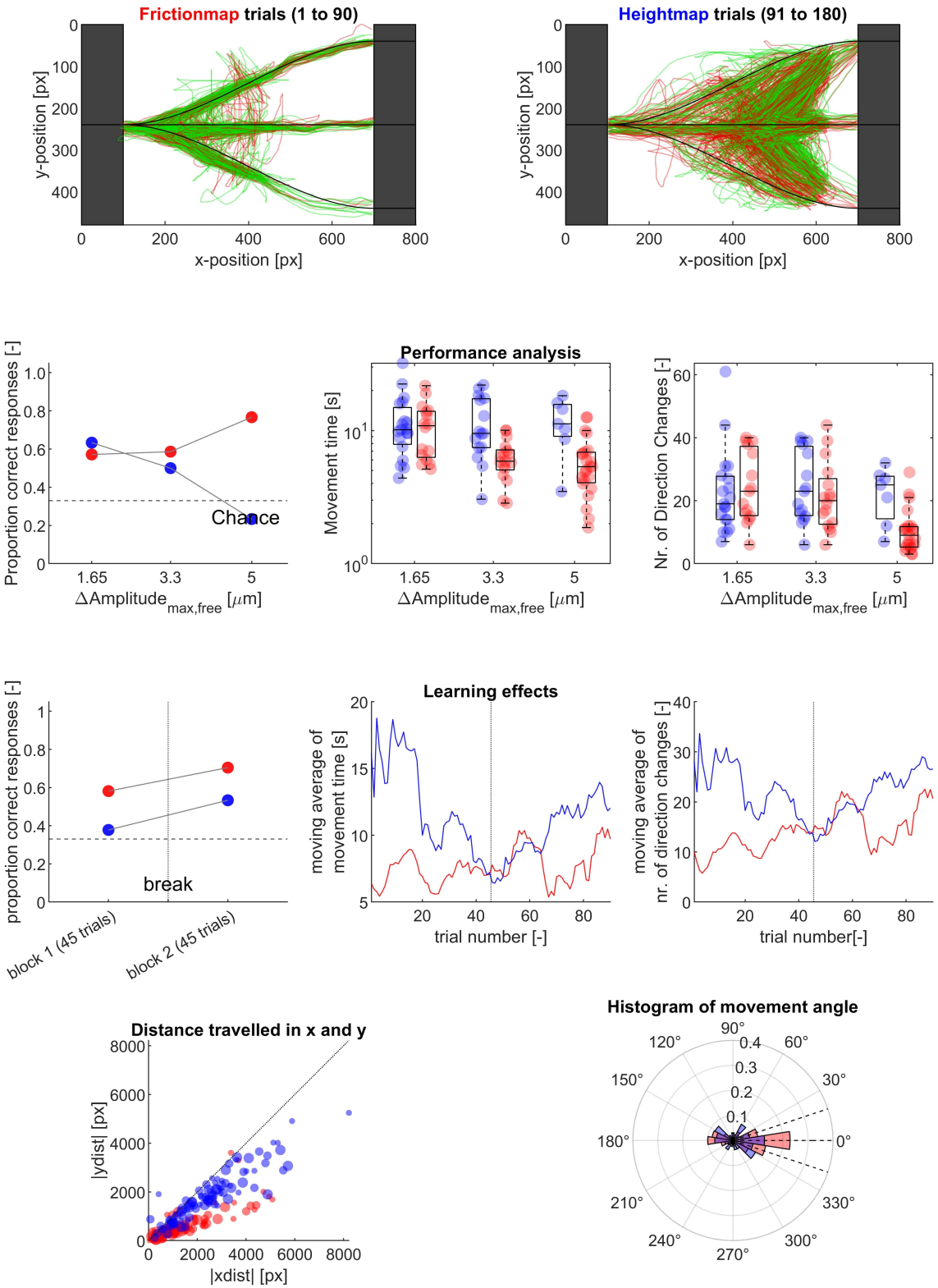

Figure L.2: Participant 1.

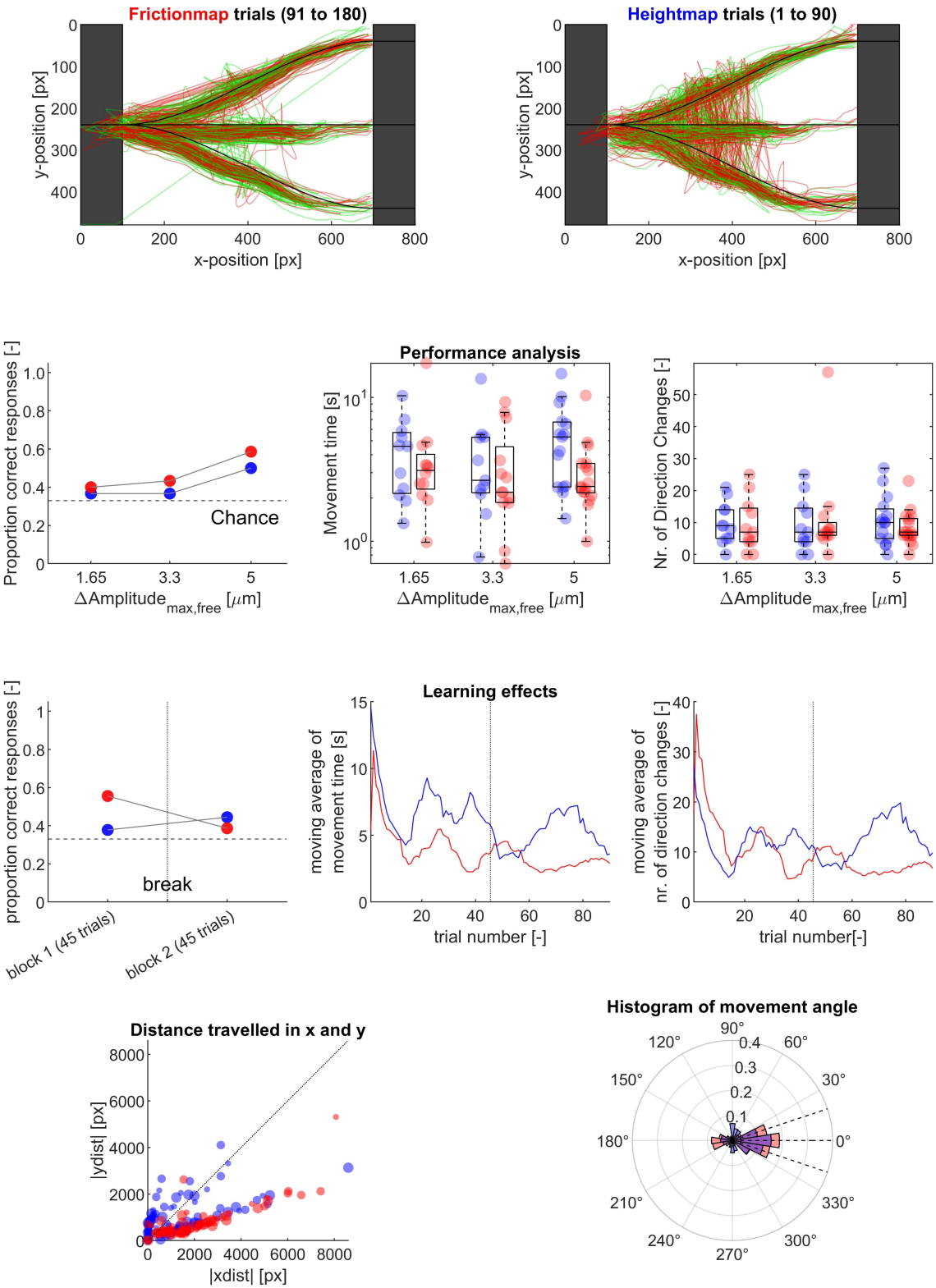

Figure L.3: Participant 2.

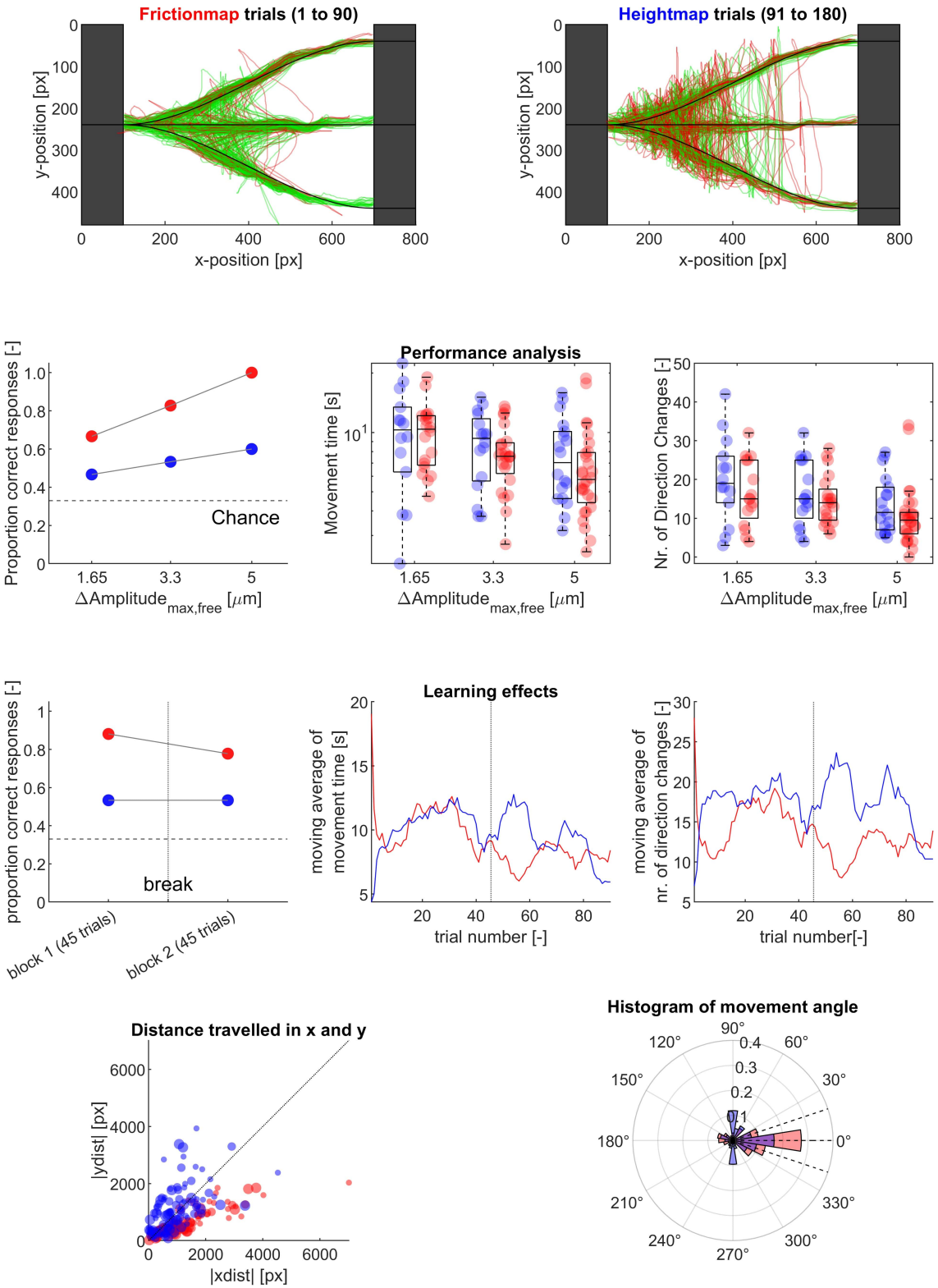

Figure L.4: Participant 3.

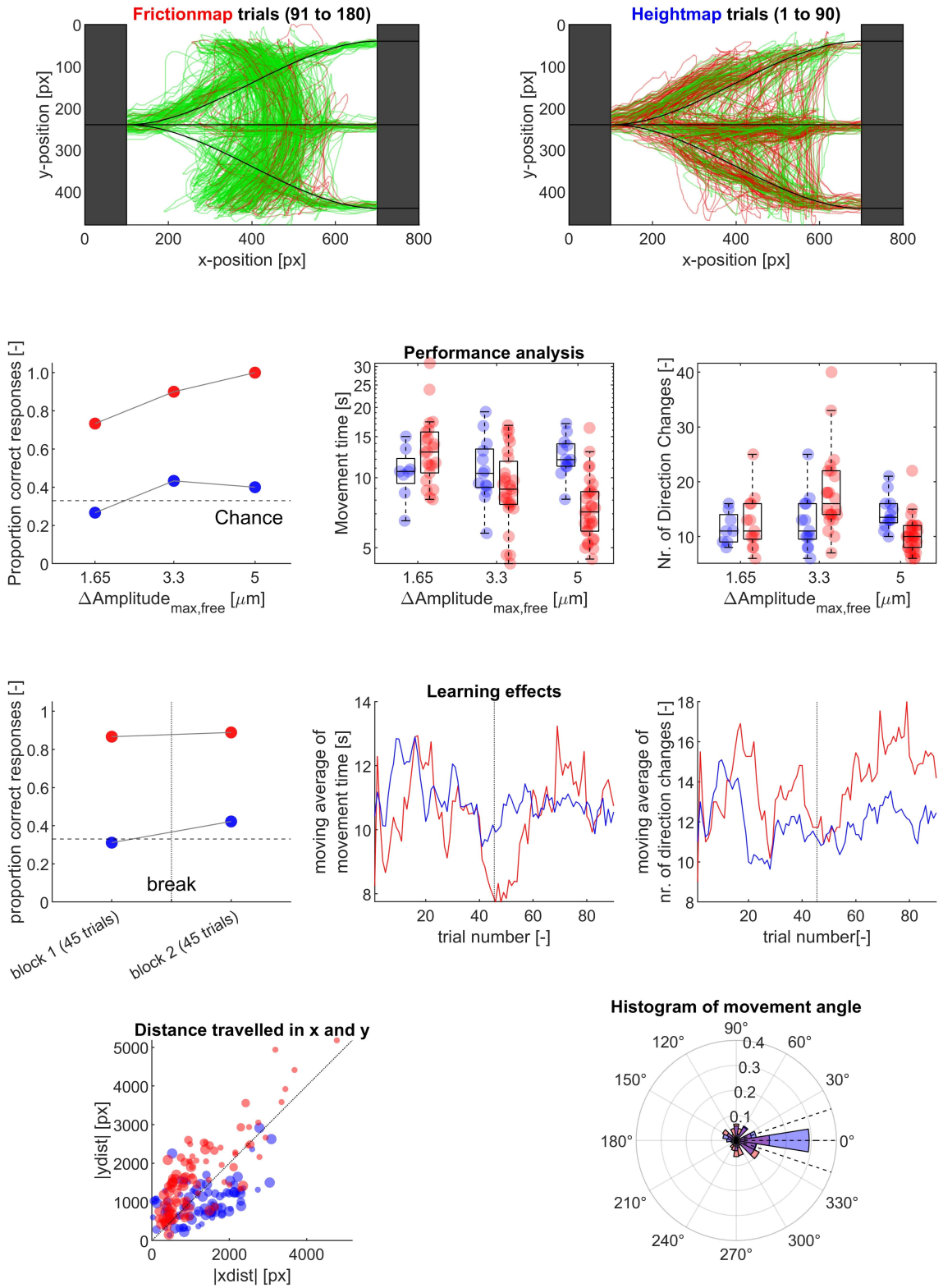

Figure L.5: Participant 4.

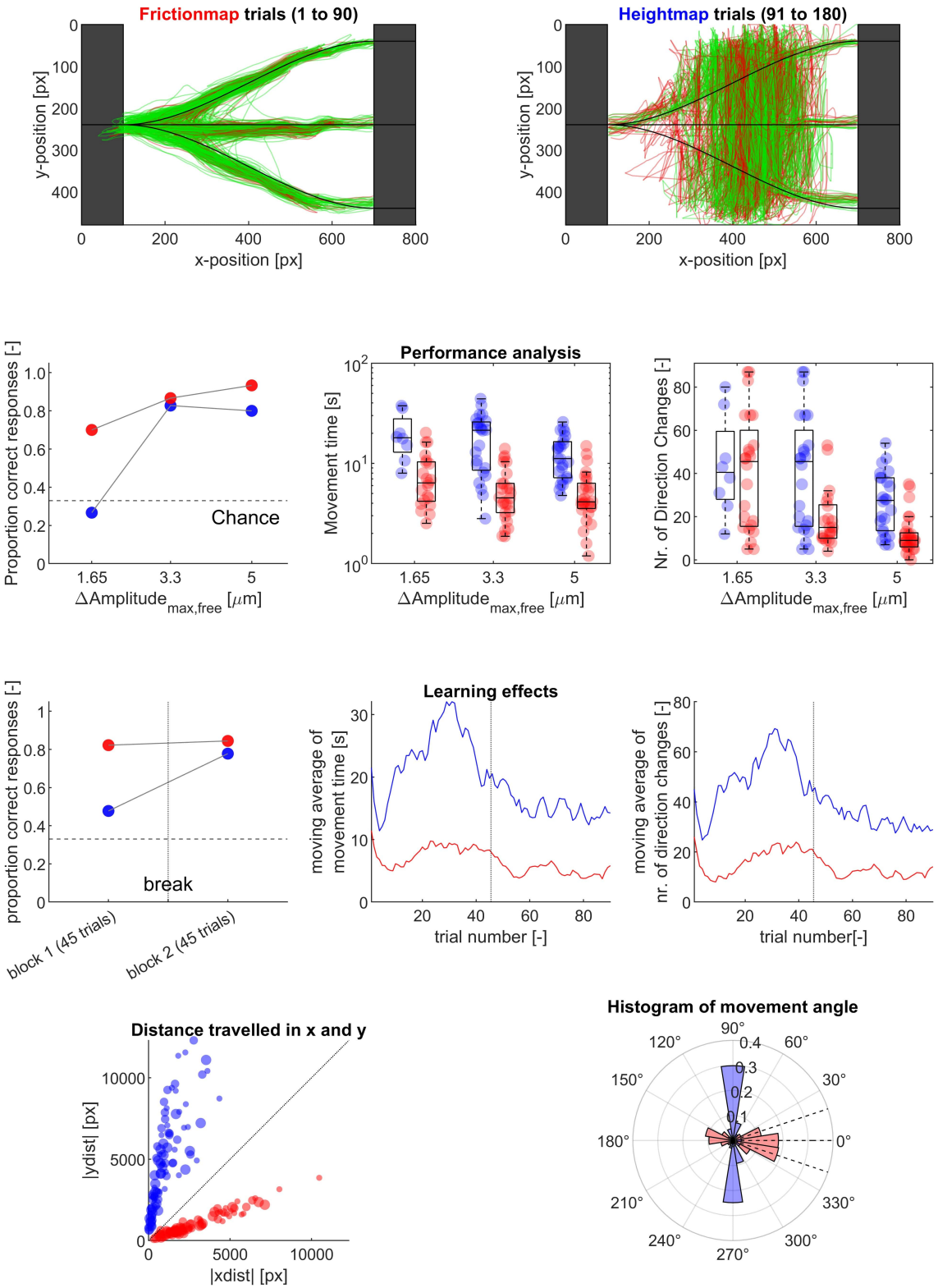

Figure L.6: Participant 5.

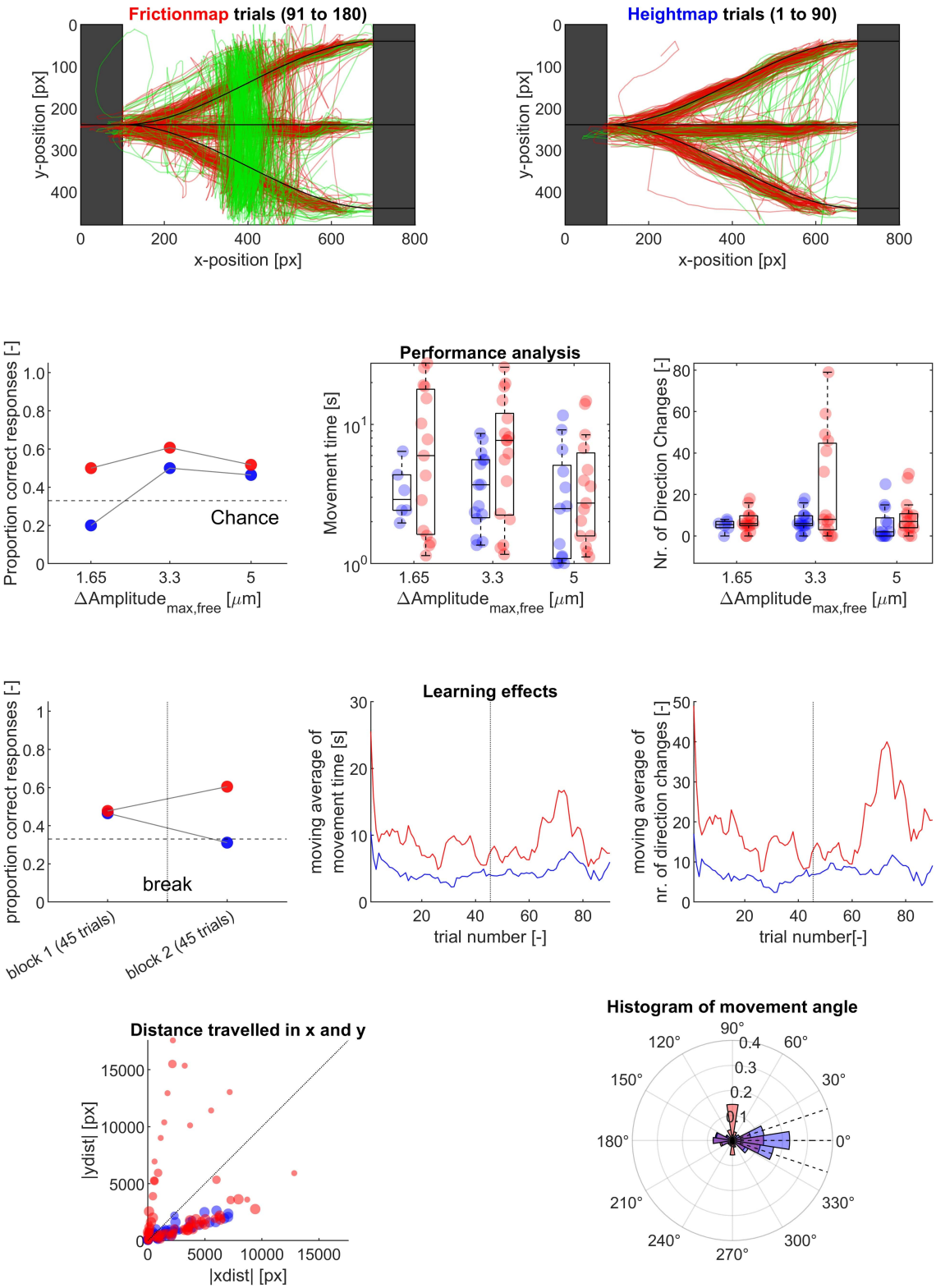

Figure L.7: Participant 6.

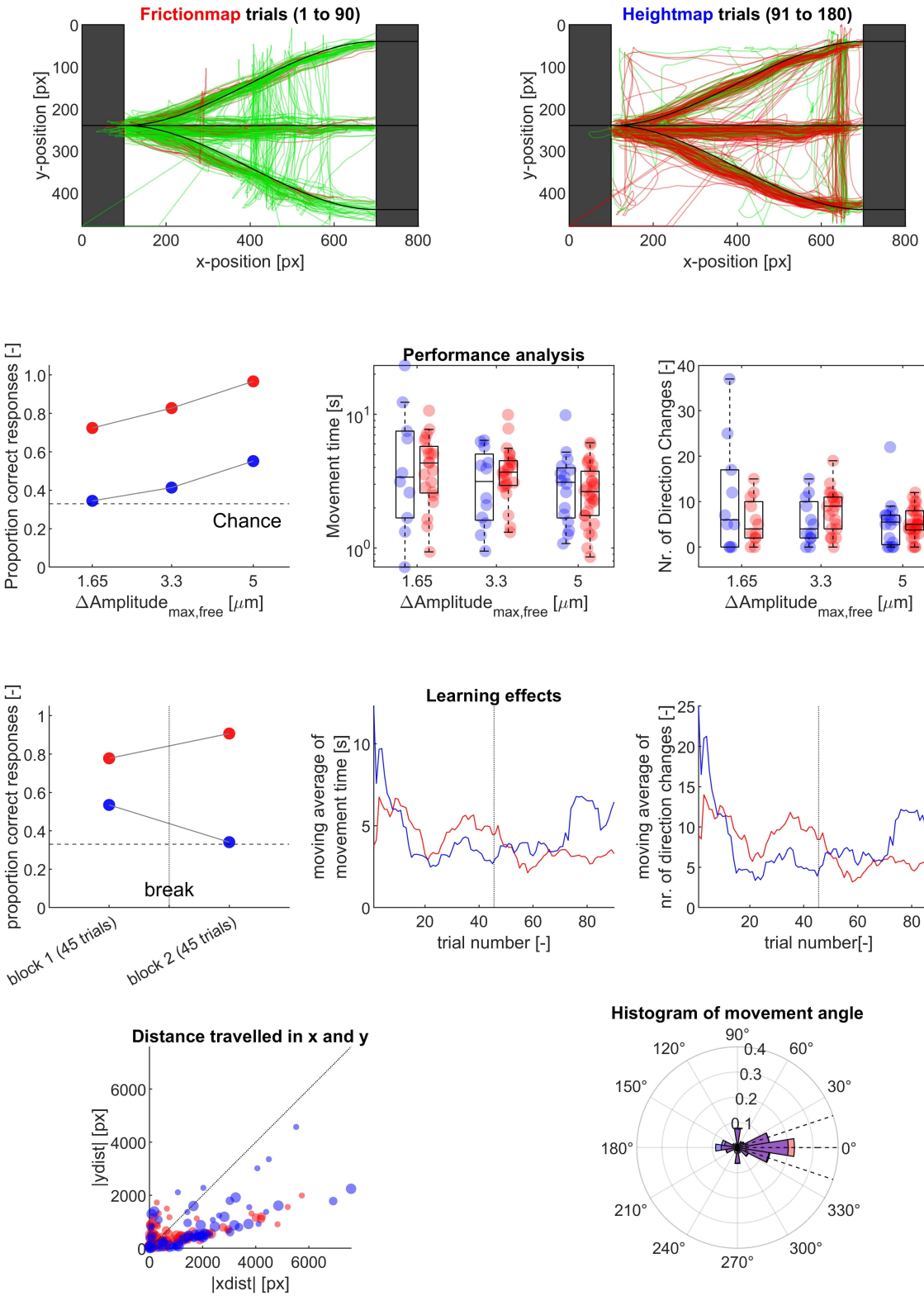

Figure L.8: Participant 7.

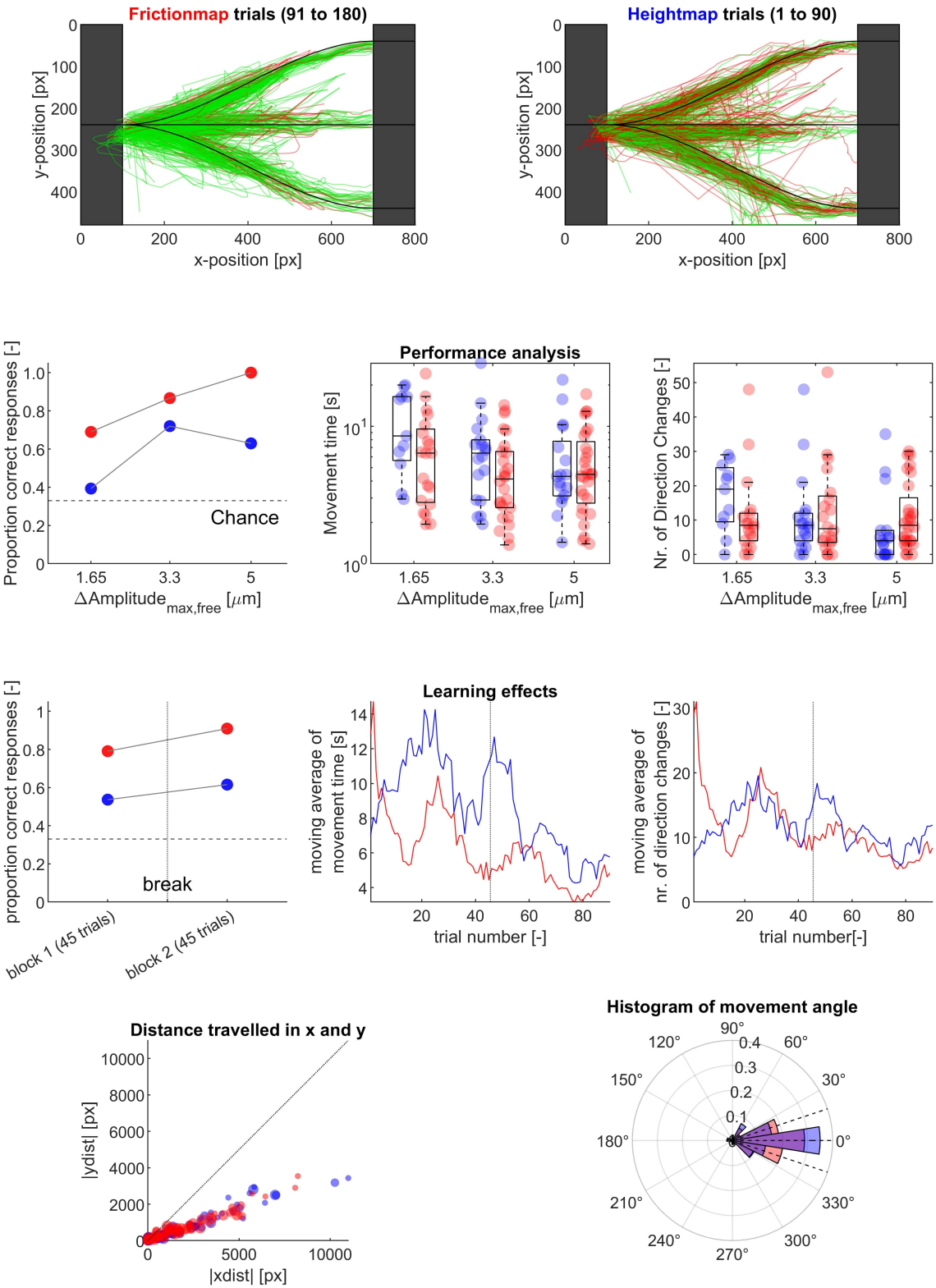

Figure L.9: Participant 8.

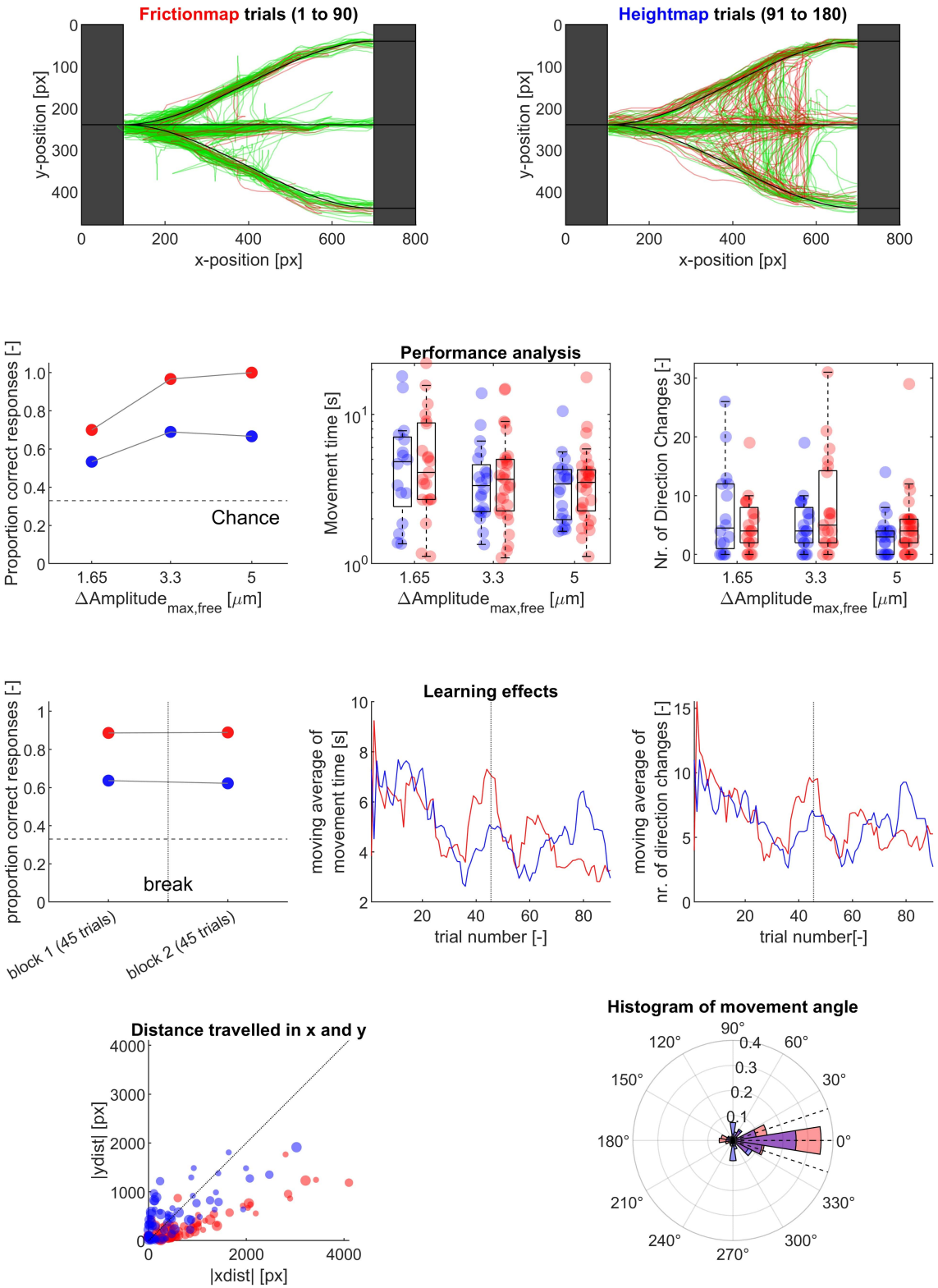

Figure L.10: Participant 9.

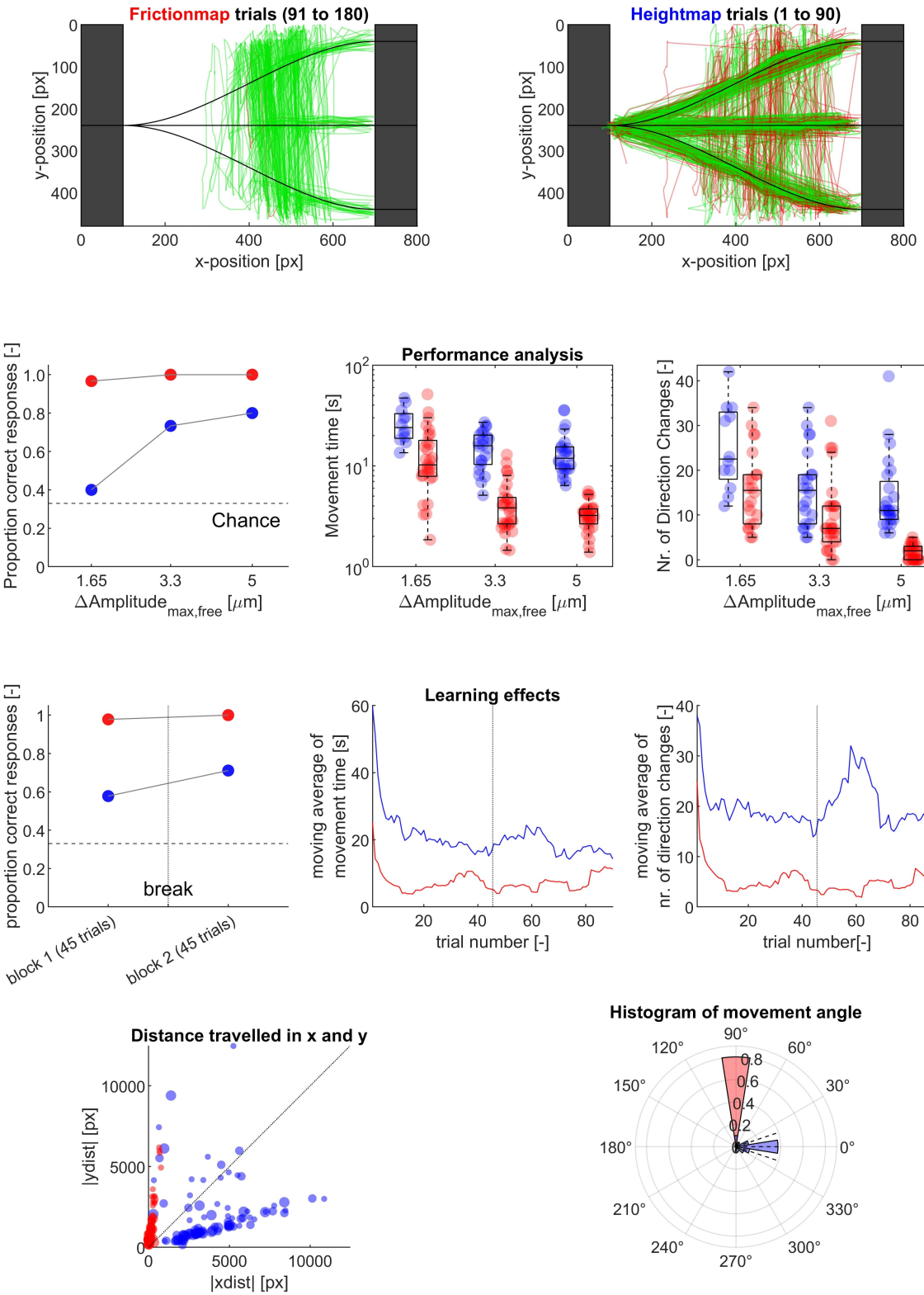

Figure L.11: Participant 10.

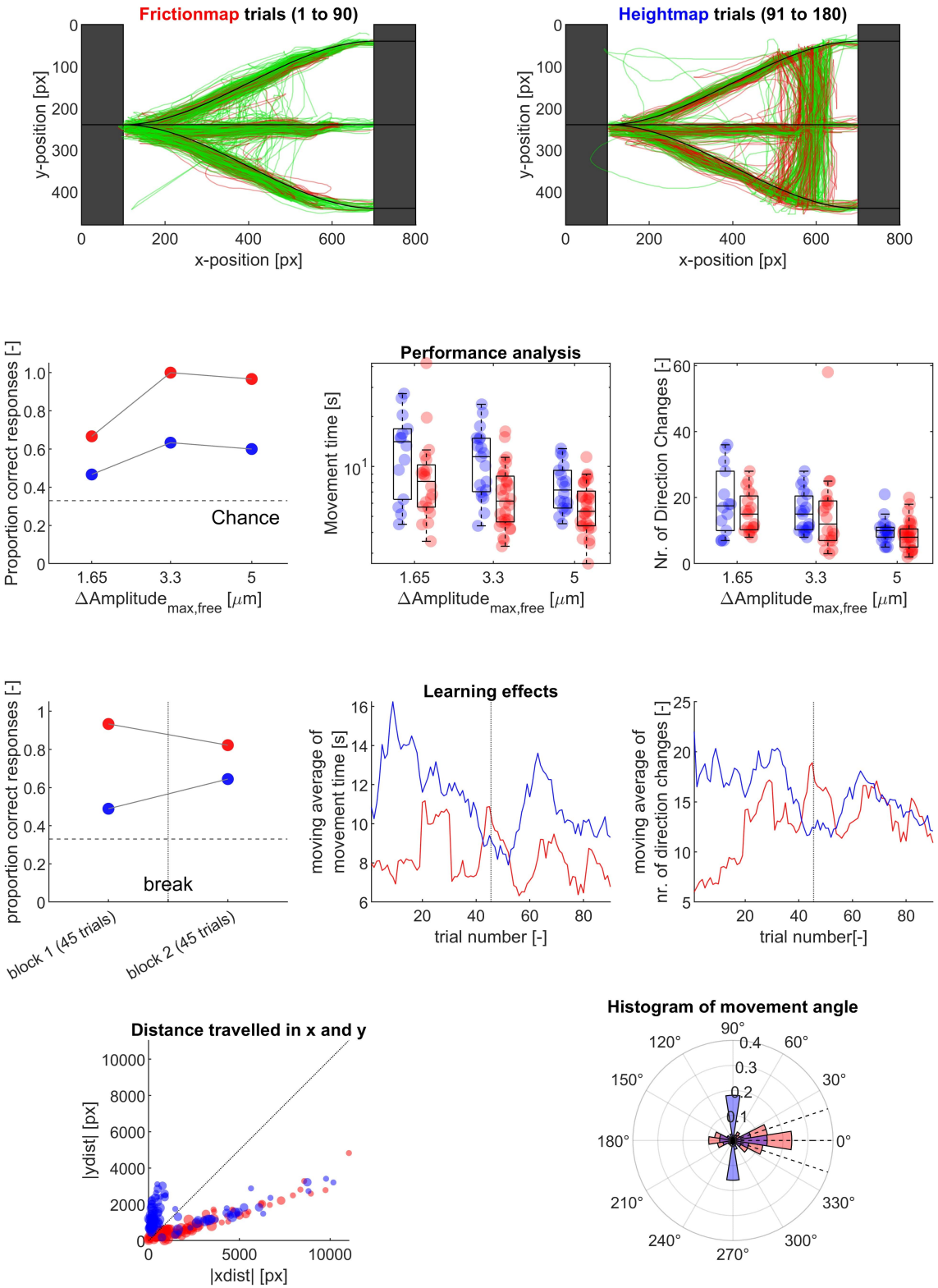

Figure L.12: Participant 11.

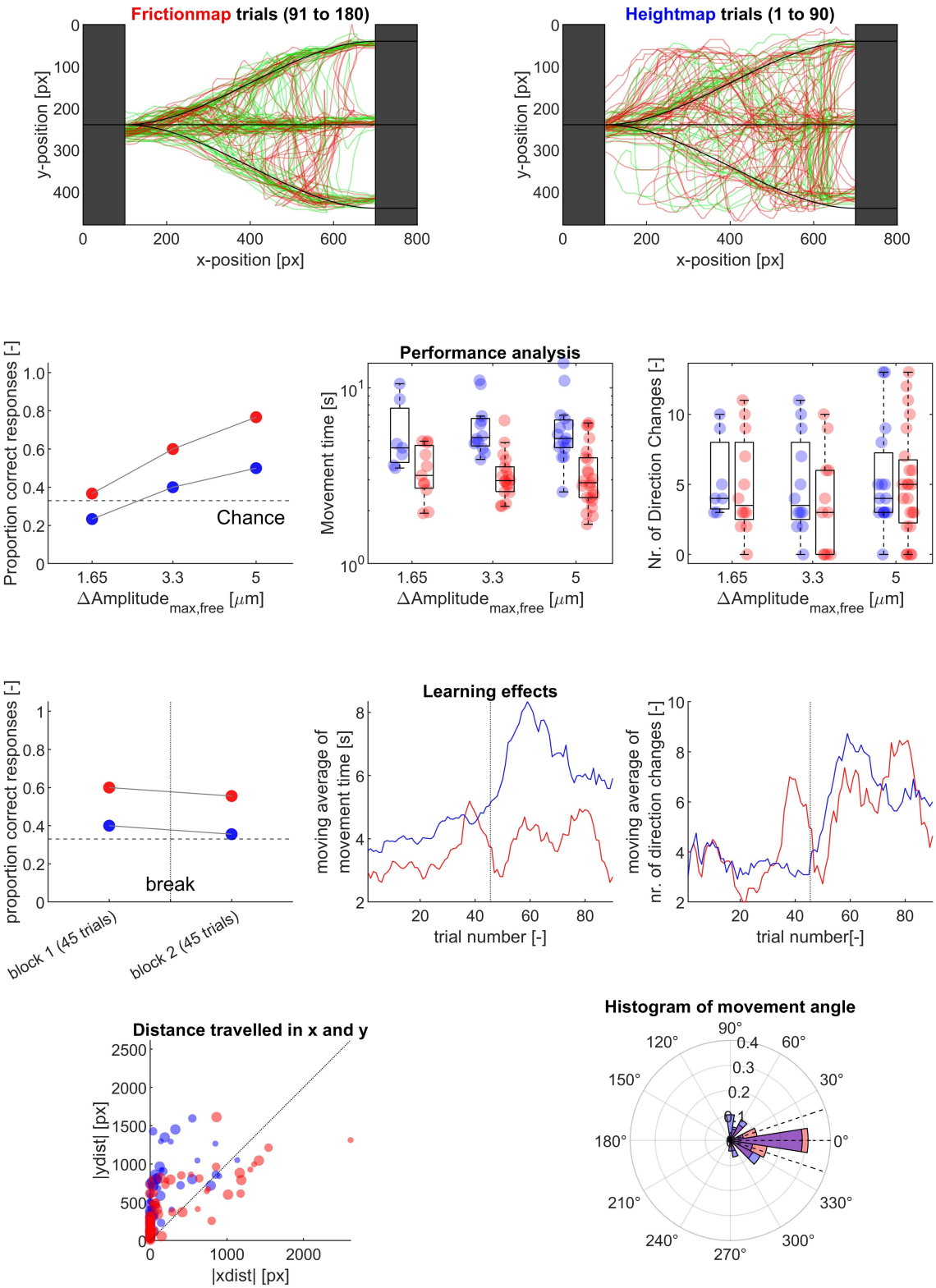

Figure L.13: Participant 12.

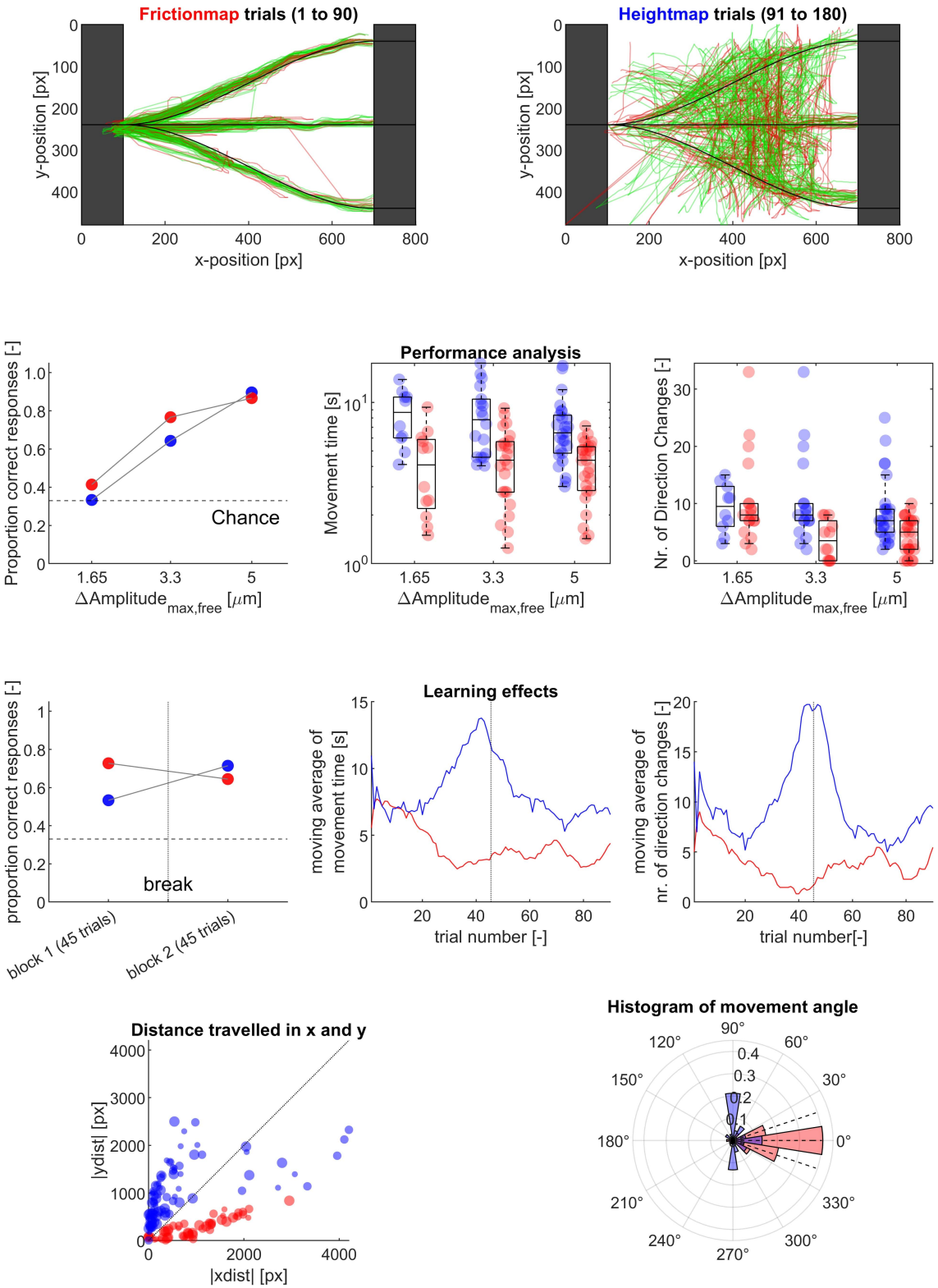

Figure L.14: Participant 13.

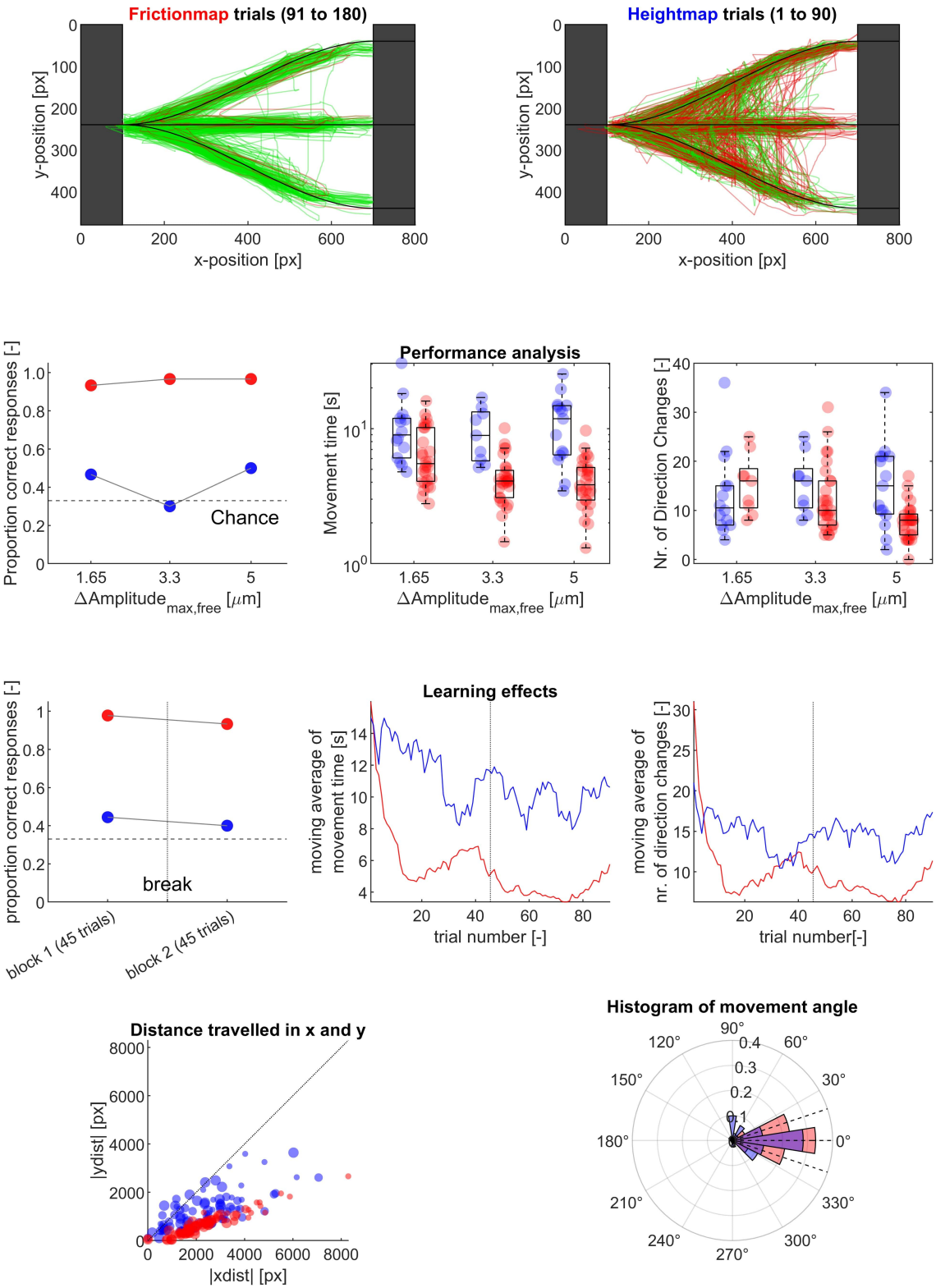

Figure L.15: Participant 14.

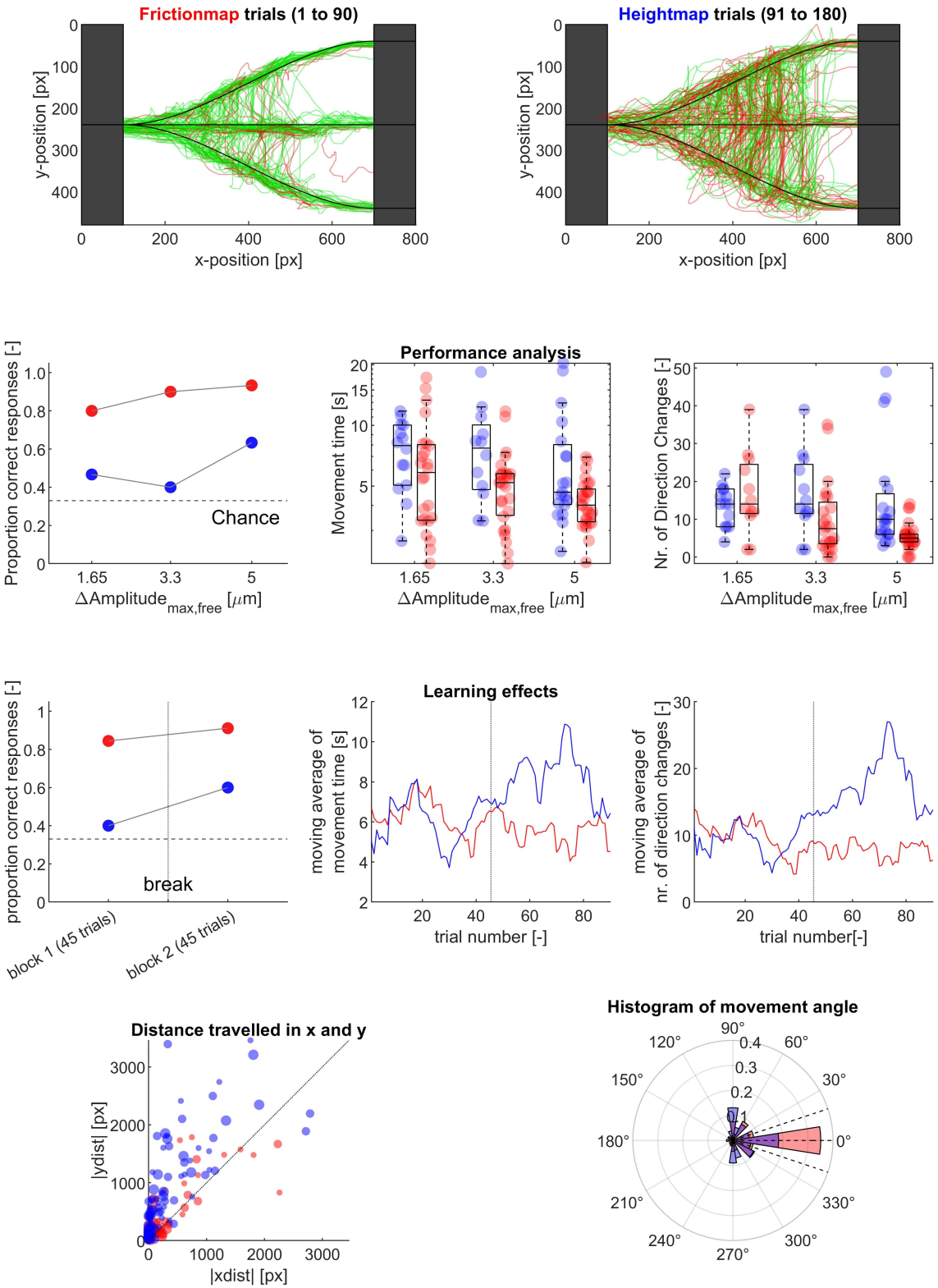

Figure L.16: Participant 15.

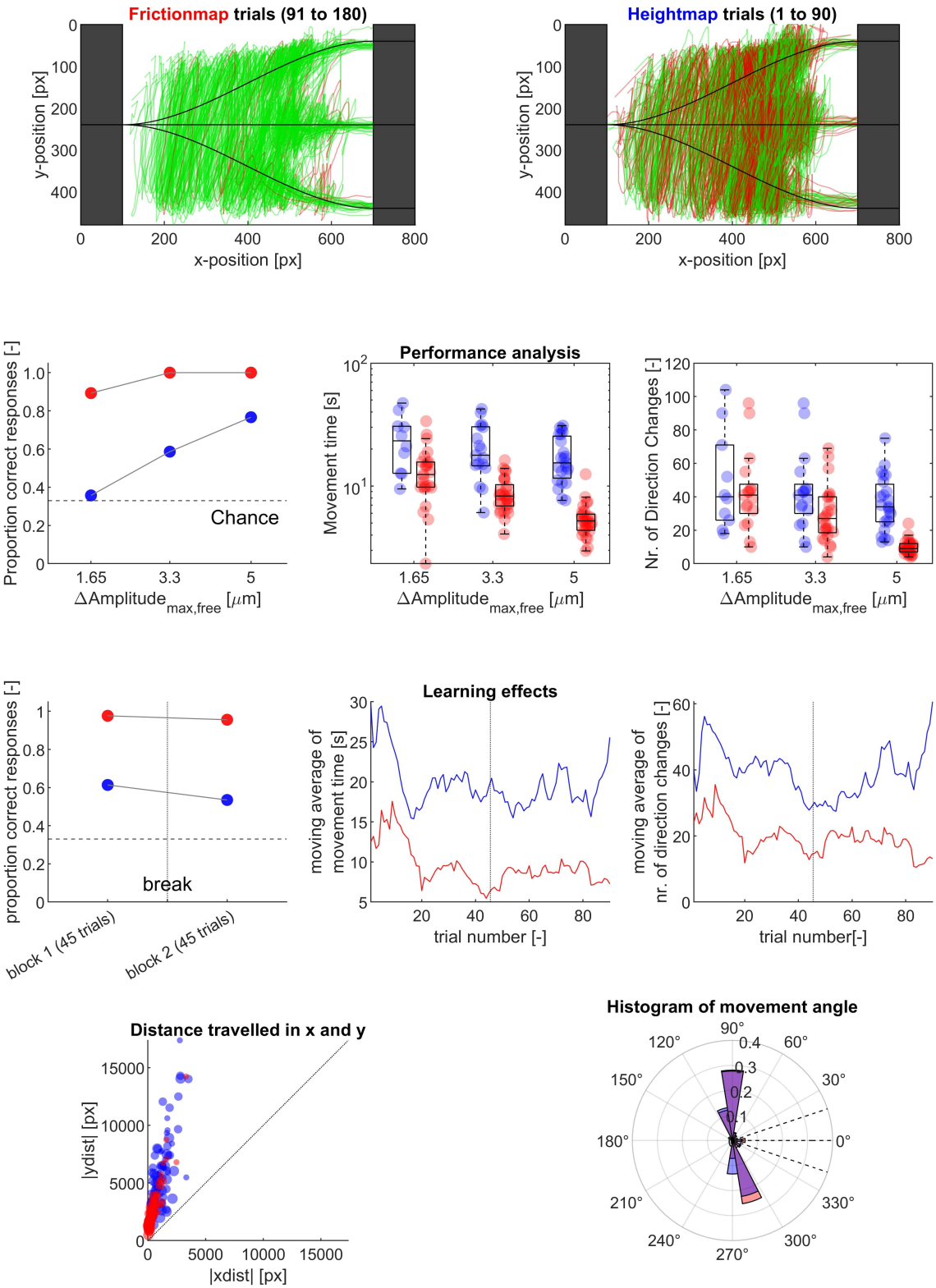

Figure L.17: Participant 16.

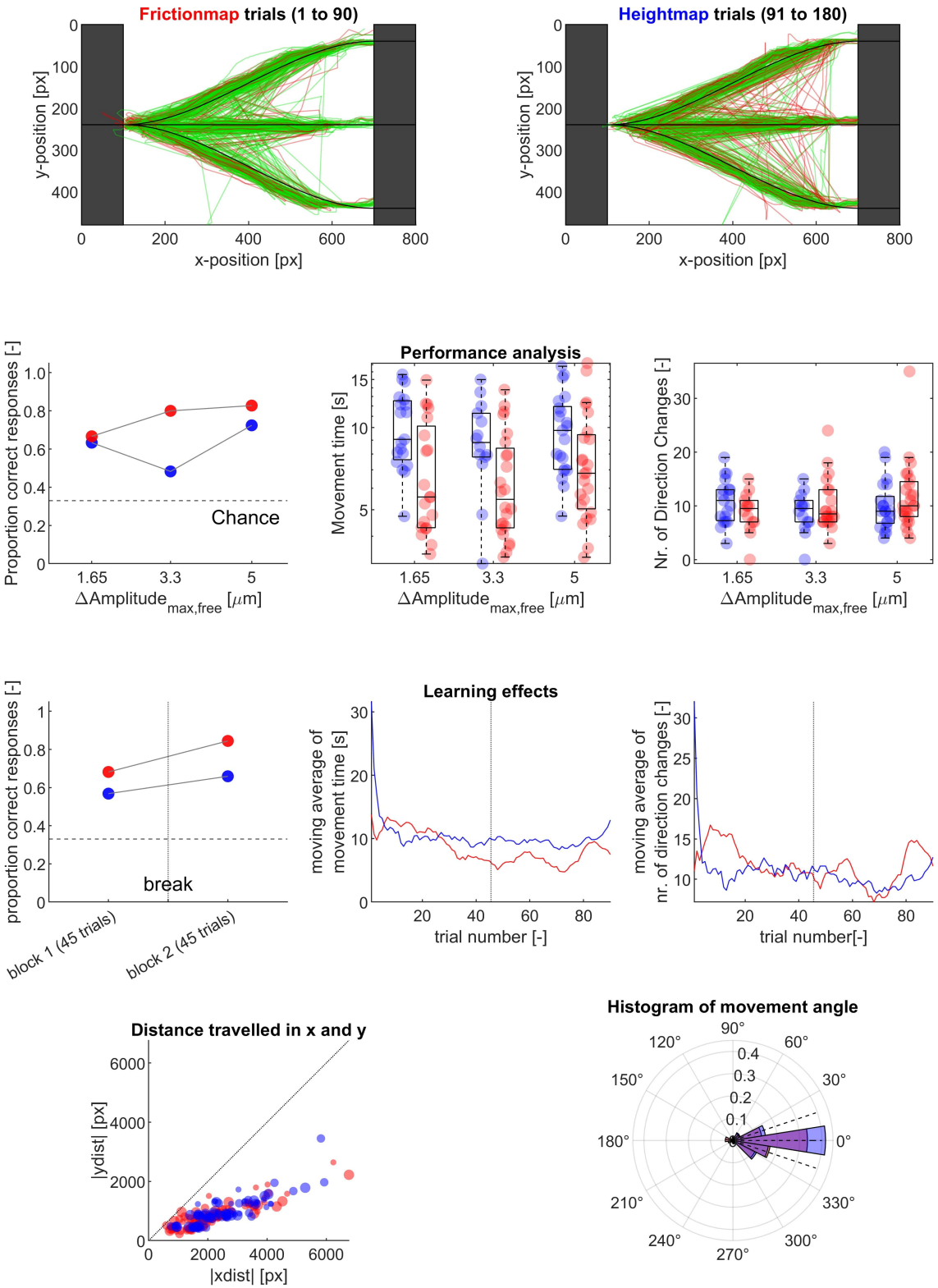

Figure L.18: Participant 17.

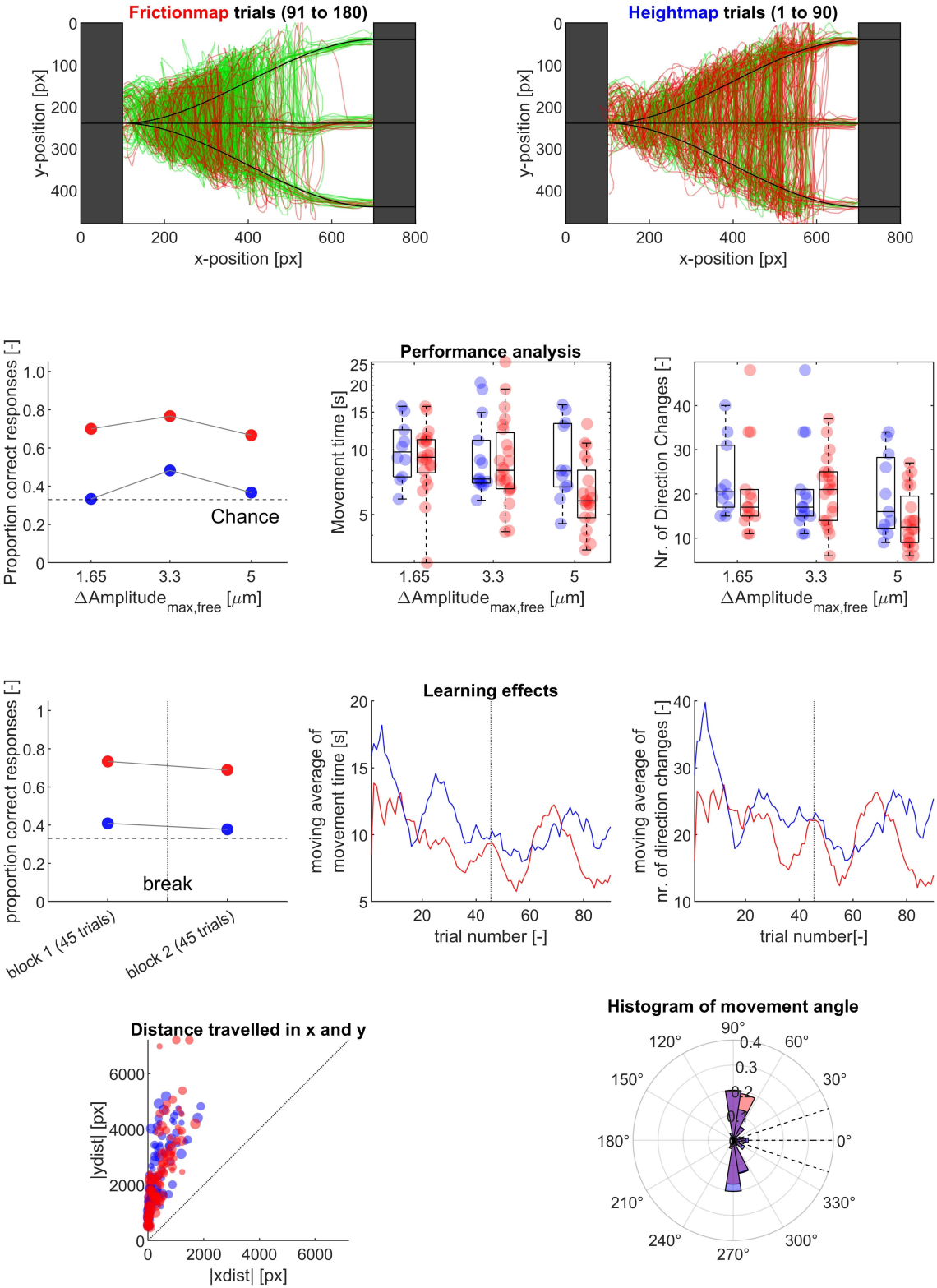

Figure L.19: Participant 18.

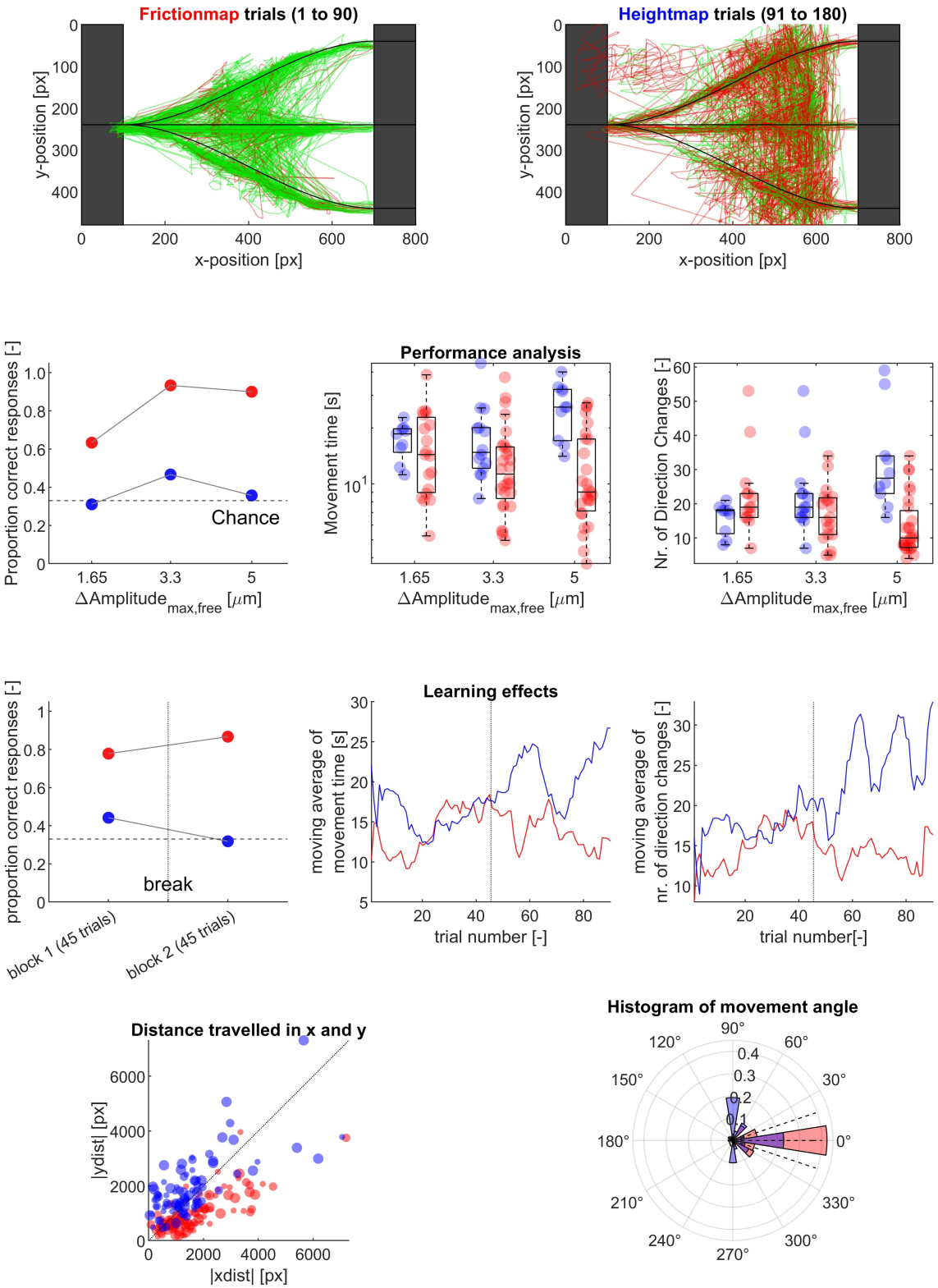

Figure L.20: Participant 19.

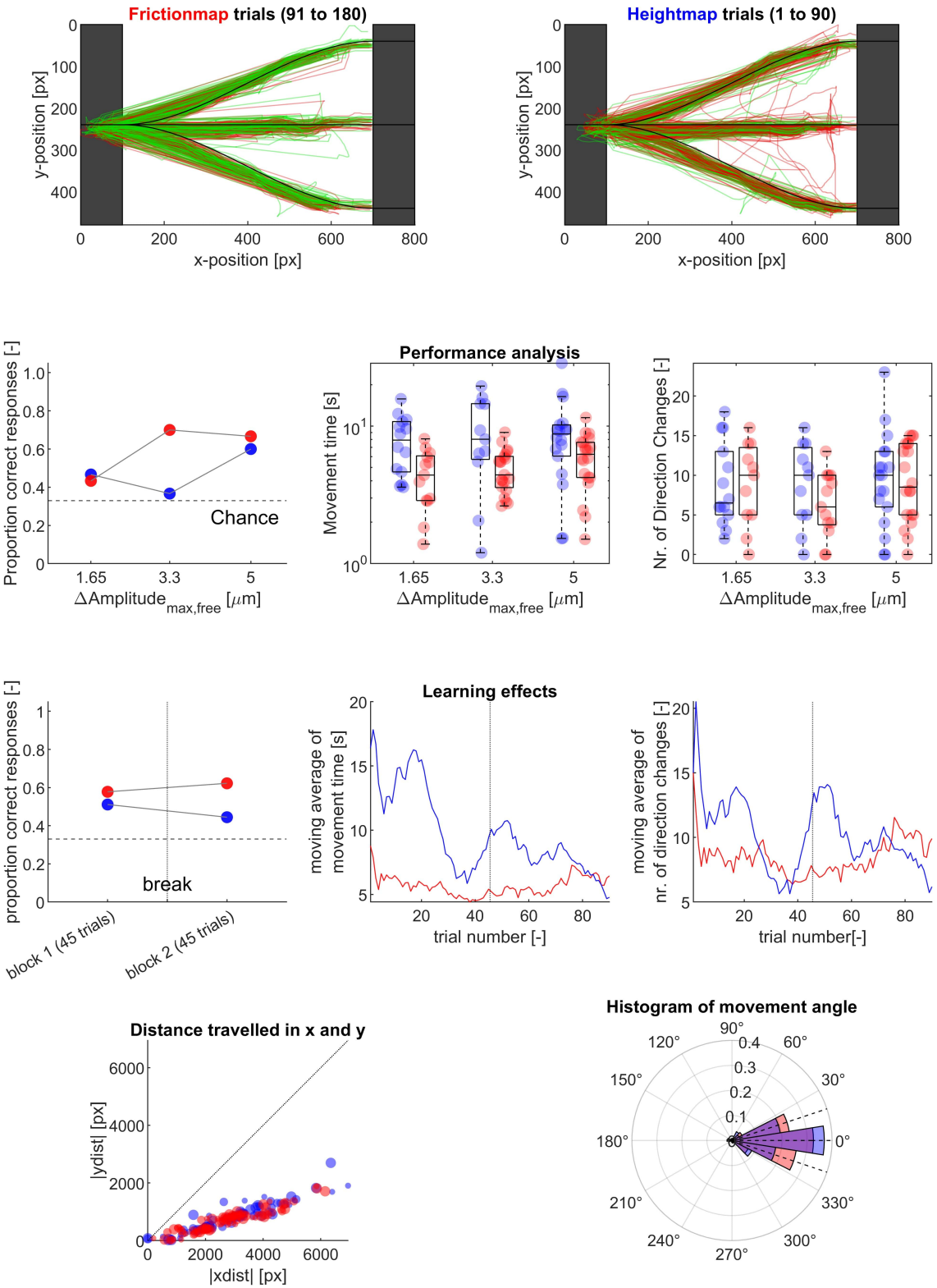

Figure L.21: Participant 20.

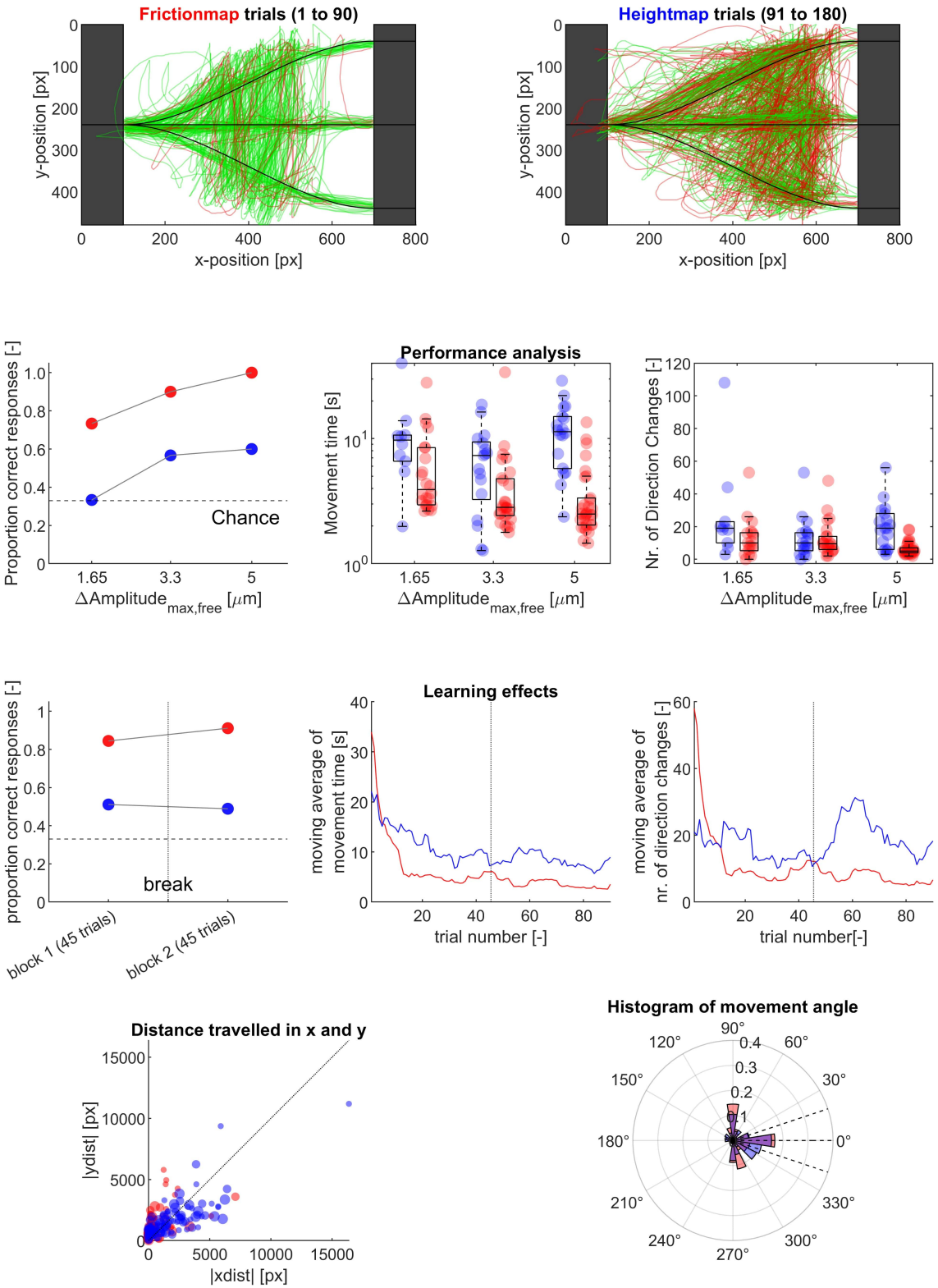

Figure L.22: Participant 21.

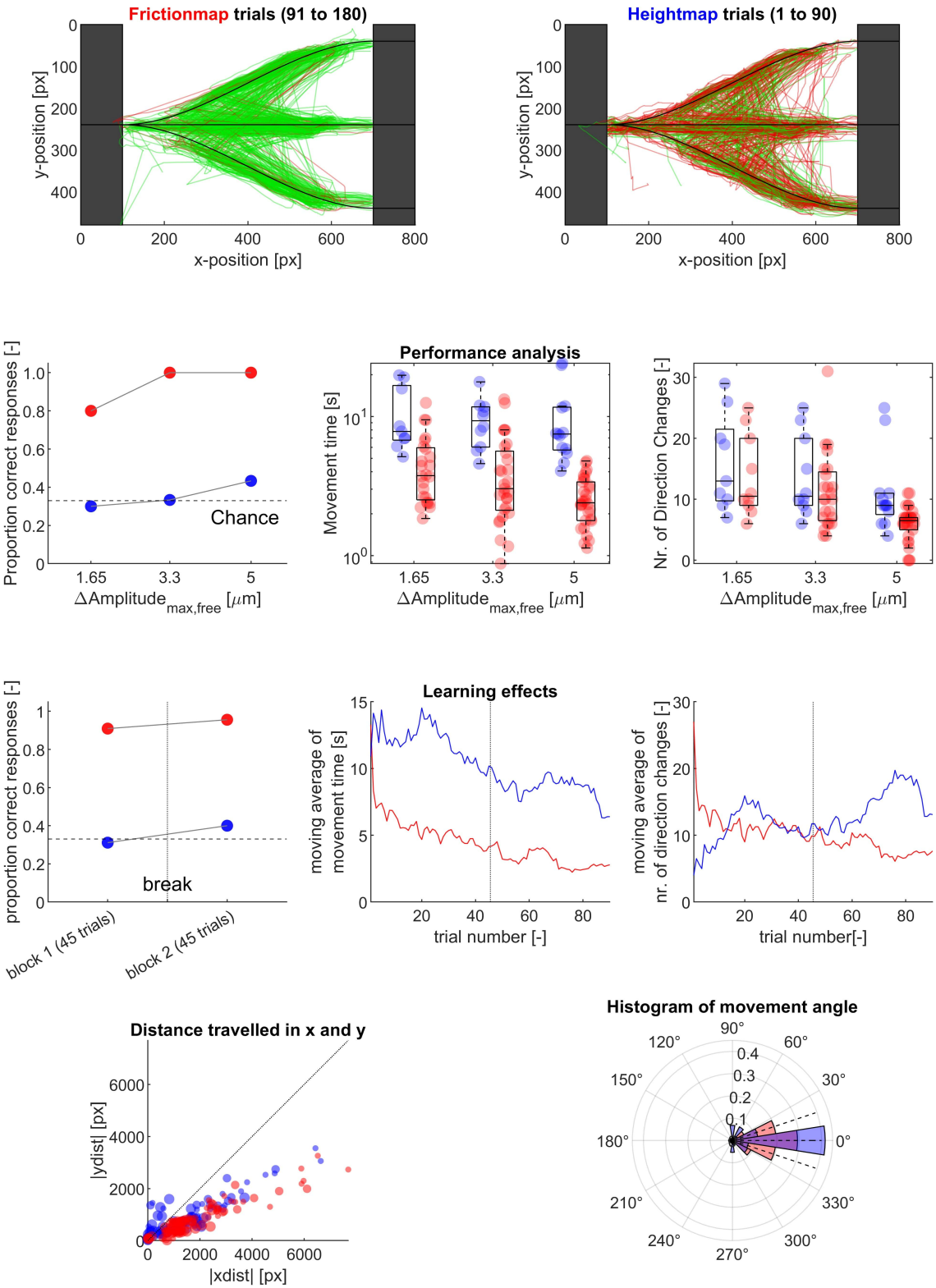

Figure L.23: Participant 22.

Bibliography

[1] Johnny Accot and Shumin Zhai. Beyond Fitts' Law: Models for Trajectory-Based HCI Tasks. Proceedings of the ACM SIGCHI Conference on Human factors in computing systems, 1997.

[2] Tammo Brans. Haptic Touchscreen Prototype (not published). Technical report, TU Delft, 2020.

[3] Daniel J. Inman. Engineering Vibration International Edition. Pearson, 4th edition, 2014.

[4] Robert D. Blevins. Formulas for natural frequency and mode shape. Van nostrand reinhold company, New York, 1979.

[5] Sergio Franco. Design with operational amplifiers and analog integrated circuits. Mcgraw-Hill Education, 4th edition, 6 2014.

[6] Géry Casiez, Nicolas Roussel, Romuald Vanbelleghem, and Frédéric Giraud. Surfpad: Riding Towards Targets on a Squeeze Film Effect. In CHI '11: Proceedings of the SIGCHI Conference on Human Factors in Computing Systems, pages 2491–2500, 2011.

[7] Vincent Levesque, Louise Oram, Karon MacLean, Andy Cockburn, Nicholas D. Marchuk, Dan Johnson, J. Edward Colgate, and Michael A. Peshkin. Enhancing physicality in touch interaction with programmable friction. In Proceedings of the SIGCHI conference on human factors in computing systems, pages 2481–2490, 2011.

[8] Géry Casiez, Nicolas Roussel, and Daniel Vogel. 1€ Filter: A simple Speed-based Low-pass Filter for Noisy Input in Interactive Systems. In CHI'12, the 30th Conference on Human Factors in Computing Systems,, pages 2527–2530, 2012.

[9] Andriy Pavlovych and Wolfgang Stuerzlinger. The Tradeoff between Spatial Jitter and Latency in Pointing Tasks. In Proceedings of the 1st ACM SIGCHI Symposium on Engineering Interactive Computing Systems, pages 187–196, Pittsburgh, PA, USA, 2009. Association for Computing Machinery.

[10] Paul M Fitts. The information capacity of the human motor system in controlling the amplitude of movement. Journal of Experimental Psychology, 47(6):381–391, 1954.

[11] Rafal Bogacz, Eric Brown, Jeff Moehlis, Philip Holmes, and Jonathan D. Cohen. The physics of optimal decision making: A formal analysis of models of performance in two-alternative forced-choice tasks. Psychological Review, 113(4):700–765, 10 2006.

[12] David S. Ebert, F. Kenton Musgrave, Darwyn Peachey, Ken Perlin, and Steve Worley. Texturing & modeling : a procedural approach. Morgan Kaufmann, 3rd edition, 2003.

[13] Felix A. Wichmann and N. Jeremy Hill. The psychometric function: I. Fitting, sampling, and goodness of fit. Perception & Psychophysics 2001 63:8, 63(8):1293–1313, 2001.